University of South-Eastern Norway

www.usn.no

FMH606 Master's Thesis 2023

Process Technology

CO_2 capture combined with calcination driven by oxyfuel combustion of green hydrogen

Glenn Nedrum

Faculty of Technology, Natural sciences and Maritime Sciences
Campus Porsgrunn

University of South-Eastern Norway

www.usn.no

Course: FMH606 Master's Thesis, 2023

Title: CO2 capture combined with calcination driven by oxyfuel combustion of green hydrogen

Number of pages: 109

Keywords: Calciner, Hydrogen combustion, Oxyfuel, Carbon capture, Electrolysis, Aspen Plus, CAPEX, OPEX, HAZID, Adiabatic flame temperature, recycled CO_2, CCS.

Student:	Glenn Nedrum
Supervisor:	Lars-André Tokheim
External partner:	Norcem AS Brevikw/Christoffer Moen

University of South-Eastern Norway

www.usn.no

Summary:

This thesis aimed to investigate the feasibility of incorporating a hydrogen and oxygen production system through electrolysis in a cement plant, specifically targeting the combustion of these gases in a calciner unit for carbon capture of the calcination process. The study was conducted in the context of Norcem Brevik cement plant in Norway, aligning with the goals of the Paris Agreement and the country's emissions targets.

A series of simulations were executed in Aspen Plus to understand the implications of various changes to the calciner system. These modifications included altering coal combustion to match real coal consumption, modifying the adiabatic flame temperature for oxy-fuel hydrogen combustion, and exploring different recycling temperature and flowrate cases for CO_2/H_2O.

The results from these simulations provided insightful data on the system's energy efficiency, the cooling demand for flue gas, compressor work, and the potential for CO_2 capture. The simulations were successful in obtaining desired parameters, providing valuable information for the overall feasibility analysis.

A detailed cost estimation was carried out, considering both CAPEX and OPEX. This analysis was crucial to understand the economic viability of the proposed modifications. The study further investigated the cost per avoided tonne of CO_2, an important aspect considering the emerging carbon capture technologies and the CO_2 tax implications.

The environmental impact and primary energy losses were also analyzed, focusing on the alignment with emission goals and the potential CO_2 emission reduction. This discussion included the prospects of the Longship project for CO_2 storage in the North Sea.

A Hazard Identification (HAZID) study was conducted to address potential safety hazards related to the production and utilization of hydrogen and oxygen in the cement plant. This study identified key hazards and recommended appropriate mitigating actions.

The thesis concluded by identifying areas for future research, including the integration of the kiln in the model, and a more detailed investigation of cooling equipment energy usage and cost.

In summary, this thesis provides a comprehensive investigation into the feasibility of integrating oxyfuel combustion of green hydrogen in a cement plant. The findings offer valuable insights for the cement industry and contribute to the broader conversation on sustainable industrial practices and carbon capture technologies.

Preface

This thesis was undertaken while working full-time, a challenging endeavor that required a considerable amount of dedication and perseverance.

I would like to express my deepest gratitude to my supervisor, Professor Lars-André Tokheim, from the University of South-Eastern Norway. His extensive technical knowledge about the cement production process was instrumental in guiding me through this research. His feedback and constructive criticism were invaluable to the shaping and completion of this thesis.

I am also deeply appreciative of the support provided by Christoffer Moen from the external partner at Norcem and HeidelbergCement Northern Europe. His industry insight and practical advice enriched my understanding of the complex issues surrounding this thesis.

A note to the reader: During the course of this thesis, Norcem underwent a rebranding process and is now known as Heidelberg Materials. Thus, references to Norcem in this document also pertain to Heidelberg Materials.

The journey to complete this thesis has been both challenging and rewarding. It has allowed me to delve deeply into a subject that is not only technically intriguing but also of great significance in terms of sustainable industrial practices and carbon capture technologies.

I hope the readers will find this work informative and inspiring in their own pursuits of knowledge and innovation.

Stavanger, May 2023

Glenn Nedrum

Contents

Nomenclature

<List symbols alphabetically, with explanations and units>

1 Introduction

This chapter provides an overview of the research undertaken in this master's thesis. It outlines the background of the study, presents the task description, and briefly describes the structure of the report. The overall aim of this research is to investigate and propose potential solutions to the identified problem in the context of CO_2 capture in cement industry.

1.1 Background

USN is one of the partners in the research project "Combined calcination and CO_2 capture in cement clinker production by use of CO_2-neutral electrical energy". The acronym ELSE is used as a short name for the project. Phase 1 of the project was completed in April 2019, and Phase 2 was started in April 2020. The goal of the ELSE project is to utilize electricity (instead of carbon-containing fuels) to decarbonate the raw meal in the cement kiln process while at the same time capturing the CO_2 from decarbonation of the calcium carbonate in the calciner.

Different concepts to implement electrification of the calciner have been discussed. One alternative is to use electricity to produce hydrogen and oxygen from water in an electrolysis process, and thereafter burn the hydrogen in oxygen in the calciner. An advantage of this is that the existing calciner may be used, maybe without doing big changes to the geometry etc.

If the hot kiln gas, the tertiary air and the carbon-containing fuels are no longer supplied to the calciner, then N_2 can be eliminated from the calciner exit gas, which will be a mixture of mainly CO_2 and H_2O. After condensation of the H_2O, the product will be more or less pure CO_2 (depending on the excess O_2 in the combustion reaction), which can be stored (or utilized in some way). Some recycling of CO_2 (or CO_2+H_2O) in the calciner may be necessary to control the temperature and the combustion properties.

1.2 Task description

This thesis investigated the following:

- A short overview of the regular calcination process used in modern kiln systems
- A short description of water electrolysis to generate H_2 and O_2
- Describing a process concept that combines electrolysis-generated H_2 and O_2 with calcination based on combustion of H_2 in O_2 (with CO_2 recycling)
- Investigating how combustion properties are affected by mixing H_2 and CO_2 (and possibly H_2O), using solid fuel combustion as a reference
- Assessment if safety aspects related to production, handling and combustion of hydrogen and oxygen in a cement kiln environment
- Mass and energy balance of the system and calculated mass flow rates, temperature, duties, etc.
- Process simulation of model of (part of) the system and simulate different cases, varying key parameters in the system
- Evaluating the main energy losses in the combined system
- Recommendation of a suitable recycling rate for CO_2 (or CO_2+H_2O)

- Creating a process flow diagram with process values for selected cases
- Creating estimates of investment costs (CAPEX) and operational costs (OPEX) of the suggested process, including calculations of cost per avoided CO_2 unit ($/$t_{CO2}$)
- Presenting key results in the form of graphical illustrations
- Discussing the results and making conclusions about the technical and economic feasibility of the concept

1.3 Thesis structure

This master's thesis is structured as follows:

- Chapter 2: Literature Review – A comprehensive review of the existing literature on cement production, CO_2 capture, and water electrolysis.
- Chapter 3: Process Concept and Design – Detailed description and design of the proposed modifications to the existing system at Norcem Brevik, including flue gas treatment, CO_2 capture, and hydrogen production with constructed process flow diagram.
- Chapter 4: Methodology – A description of the research methodology, including the use of Aspen Plus and Aspen Process Economic Analyzer for process simulation and economic analysis.
- Chapter 5: Process Simulation – Presentation of the Aspen Plus model development, verification, and results for different cases of the modified calciner system and alkaline electrolyser.
- Chapter 6: Economic Analysis – A detailed economic analysis of the proposed system modification, including capital investment costs, operational expenses, and cost per avoided tonne of CO_2.
- Chapter 7: Discussion – Analysis and interpretation of the simulation results and economic analysis, comparison with alternative CO_2 capture technologies, and evaluation of energy efficiency and environmental impact.
- Chapter 8: Conclusion – Summary of the findings, implications and contributions, recommendations for future research, and final remarks.

2 Literature Review

This chapter offers a comprehensive review of the existing literature on the modern kiln system in cement production process, CO_2 capture, and water electrolysis, providing a solid foundation for the development of the proposed system modifications.

2.1 Modern kiln system

The system of interest in this master thesis is the modification of the modern cement kiln process. In modern kiln system in the cement industry, there are two combustion zones. The combustion zones are divided by the calciner, where decarbonation happens at around 900℃, and the rotary kiln, where clinker minerals are formed at temperatures of approximately 1400℃ [1].The most common type of modern kiln is the dry process preheater with a calciner upstream the kiln. It consists of a multi-stage cyclone preheater, a calciner, a rotary kiln, and a clinker cooler [2], as shown in figure 2.1.

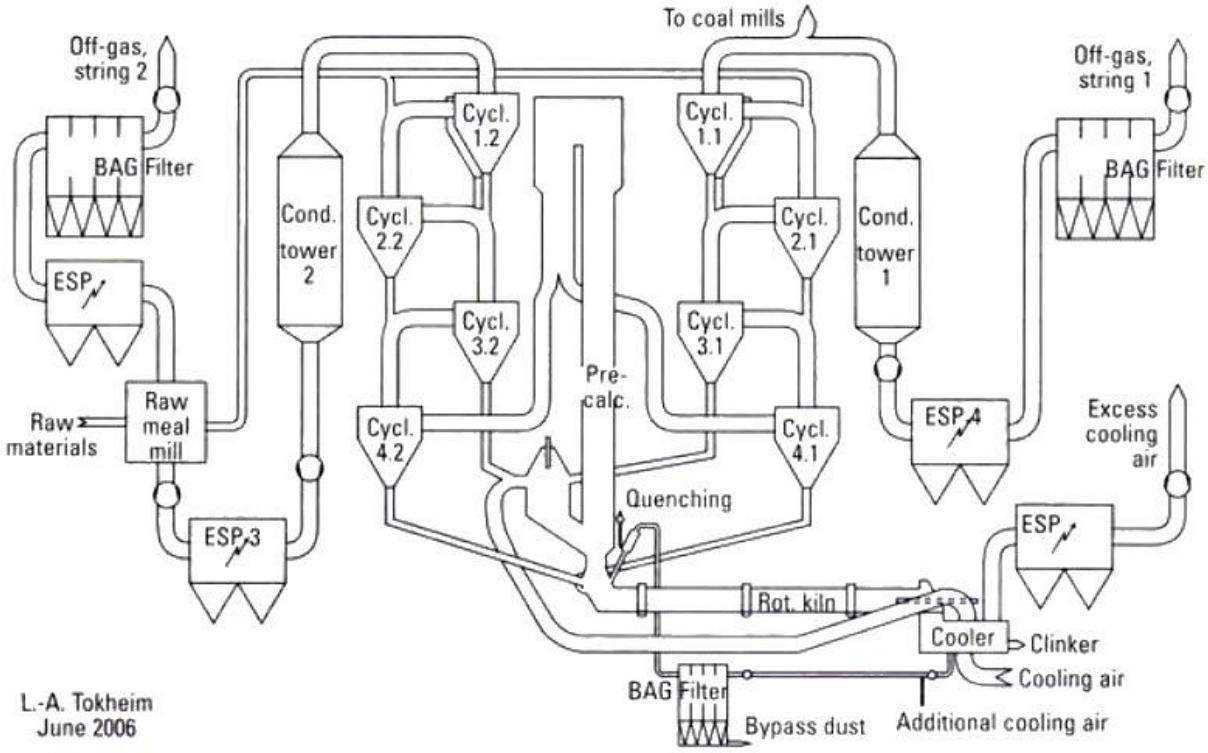

Figure 2.1 Sketch of modern kiln system (Kiln 6 at Norcem Brevik) created by L.-A. Tokheim [2]

This system has two parallel 4-stage preheater cyclones. In the pneumatic conveying regime, particles are conveyed through a pipeline by suspending them in a high-velocity stream of hot gases. This method ensures that the particles are entrained and thoroughly mixed with the hot gases, facilitating effective heat transfer through radiation, convection, and conduction. Modern calciners are designed to operate in this regime, as it allows for efficient fuel combustion and heat utilization. The use of pneumatic conveying in calcination processes ensures that the materials are evenly distributed and heated, resulting in consistent product

quality. Additionally, the pneumatic conveying regime minimizes material buildup and reduces the risk of fouling or clogging in the process equipment, which improves process efficiency and reduces maintenance costs. Overall, the pneumatic conveying regime is a highly effective and widely used method in modern calciners for achieving efficient heat transfer and ensuring optimal process performance [3]. Meal is here heated up towards 650℃ before it enters the calciner. This is here the calcination reaction occurs:

$$CaCO_3 \rightarrow CO_2 + CaO$$

Approximately 95% of this reaction occurs at this stage. It is crucial not to exceed this calcination percentage prior to the rotary kiln, as the thermal energy required for the reaction is significantly higher than heating the products above the desired 900℃. As a result, it becomes challenging to regulate the temperature within the kiln.

Next, the pre-calcined meal is introduced into the rotary kiln, where it undergoes complete calcination and clinker is produced. This process typically occurs at an operating temperature of 1400°C. To achieve the desired temperature of the clinker for further processing, a cooler is utilized [2].

A modern kiln system designed to minimize heat loss, reduce fuel consumption, allow for alternative fuel combustion, lower CO_2 emissions, and improve overall productivity. The system is a highly energy-efficient and more environmentally friendly system used for clinker production.

2.1.1 Challenges and future research directions

Despite the advances made in modern kiln systems with calciners, there remain several challenges and opportunities for future research and development. Some key areas of interest include:

1. Further optimization of energy consumption and heat recovery: Continuous improvement in the design and operation of kiln systems can lead to additional energy savings and emission reductions. Investigating novel heat recovery techniques and optimizing heat exchanger designs are potential areas for future research [4].
2. Integration of CO_2 capture technologies: The cement industry is under increasing pressure to reduce its carbon footprint. Integrating CO_2 capture technologies into existing and future kiln systems can help the industry meet its emission reduction targets. Research into cost-effective and energy-efficient CO_2 capture methods tailored for the cement industry is essential [5].
3. Utilization of alternative fuels and raw materials: The use of alternative fuels and raw materials can further reduce the environmental impact of cement production. However, challenges related to the quality and availability of these materials, as well as potential impacts on product quality, need to be addressed through further research and development [4].
4. Development of novel calcination technologies: Investigating innovative calcination methods, such as the use of renewable energy sources or advanced materials, can lead to the development of more sustainable and efficient calcination processes in the future [6].

By addressing these challenges and exploring new research directions, the cement industry can continue to improve its energy efficiency, reduce CO_2 emissions, and enhance the sustainability of its operations.

2.2 Carbon capture and storage

The International Energy Agency (IEA) latest report from 2021, *Net Zero by 2050*, calls for a substantial reduction in CO_2 emissions from the cement sector by 2050, with carbon capture and storage (CCS) playing a key role in achieving this goal [7]. According to the report, CCS deployment should be expanded significantly in the cement sector to help reduce emissions. By 2030, around 370 million tonnes of CO_2 should be captured from cement production, rising to around 1.5 gigatonnes by 2050. This would represent a major increase in CCS deployment, as only a small fraction of CO_2 emissions from cement production are currently being captured and stored. The report emphasizes the need for a combination of measures to achieve the necessary emission reductions, including increased energy efficiency, a shift towards low-carbon fuels, greater use of alternative cementitious materials, and the deployment of innovative low-carbon cement production technologies. CCS, as a key component of the overall strategy, will help the cement sector reach net-zero emissions by 2050. According to the 2018 report, achieving the 2°C scenario goal by 2050 would require CCS to account for 48% of the emission reduction in the cement sector [8].

2.2.1 CO_2 emission from cement production

Today, the only option to decarbonize some of the most important industrial sectors in the world, such as cement production, is through CCS (carbon capture and storage). This is significant since the cement industry is responsible for about 8% of the global CO_2 emissions [5]. 2/3 of this emission comes from one of the key reactions occurring in the calcination process:

$$CaCO_3 \rightarrow CO_2 + CaO,$$

where the rest of the emission comes from combustion of fuels [1]. Due to the significant thermal energy requirements and the calcination product, a medium-sized cement plant can emit approximately 1 million tonnes of CO_2 each year. With thousands of cement plants situated worldwide and the demand for production on the rise, the necessity to reduce CO_2 emissions becomes increasingly crucial.

Norcem has been proactive in adopting sustainable practices in its operations, particularly in the area of fuel consumption. Traditionally, coal has been the dominant fuel source in the cement industry due to its abundance, low cost, and high energy density. However, recognizing the environmental consequences of coal combustion, Norcem has been working diligently since the mid-eighties to increase the use of alternative fuels in its production processes [2]. These alternative fuels include animal meal, liquid hazardous waste, refuse derived fuels, and solid hazardous waste. Norcem steadily increased the use of alternative fuels to 35% of the thermal energy needed in the kiln. However, limitations to temperature and environmental limitation stopped them from increasing further. In 2004 a modification to allow for more utilization of alternative fuels, including modification of waste feeding system, and installation of chlorine bypass system was implemented. Further improvement was conducted in 2006 to enlarge the kiln hood to reduce the dust circulation between the

cooler and the kiln, allowing for increased production. These modifications have allowed for operation of 60% alternative fuels. By diversifying its fuel portfolio, Norcem has managed to significantly reduce its CO_2 emissions and environmental footprint, while continuing to meet the increasing demands for cement in a sustainable manner. This transition serves as a model for other cement producers to follow in their quest to mitigate the environmental impact of their operations.

In the not-so-distant future, when renewable energy sources largely replace conventional fuels, crucial industrial production processes, such as cement clinker manufacturing, will predominantly rely on electricity or hydrogen produced from electricity rather than CO2-emitting combustion processes. This is where the ELSE (abbreviation for "ELektrifisering av SEmentproduksjonen") project comes in.

The Norcem Brevik facility is mainland Norways third largest source of CO_2 emission and has a yearly emission of 750 000 tonne CO_2 [9]. The ELSE project is a project that aims to electrify the cement production process and capture CO_2 emission from the Norcem Brevik plant or other cement plants. The project involves five partners; USN, IFE, SINTEF Industry; Kanthal and Norcem. The objective includes specifying a feasible concept and verifying concept through experiments. The project seeks to determine the technical and economic feasibility of cement production with the reduction and possible capture of CO_2 emission by use of renewable electrical energy.

2.2.2 Oxy-fuel combustion carbon capture

Oxy-fuel combustion is an innovative method of burning fuels that involves the use of oxygen and recycled flue gas for the combustion process, as seen in figure 2.2. The key differences between oxy-fuel combustion with coal and conventional combustion with coal are found in the heat transfer, coal reactivity, and emissions [10]. In conventional coal-fired combustion, air is used for the combustion process, and the nitrogen present in the air dilutes the concentration of CO_2 in the flue gas. However, during oxy-fuel combustion, a combination of oxygen and recycled flue gas is used for fuel combustion, which results in a gas mixture consisting mainly of CO_2 and water with a high concentration of CO_2 that is ready for sequestration.

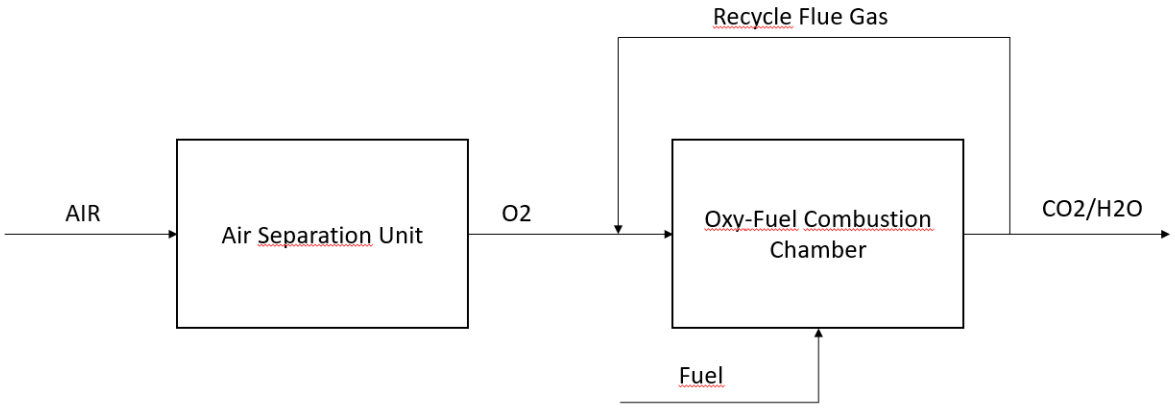

Figure 2.2 Oxy-Fuel CO_2 capture

The recycled flue gas also plays an important role in oxy-fuel combustion by controlling the flame temperature and making up for the missing nitrogen, which is essential to ensure that there is enough gas to carry the heat through the boiler. Overall, oxy-fuel combustion offers several benefits, including reduced emissions and improved efficiency, making it a promising technology for cleaner and more sustainable energy production [10]. However, the oxy-fuel capture technology comes with an energy penalty due to the need to produce high purity oxygen in an Air Separation Unit.

In cement production, the implementation of oxy-fuel technology requires adaptations to the combustion equipment and recycling of flue gas as the oxidizer composition has a significant impact on the flame characteristics in the rotary kiln, affecting numerous combustion properties such as the flame temperature [8]. It is crucial to maintain the same heat transfer to the clinker to ensure product quality and process efficiency.

Research conducted by the European Cement Research Academy investigated the impact of oxy-fuel combustion on clinker composition and properties, concluding that there were no major differences in its composition, structure, and properties [8]. It was found that good-quality cement could be successfully produced in an oxy-fuel atmosphere, with similar phase and chemical compositions, and comparable compressive strength to commercially available cements.

Implementing oxy-fuel technology in a cement plant also requires optimizing the entire process for energy efficiency, as the volumes and composition of gases flowing through the system differ from conventional cement production process. One constraint is the high energy cost of oxygen separation, necessitating its supply in as near stoichiometric quantities as possible, complicating combustion completeness [8]. Significant research has been conducted on oxy-fuel combustion of coal in the past decade, motivated by CO_2 capture from coal-fired power generation, given increased understanding of the process [8].

In 2018, the European Cement Research Academy (ECRA) announced the implementation of oxy-fuel capture technology in two cement plants in Europe, located in Colleferro (Italy) and Retznei (Austria) [11].

Barker et al. stated in their study that using oxy-combustion only in the calciner could reduce approximately 61% of the CO_2 emissions resulting from traditional cement production [12]. However, implementing oxy-combustion in both the calciner and the kiln could potentially result in nearly 100% avoidance of CO_2 emissions, although significant technical uncertainties remain with this approach.

One of the major drawbacks of oxy-combustion technology is the sharp increase in power consumption compared to the traditional process. This increase is primarily due to oxygen production and CO_2 cooling, compression and purification. Moreover, when factoring in the CO_2 emissions from fossil fuel power generation, the overall reduction in CO_2 emissions attributable to oxy-combustion, for the calciner, decreases from 61% to 52 [12]. However, this is not an issue for power from electricity with renewable energy sources like 99% of the electricity in Norway. Although oxy-fuel technology is being tested in existing plants, further research is necessary to determine its feasibility as a practical option for the cement industry [4].

2.2.3 Post-combustion carbon capture

Post-combustion carbon capture is a technology that focuses on capturing carbon dioxide from flue gas generated from fossil fuel combustion, such as coal, natural gas, or oil. Since the 1960s, when the most widely used technology (amine scrubbing) was being utilized to separate capture CO_2 at American oil fields and compressed back into the reservoirs for enhanced oil recovery, this technology has been studied and developed and is considered the most mature carbon capture technology [13]. The technology is almost the same being used today. Since 1996, the Sleipner field has captured 23 million tonne CO_2.

Post-combustion typically employs chemical absorption techniques, where the flue gas is passed through a solvent, often an amine-based solution, which binds to the CO_2. The CO_2-rich solvent is then heated to release the captured CO_2, which can be captured.

The technology has a high capital investment, which makes it a challenge for industries to implement. The process is also incredibly energy demanding. The efficiency of post-combustion carbon capture can be limited when the CO_2 content in the gas is low, as this reduces the amount of CO_2 that can be captured and increases the energy demand for the capture process.

Despite these challenges, the benefits of reducing greenhouse gas emissions make post-combustion carbon capture one of the important technologies for mitigating the impacts of climate change.

Post-combustion technologies are considered end-of-pipe solutions that do not require fundamental modifications to the clinker-burning process. As a result, they are suitable for both new kilns and retrofitting of existing ones [4]. Currently, this technology is being installed at Norcem Brevik to capture around half of the CO_2 emission from the cement plant.

2.2.4 Pre-combustion carbon capture

Pre-combustion is a process that involves partially combusting the fuel and introducing hot steam to produce a mixture of carbon dioxide, carbon monoxide (CO), and hydrogen, like the process of syngas production. The resulting gas mixture is then separated, and the hydrogen is extracted from the carbon dioxide using physical or chemical methods. The hydrogen is then used as fuel, ultimately producing water as a combustion product [14]. However, this only removes the CO_2 emission from the fuel and not emission from the calcination process. To remove the CO_2 product from calcination, there must be implemented further post-combustion or oxy-fuel combustion. Therefore, this carbon capture technologies are not suitable for the cement industry. Instead, it is more appropriate to explore CO_2 capture technologies that are specifically designed for the cement production process [4].

2.2.5 Longship project

Norcem Brevik is today building a post-combustion carbon capture plant which will be a part of the Longship project. The plant will capture around half of the CO_2 emissions [15]. Norcem has ambition about zero carbon emission by 2030 [16].

Longship was launched on September 21, 2020. Longship is the Norwegian government's investment in CO_2 management and is a full-scale CO_2 management project that will demonstrate the capture of CO_2 from industrial sources, transport and safe storage of CO_2. Norway has excellent prospects to develop CCS due to the storage capacity inside the geological layers on the Norwegian continental shelf [5].
At the Hafslund Oslo Celsio waste incineration facility and the cement plant Norcem Brevik, CO_2 will be extracted, liquefied, and transported via ship. After that, it will be moved to an terminal northwest of Bergen, where it will be pumped through pipes into the north sea and securely kept 2,600 meters below the seabed. The terminal can initially hold 1.5 million tonnes of CO_2 annually, while the pipeline to the reservoir is built to hold 5 million tonnes. Northern Lights, which oversees the transportation and storage at Longship, plans to increase its capacity to 5 million tonnes annually through a number of expansion stages and expand its clientele [17].

2.3 Water electrolysis

In recent years, the hydrogen economy and water electrolysis have emerged as prominent topics in the discourse on net-zero emissions pathways. This discussion is primarily driven by the adoption of hydrogen-specific strategies by over 30 countries and a concerted effort by the European Union to augment electrolyser capacity from the current 0.1 GW to 40 GW by 2030 [18]. The International Energy Agency (IEA) projects that the global electrolyser capacity will witness an exponential growth from 0.2 GW today to 33,000 GW by 2070 [18]. This review aims to explore various electrolyser technologies and their operational principles.

Water electrolysis, a critical process in hydrogen production, involves splitting water molecules into hydrogen and oxygen using electricity. This overall reaction is endothermic ($\Delta H > 0$) and nonspontaneous ($\Delta G > 0$), thus necessitating energy input to sustain the reaction [18]. The electrolysis process requires both electric and thermal energy input.

In an adiabatic system where all the energy needed for the electrochemical process is provided by electricity, the minimum voltage required to execute water electrolysis is the thermoneutral cell voltage. The potential of the cell surpassing the thermoneutral voltage implies that no external heat is required for conducting the electrochemical reaction. Contrarily, heat is generated in the process, directly proportional to the difference between the cell voltage and the thermoneutral voltage as seen below [18].

$$E_{el} = (V_{cell} + V_{tn}) * I$$

This generated heat can be quantified through the excess heat voltage from the cell voltage and contributes to a rise in the temperature of the electrolyte flow and the gases produced in the stack. It is crucial to continuously remove this excess heat to ensure a constant operating temperature.

2.4 Proton-exchange membrane electrolyser

Proton-exchange membrane (PEM) electrolysis was first developed in 1966 by General Electric Co., drawing on technology from fuel cells produced for the US space programme [18]. Initially, PEM-electrolysers were primarily used for oxygen production in anaerobic

systems, such as spacecrafts and underwater applications. However, recent years have seen growing interest in PEM for hydrogen production and clean energy systems.

Water splitting in PEM occurs in the cell's central component, the membrane-electrode-assembly (MEA). The MEA comprises a thin (90 - 200 µm) catalyst-coated membrane that separates the anode from the cathode. This porous material allows H+ protons to pass from the anode to the cathode.

The catalysts are typically platinum for the cathode, and iridium or ruthenium for the anode. These catalysts, in finely particulated form to maximize surface area for reactions, are coated either directly on the membrane or onto porous transport layers that facilitate the flow of current and produced gases. The bipolar plates, which also serve as circulators for water and product gases, construct the anode and cathode. Oxygen and hydrogen gases are collected from the backs of the porous transport layers to gas manifolds. Water circulation serves not only as a feedstock for the reactions but also aids in removing excess heat produced during operation [18].

Table: 2.1 CAPEX stack cost PEM [19]

Electrolyser	Moduler [MW]	CAPEX 2017 [€/kW]	CAPEX 2025 [€/kW]
PEM	20	1200	700

Despite their efficiency, PEM electrolysers are currently costlier than alkaline electrolysers. Table 2.1 shows the CAPEX stack cost for 2017 and an assumed CAPEX stack cost for 2025 with maturity of technology. This high cost is primarily due to the valuable noble metals used for the membrane catalyst, particularly platinum, which has a high and fluctuating price, making future cost predictions challenging [18].

2.4.1 Alkaline electrolyser

Alkaline water electrolysis (AWE) is a well-established technology for the electrochemical splitting of water. The electrolysis cell in AWE consists of a positive anode, a negative cathode, an alkaline solution, and a diaphragm or membrane that facilitates the passage of hydroxide ions (OH-) [18]. The electrolyte is typically a 25 - 30% aqueous solution of potassium hydroxide (KOH) or sodium hydroxide (NaOH). KOH is usually preferred due to its superior ionic conductivity and lower CO2 solubility, which mitigates the risk of carbonate formation and subsequent decrease in conductivity.

Additives are often used to enhance the ionic activity of the electrolyte and to reduce its aggressiveness. The anode and cathode are typically nickel-coated iron or other Ni-based alloys with porous or mesh-structures, designed to maximize the surface area for reactions. The alkaline environment eliminates the need for expensive acid-resistant cell materials [18].

One limitation of AWE is that the diaphragm separating the electrodes is not entirely gas-tight, leading to some diffusion of oxygen and hydrogen from one side to another.

Table: 2.2 CAPEX stack cost AEL [19]

Electrolyser	Moduler [MW]	CAPEX 2017 [€/kW]	CAPEX 2025 [€/kW]

Alkaline	20	750	480

Despite this, AWE remains the most economical option among the electrolyser types, boasting relatively high electric efficiency. Table 2.2 shows the CAPEX stack cost for 2017 and an assumed CAPEX stack cost for 2025 with maturity of technology [18].

2.5 Process economics

There are multiple factors affecting the feasibility of expanding a process plant, such as energy design optimalization, maturity of technology, electrical prices, etc.

2.5.1 Fixed capital investment

Fixed capital investment refers to the total cost associated with designing, constructing, and installing a plant, including the required site modifications. It consists of four main components: Inside Battery Limits (ISBL) investment, which represents the cost of the plant itself; Offsite (OSBL) investment, which includes the cost of site infrastructure modifications; engineering and construction costs; and contingency charges.

The accuracy of a cost estimate is dependent on the level of design detail available, the accuracy of the cost data, and the time spent preparing the estimate. Early in a project, only an approximate estimate is justified due to the limited information available.

2.5.2 Classification of capital cost estimates

The Association for the Advancement of Cost Estimating International (AACE International) classifies capital cost estimates into five types according to their accuracy and purpose [20]. The two types pertinent to the early stages of a project are the Order of Magnitude estimates, which have an accuracy of ±30–50%, and Preliminary estimates, which have an accuracy of ±30%. Both are used to make coarse choices between design alternatives and are based on limited cost data and design detail.

2.5.3 Shortcut methods for capital cost estimates

Several shortcut methods have been developed for making quick (Class 5) capital cost estimates without completing a detailed plant design. These methods allow for estimates of total plant cost to be made within ±50% accuracy for preliminary studies and can also provide a rough check on more detailed estimates developed later in the process.

2.5.4 Sources of purchased equipment costs

The best source for purchased equipment costs is recent data on actual prices paid for similar equipment. Engineers working for Engineering, Procurement, and Construction (EPC) companies often have access to large amounts of high-quality data. However, design

engineers outside the EPC sector must rely on cost data from the open literature or use cost estimating software, such as the suite of tools licensed by Aspen Technology Inc.

2.5.5 Aspen Process Economic Analyzer

Aspen Technology's Aspen ICARUS™ Technology is a cost estimating program that estimates equipment costs, bulk costs, and installation costs from the costs of materials and labor. The models in ICARUS™ are developed by a team of cost engineers and are updated annually. The Aspen Process Economic Analyzer software, which uses Aspen ICARUS™ Technology, can provide reasonably good estimates when used properly.

2.5.6 Equipment costs

For design engineers who lack access to reliable cost data or estimating software, the correlations given in table 2.1 can be used for preliminary estimates. These correlations are only valid between the lower and upper values of S indicated, with prices for carbon steel equipment except are noted in the table 7.1 in the Chemical Engineering Design book [20]. Extrapolation to other materials, year, and currency can then be performed before implementing in used CAPEX or OPEX estimation technique.

2.5.7 Cost per avoided CO_2 unit

The study by Barker et al. in 2009 assessed the costs of implementing post-combustion and oxy-fuel technologies in new cement plants [12]. According to their findings, oxy-fuel technology was estimated to cost \$56/t CO_2 avoided for a 1 Mt/yr cement plant in Europe and \$32.2/t for a 3 Mt/yr plant in Asia. On the other hand, post-combustion capture was estimated to cost \$149.8/t CO_2 for a 1 Mt/yr European cement plant and \$82.6/t for a 3 Mt/yr Asian plant. These costs were significantly higher than those of oxy-fuel technology due to lower economies of scale and additional requirements, such as flue-gas desulphurization, NOx reduction, and steam generating plant installation.

However, it should be noted that the technology has advanced since 2009. An article from 2019 showed the cost per avoided CO_2 with post-combustion CO_2 capture to be \$71.71/t for standard post-capture and \$42.81/t for advanced post-combustion with waste heat utilization, indicating a decrease in cost [1]. Additionally, an electrically heated calciner was studied, and the cost per avoided tonne CO_2 was estimated to be \$80.27/t, showing promising results for the use of this technology in the cement industry.

3 Process Concept and Design

This chapter presents the existing Norcem Brevik, and the detailed description and design of the proposed modifications to the existing process, focusing on oxy-fuel combustion with hydrogen, flue gas treatment with CO_2 capture, and H_2/O_2 production with electrolysis, as well as the optimization of heat exchange within the system. This chapter also presents the modified process flow diagram.

3.1 Norcem Brevik system description

This subchapter provides a description of the cement production process at Norcem Brevik, including the transportation and processing of raw meal, preheating in cyclones, calcination in the calciner, clinker production in the kiln, cooling of the clinker, flue gas from the kiln and calciner. The simplification of the process can be seen in the block diagram in figure 3.1.

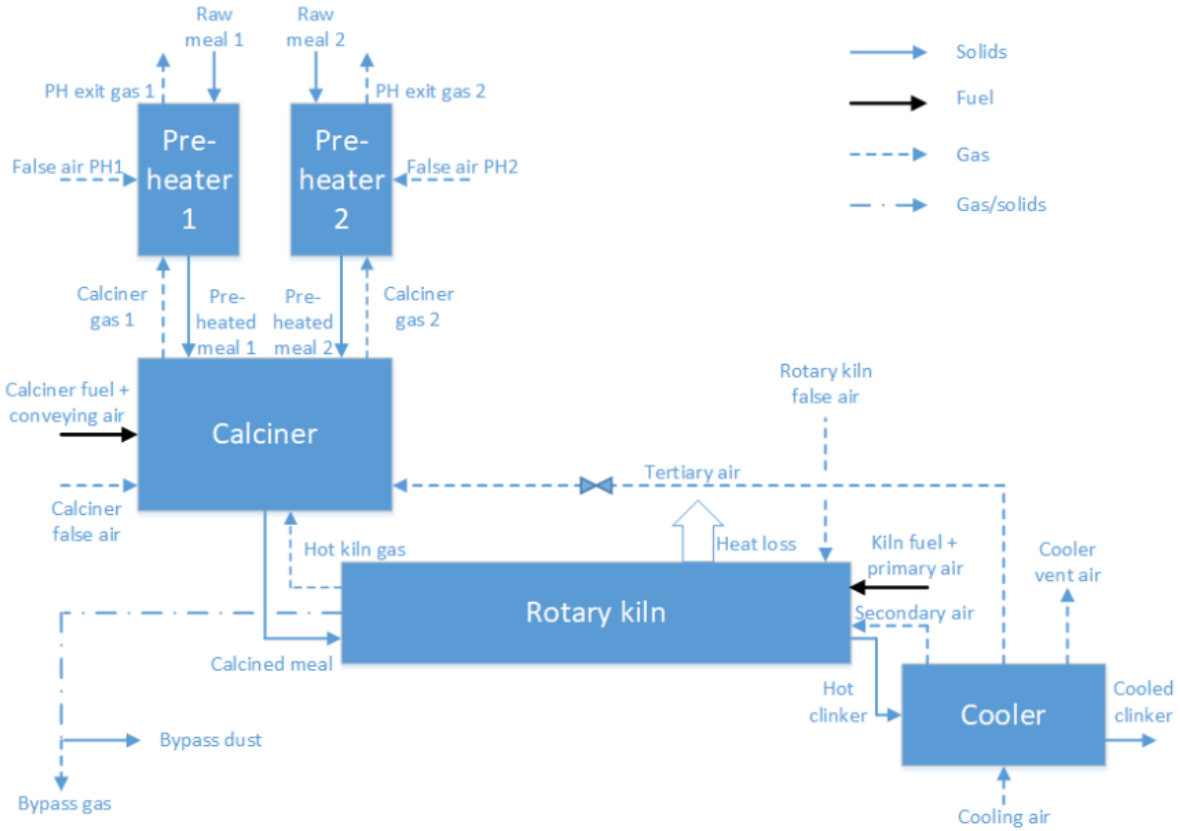

Figure 3.1: Cement kiln process with preheater and calciner [21]

3.1.1 Raw meal transportation and preparation

The cement production process begins with the extraction and preparation of raw materials, which typically consist of limestone, quartz, and other additives. These raw materials are crushed, grounded, and blended in proper proportions to form a homogenized raw meal, which is then transported to the preheating stage. The transportation of raw meal can be

achieved through various means, such as conveyor belts, bucket elevators, or pneumatic transport systems.

3.1.2 Cyclone preheaters

Before entering the calcination stage, the raw meal undergoes a preheating process using a series of cyclone preheaters. These preheaters are designed to utilize the hot exhaust gases from the kiln and calciner to heat up the raw meal, increasing its temperature and reducing the energy required for calcination. As the raw meal moves through the preheater stages, it undergoes some minor chemical and physical changes that prepare it for the calcination process. The meal exits the preheaters at around 650 °C.

3.1.3 Calciner

In modern cement production processes, as explored in the literature review, calcination typically occurs in a separate calciner vessel, which is connected to the rotary kiln. The calciner is responsible for the partial calcination of the raw meal, during which the calcium carbonate ($CaCO_3$) in the meal is converted into calcium oxide (CaO) and carbon dioxide (CO_2). This process occurs at temperatures of approx. 900°C and accounts for close to 94% of the total calcination in the cement production process.

3.1.4 Kiln

Following calcination, the partially calcined meal enters the rotary kiln, where the remaining calcination takes place, and clinkers are formed at temperatures at 1450°C. The rotary kiln is a long, cylindrical vessel that rotates around its axis to facilitate the transport and mixing of the raw meal. The hot clinker produced in the kiln is discharged into a clinker cooler for further processing.

3.1.5 Clinker cooler

The clinker cooler plays a crucial role in the cement production process by cooling the hot clinker from the kiln to a temperature suitable for further processing and storage. The cooling process also recovers heat from the clinker. This heated air is used as secondary air to combust fuel in the kiln and as tertiary air to combust fuel in the calciner, improving the combustion efficiency. The cooled clinker is then transported to a storage facility and then to the grinding and blending stage.

3.1.6 Flue gas

Flue gases generated from the kiln and calciner contain various pollutants, including particulate matter, nitrogen oxides (NOx), sulfur oxides (SOx), and CO_2. These gases must be treated before being released into the atmosphere to comply with environmental regulations. The flue gas treatment system includes electrostatic precipitators and bag filters to remove particulate matter as seen in figure 2.1, and selective non-catalytic reduction system to reduce NOx emissions, and a gas suspension adsorber to reduce SO_x emissions.

3.1.7 Clinker processing and cement production

The cooled clinker is grounded together with gypsum and other additives to produce the final cement product. This grinding process is accomplished using grinding equipment. The gypsum acts as a set regulator, controlling the hydration reactions in the cement and preventing rapid setting. Other additives may be included to produce specific cement types or to enhance specific properties of the cement, such as strength or workability.

3.1.8 Cement storage and transport

Once the final cement product is produced, it is stored in silos before being dispatched to customers. The cement is transported in bulk, using ships and specialized trucks.

In summary, the cement production process encompasses several key stages, including the transportation and preparation of raw meal, preheating in cyclones, calcination in the calciner, clinker production in the kiln, cooling of the clinker, flue gas treatment, and the processing and storage of the final cement product. Each stage plays a critical role in the overall efficiency and environmental performance of the cement production process, and modern advancements in technology and process optimization continue to improve the sustainability of cement manufacturing.

This thesis will focus on the calciner.

3.2 Modification concept

3.2.1 Introduction to the modified concept

The calciner is the most energy-intensive equipment and the largest contributor of CO_2 in the cement production process. To decrease the CO_2 emission, modifying only the calciner with hydrogen driven oxy-fuel combustion is an alternative.

The modified calciner oxyfuel combustion with hydrogen concept provides a promising solution to achieving significant CO_2 emission reductions. Distinct from the conventional oxyfuel combustion, which relies on the combustion of fossil fuels in an oxygen environment, the modified concept proposes the usage of hydrogen as fuel to eliminate CO_2 from combustion. The combustion of hydrogen generates water as seen in equation:

$$H_2 + O_2 \rightarrow H_2O,$$

fundamentally reducing the CO_2 emissions associated with traditional cement production processes. The calcination reaction process generates pure CO_2. The result is a flue gas composed of CO_2 and H_2O from the calciner that can be easily separated, and CO_2 can be captured for storage. By modifying the calciner, it is possible to potentially reduce at least 70% of the CO_2 emissions from clinker production [22].

This approach aims to adopt the existing plant process parameters, ensuring a smooth transition from the conventional modern kiln method to the modified concept. It represents a transformative shift in cement manufacturing, with a strong emphasis on environmental sustainability, energy efficiency, and emission reduction.

3.2.2 Modified concept overview

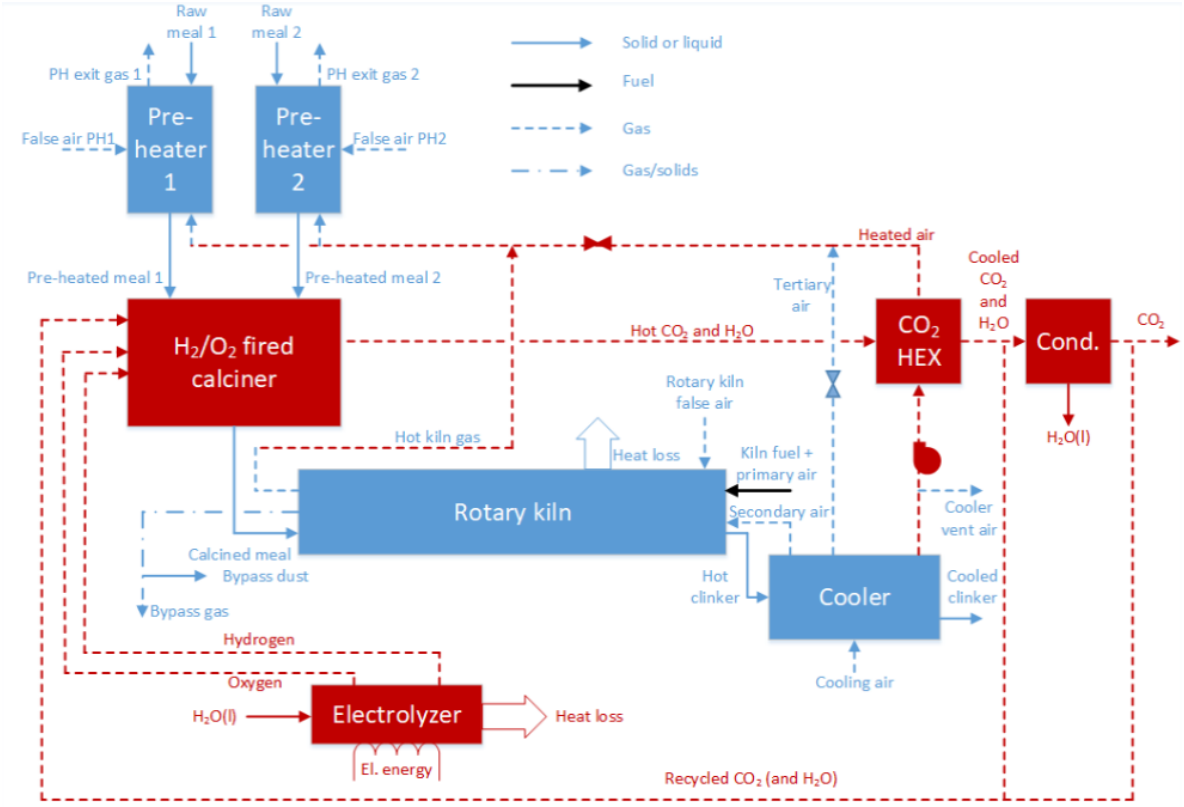

Figure 3.2: Modified cement kiln process with hydrogen oxyfuel combustion [21]

Figure 3.2 shows the block diagram of the proposed modified oxyfuel combustion process and can be broken down into a series of critical steps.

3.2.2.1 Calciner modification with flue gas treatment and flue gas recycle

The calciner is modified to facilitate the combustion of hydrogen in an oxygen-rich environment. This process creates a flue gas primarily composed of water vapor and CO_2. The flue gas is then treated before capturing the CO_2. Some of the flue gas is recycled back, with a compressor, into the calciner to reduce the adiabatic flame temperature.

3.2.2.2 Production of H_2 and O_2

Hydrogen and oxygen are produced through the electrolysis of water, powered by renewable energy sources. The water electrolysis technology selected was the alkaline electrolyser, considering its cost-effectiveness. While the proton exchange membrane (PEM) technology was also evaluated as a potential alternative due to its high efficiency, its initial investment cost would have been significantly higher in this industrial size application. Despite the anticipated decrease in the cost of PEM technology, there are concerns about its long-term viability due to the utilization of noble metals. These uncertainties arise from the potential fluctuations in the availability and affordability of these metals in the future.

The alkaline electrolyser is specifically based on NEL Hydrogen's A3880 model and sized up to H_2 production need, which the model allows for with multiple parallel units. The electrolyser is modified to high cell pressure (6.7 bar) to avoid the need for gas compressors.

Water with KOH, electrolyte, is introduced to the cell where a percentage of the water is converted to hydrogen and oxygen. At the cathode exit, hydrogen gas and water exit. Simultaneously, oxygen gas and water leave at the anode exit. The distinct gases are separated from the electrolyte water in their respective knockout drums. Here, the gases are stripped of entrained water droplets, and separated water is recycled back to the electrolytic cell.

The recycled electrolyte water is cooled on the way back to the electrolyser cell by a heat exchanger. This step is critical to controlling the temperature and production efficiency within the electrolyser cell for efficient operation. Additional water is also supplied to one of the knockout drums to compensate for the water consumed during electrolysis.

The distinct hydrogen and oxygen gases from the knockout drums are then further cooled, leading to more water condensation in a subsequent knockout drum. This step also acts as a buffer tank, short-term storage, for the gases and aids in maintaining a steady supply to the calciner. The condensed water from this stage is returned to the initial knockout drums, ensuring optimal water utilization in the system, and reducing the cooling need before reentering the cell. The gases are then dried in separate dryers to remove any residual moisture, ensuring they are in the optimal state for combustion in the calciner.

3.2.2.3 Heat exchange between air from clinker cooler and hot flue gas

The residual heat from the hot flue gas is harnessed and transferred to ~~the cooler air from~~ the clinker cooler. This energy recovery step boosts the overall process efficiency, reducing the energy demand of the cement manufacturing process.

3.2.2.4 Separation of CO_2 and water in flue gas

Following heat recovery, the flue gas undergoes a separation process where water vapor is condensed, and CO_2 is captured. This step results in a CO_2 stream that goes through a dryer, separated and concentrated, ready for further processing. The battery limit, the boundary where the research of this thesis ends, is established upstream the compressing of the captured CO_2 for transport. The more detailed modification can be seen in the created process flow diagram in figure 3.3.

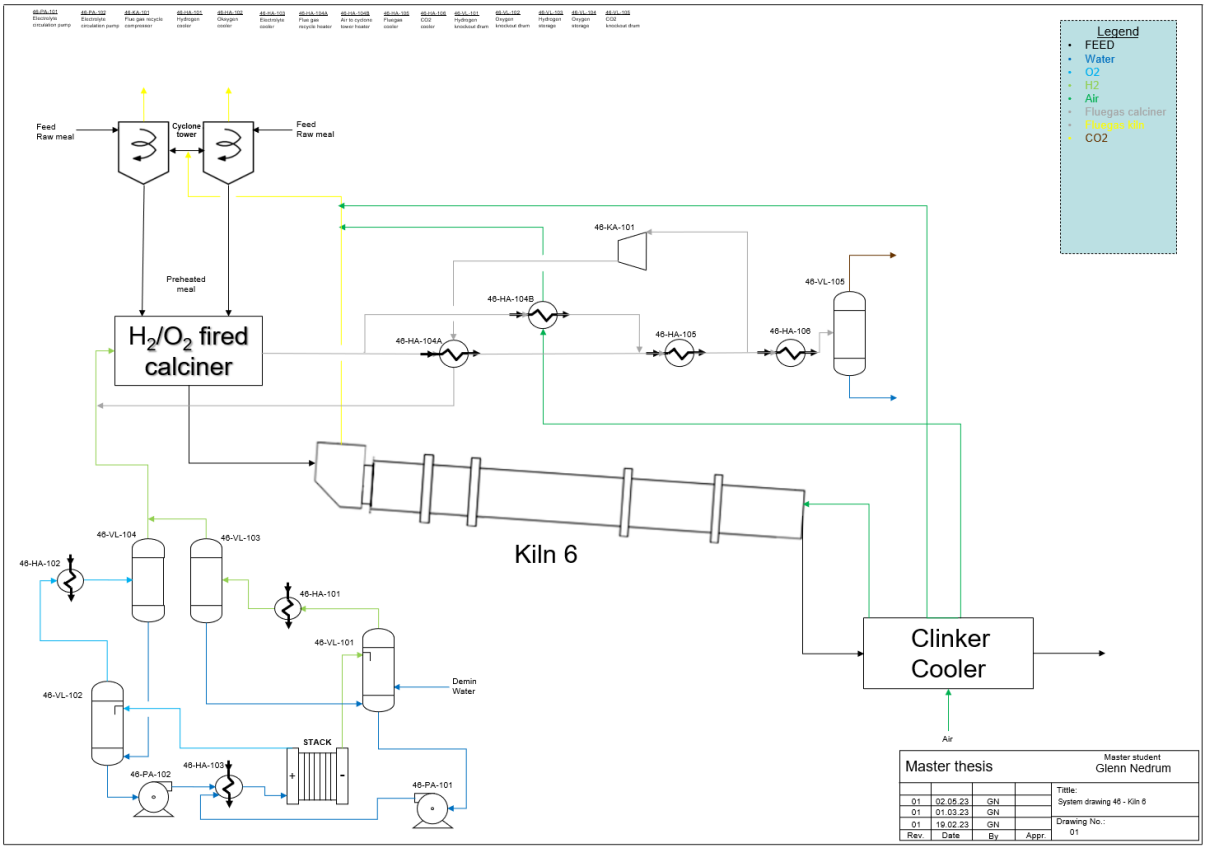

Figure 3.3: Modified Concept - Process Flow Diagram

In this modified process, the flue gas will no longer be utilized to preheat the raw meal in the cyclone preheaters as seen in figure 3.1. Instead, the air used to cool the clinker, which was previously used as the oxidizing agent for the fuel in the calciner, will now heat exchange with the flue gas in a heat exchanger. This heated air will then be directed to the preheater cyclones to preheat the raw meal before it enters the calciner. Furthermore, the flue gas from the kiln, which in a conventional modern process would travel to the calciner, will now bypass the calciner before going to the cyclone preheaters. This change ensures the preheating of the raw meal before it enters the calciner, optimizing the overall energy efficiency of the process.

3.2.3 Benefits and challenges of the modified concept

The transition to the modified presents numerous advantages. Most significantly, it offers a substantial reduction in CO_2 emissions, capture of an immense amount of CO_2, and a cost avoidance of buying coal for fuel. Furthermore, the incorporation of hydrogen combustion opens the possibility for the cement industry to utilize renewable energy sources, contributing to a more sustainable and environmentally friendly future. While the modified oxyfuel combustion concept presents transformative potential for the cement industry, it is not without challenges that need to be addressed.

One of the significant challenges is maintaining the control of the adiabatic flame temperature in the calciner. The selection of the gas recycling temperature, flow rate and/or composition will all have an impact on the system's mass and energy balance. This implies

that there is a possibility to optimize for a recycling mixture of CO_2 and water or CO_2 only. The combustion of hydrogen with oxygen results in a higher adiabatic flame temperature compared to coal fuel, which could lead to equipment damage if not adequately managed. To ensure the sustainability of the process, effective flue gas recycling and temperature control strategies must be implemented. The recycling rate and temperature of the recycled flue gas directly affects the flame temperature, cooling need of flue gas, and consequently the overall system energy efficiency. Therefore, striking an optimal balance between these parameters is essential for the successful implementation of this concept.

Moreover, the cooling requirement of the flue gas presents a complex energy optimization problem. The flue gas needs to be cooled before it undergoes water condensation and CO_2 capture. However, excessive cooling could lead to energy inefficiencies, while inadequate cooling could hamper the CO_2 capture process. Therefore, a careful analysis of the cooling requirements and optimal strategies is necessary.

Alkaline electrolysis is a mature technology and is currently the most cost-effective choice for large-scale hydrogen production. However, the design and operation of the electrolyser come with their own challenges. The reaction rate of water to hydrogen and oxygen in the electrolyser is a critical parameter, affecting the efficiency of hydrogen production. Furthermore, the recycling rate of the electrolyte is crucial for controlling the temperature within the electrolyser cell that could lead to overheating if not properly managed.

These challenges and uncertainties underline the need for comprehensive research and investigation, which this thesis aims to undertake. The goal is to understand the intricacies of the modified concept, optimize the process parameters for energy efficiency, and devise effective solutions to overcome the associated challenges. Furthermore, it’s critical to investigate the cost of the proposed concept. This work aims to contribute to the ongoing efforts to transform the cement industry towards a more sustainable and environmentally friendly future with renewable energy sources.

4 Methodology

This chapter outlines the research methodology used in this study, including research method, application of Aspen Plus and Aspen Process Economic Analyzer for process simulation and economic analysis, as well as the application of HAZID for safety considerations. The chapter also includes derivation of mass and energy balance equations.

4.1 Research design, literature survey and data collection

This thesis's research approach adopts a methodical strategy to examine approaches to modify a cement calciner for hydrogen-oxyfuel combustion. This process includes a thorough analysis of the existing literature, the gathering of data from multiple sources, and the use of simulation software to simulate the suggested concept's process and cost.

This methodical approach provides a thorough investigation of the subject, integrating both theoretical and practical viewpoints. The research design includes evaluating the current state of technology and identifying potential challenges and opportunities. The researched hydrogen-oxyfuel combustion concept is then designed, taking into consideration the relevant assumption and limits. The research also explores optimization methodologies and assesses the viability of the idea as potential solutions to the challenges that have been identified.

To comprehend the cement production process, oxyfuel combustion utilization, and the usage of hydrogen in such systems, a thorough literature review was carried out. To locate relevant research papers, articles, and reports, different academic databases were searched, including ScienceDirect and Google Scholar. The review concentrated on the fundamentals of oxyfuel combustion, how it is used to make cement, how carbon is captured, and what problems this method has.

The mechanisms of calcination and clinker formation, the benefits, and drawbacks of oxy-fuel combustion in the production of cement, and the potential for producing hydrogen and oxygen in an electrolyser as a fuel source were among the main topics of interest. The evaluation also looked at current cost estimation strategies and methodologies for process improvement in process systems.

The collection of data, which provides the necessary inputs for modeling and analysis, is an essential component of this study. Several sources, including published research, industry reports, and technical specifications from equipment manufacturers, were used to gather the data. The fundamental data, such as the specific parameters of the data existing cement plant and the characteristics of the materials, were collected directly from the plant. Secondary data, including equipment cost estimates, were gathered from existing literature and database in Aspen Plus Economic Analyser. The data were then used to develop the Aspen Plus model and to perform the necessary calculations and analyses.

In the case of the electrolyser, particular information on efficiency, cost and operating conditions was obtained from the online-available technical specifications of the NEL Hydrogen A3880 model and from an article including electrolyser cost estimation per megawatt.

4.2 Mass and energy balance derivation

4.2.1 Provided process values

Table 4.1: Provided process values.

Symbol	Value	Unit	Note
$\dot{m}_{preheated\ meal}$	205 000	$\frac{kg}{h}$	Provided value by plant
w_{CaCO_3}	0,77	$\frac{kg}{kg}$	Provided value by plant
η_{calc}	94	%	Provided value by plant
$T_{preheated\ meal}$	658	°C	Provided value by plant
$T_{calciner}$	900	°C	Provided value by plant

4.2.2 Constants

Table 4.2: Constants used for calculation.

Symbol	Value	Unit	Note
$LHV_{H_2,mol}$	242	$\frac{kJ}{mol}$	[23]
F	96,485	$\frac{kC}{mol}$	[24]
$e^-_{H_2}$	2		[25]
Cp_{CaCO_3}	129,7389905	$\frac{J}{mol * K}$	Provided value by plant - interpolation at 900C
Cp_{SiO_2}	70,6915	$\frac{J}{mol * K}$	Provided value by plant - interpolation at 900C
Cp_{H_2}	28,84	$\frac{J}{mol * K}$	At 25C [26]

Cp_{O_2}	29,39	$\frac{J}{mol * K}$	At 25C [26]
Cp_{H_2O}	45,539005	$\frac{J}{mol * K}$	Interpolation at 900C [26]
$\Delta H^o_{f,CaCo_3}$	$-1202,06534$	$[\frac{kJ}{mol}]$	Provided value by plant - interpolation at 900C
$\Delta H^o_{f,CaO}$	$(-640,3182495)$	$[\frac{kJ}{mol}]$	Provided value by plant - interpolation at 900C
$-\Delta H^o_{f,Co_2}$	$(-394,9869575)$	$[\frac{kJ}{mol}]$	Provided value by plant - interpolation at 900C

4.2.3 Calciner

The mass balance of the system can be described by the following equation:

$$\frac{dm}{dt} = \dot{m}_i - \dot{m}_o + \dot{m}_g$$

Where $\dot{m}_i$ is the mass flow into the system, $\dot{m}_o$ is the mass flow out of the system, and $\dot{m}_g$ is the mass generated in the system.

Since there is no mass generated in the system:

$$\dot{m}_g = 0$$

And for a steady state system:

$$\frac{dm}{dt} = 0$$

Hence:

$$\dot{m}_i - \dot{m}_o = 0$$

And:

$$\dot{m}_i = \dot{m}_o$$

Input:

$$\dot{m}_{preheated\ meal} = \dot{m}_{CaCO_3} + \dot{m}_{SiO_2}$$

$$\dot{m}_{H_2}$$

$$\dot{m}_{O_2}$$

Output:

$$\dot{m}_{CaO}$$

$$\dot{m}_{CO_2}$$

$$\dot{m}_{H_2O}$$

$$\dot{m}_{SiO_2}$$

$$\dot{m}_{CaCO_3,non\ reacted}$$

Then:

$$\dot{m}_{preheated\ meal} + \dot{m}_{H_2} + \dot{m}_{O_2} = \dot{m}_{CaO} + \dot{m}_{CO_2} + \dot{m}_{SiO_2} + \dot{m}_{H_2O} + \dot{m}_{CaCO_3,non\ reacted}$$

By splitting the preheated meal into $\dot{m}_{CaCO_3}$ and $\dot{m}_{SiO_2}$, we get:

$$\dot{m}_{CaCO_3} + \dot{m}_{SiO_2} + \dot{m}_{H2} + \dot{m}_{O_2} = \dot{m}_{CaO} + \dot{m}_{CO_2} + \dot{m}_{SiO_2} + \dot{m}_{H_2O} + \dot{m}_{CaCO_3,non\ reacted}$$

From here we can calculate the mass flows:

$$\dot{m}_{CaCO_3} = w_{CaCO_3} * \dot{m}_{preheated\ meal}$$

$$\dot{m}_{SiO_2} = (1 - w_{CaCO_3}) * \dot{m}_{preheated\ meal}$$

$$\dot{m}_{CaCO_3,reacted} = \eta_{calc} * \dot{m}_{CaCO_3}$$

$$\dot{m}_{CaCO_3,non\ reacted} = \dot{m}_{CaCO_3} - \dot{m}_{CaCO_3,reacted}$$

To calculate the mass flow of CaO and CO_2 we need to look at the balanced reaction equation for CaCO3:

$$CaCO_3 \rightarrow CaO + CO_2$$

$$\dot{n}_{CaCO_3,reacted} = \frac{\dot{m}_{CaCO_3,reacted}}{M_{CaCO_3}}$$

Where $\dot{n}_{CaCO_3,reacted}$, is the mole flow of the reacted carbonate and M_{CaCO_3} is the molar mass. From this we can obtain the molar flow of CO_2 and CaO out of the calciner:

$$\dot{n}_{CaCO_3,reacted} = \dot{n}_{CO_2} = \dot{n}_{CaO}$$

Hence,

$$\dot{m}_{CaO} = \dot{n}_{CaO} * M_{CaO}$$

$$\dot{m}_{CO2} = \dot{n}_{CO_2} * M_{CO_2}$$

The mass flow of H_2, O_2, and H_2O is dependent upon the energy balance of the system, so we will start by examining the energy balance before we continue with the mass balance.

The energy balance of the system can be described by this equation:

$$E_{in} = E_{out}$$

Where the energy into the system is the energy from combusting hydrogen and oxygen in the calciner, and the energy out is the energy required to react $CaCO_3$, heat the preheated meal, heat H_2, heat O_2, and heat H_2O. The total energy balance can be described by:

$$E_{H_2,comb} = E_{CaCO_3,reacted} + Q_{preheated\ meal} + Q_{H_2} + Q_{O_2} + Q_{H_2O}$$

To find the $CaCO_3$ reaction energy in the calciner, we need to obtain the heat of reaction first:

$$\Delta H^o_{CaCo_3} = \Delta H^o_{f,CaCo_3} - \Delta H^o_{f,CaO} - \Delta H^o_{f,Co_2}$$

Then:

$$E_{CaCO_3,reacted} = \dot{n}_{CaCO_3,reacted} * \Delta H^o_{CaCo_3}$$

For heating the preheated meal, the energy needed can be obtained by:

$$Q_{preheated\ meal} = \dot{n}_{preheated\ meal} * Cp_{preheated\ meal} * \Delta T_{preheated\ meal}$$

Where:

$$\dot{n}_{preheated\ meal} = \frac{\dot{m}_{CaCO_3}}{M_{CaCO_3}} + \frac{\dot{m}_{SiO_2}}{M_{SiO_2}}$$

We know the energy needed to react $CaCO_3$ to CaO and CO_2, and the energy to heat preheated meal. However, the energy needed to heat H_2, O_2 and H_2O and the energy gained from combustion is dependent on the molar flow of the species or mass flow, which we do not know yet. We can solve for the unknowns by using the shared unknown molar flow of hydrogen. We know the energy from combustion of H_2 and O_2 can be given by the lower heating value of hydrogen and the unknown molar flow of hydrogen.

To solve this problem, we need to consider the energy required to heat hydrogen, oxygen, and H_2O. Assuming that specific heat values are constant over the temperature range. Now, considering the unknow molar flow, $\dot{n}_{H_2}$, we can obtain the energy needed to heat H_2, O_2 and H_2O by the following equations:

$$Q_{H_2} = \dot{n}_{H_2} * Cp_{H_2} * \Delta T_{H_2}$$

$$Q_{O_2} = \dot{n}_{O_2} * Cp_{O_2} * \Delta T_{O_2}$$

$$Q_{H_20} = \dot{n}_{H_2O} * Cp_{H_20} * \Delta T_{H_20}$$

The energy gained from combustion can be shown by introducing the lower heating value of hydrogen:

$$E_{H_2,comb} = \dot{n}_{H_2} * LHV_{H_2}$$

Furthermore, the balanced equation the combustion reaction is:

$$H_2O \rightarrow H_2 + \frac{1}{2}O_2$$

Then, by using the stoichiometric relationship between hydrogen, oxygen, and water:

$$\dot{n}_{O_2} = \frac{1}{2}\dot{n}_{H_2}$$

$$\dot{n}_{H_2O} = \dot{n}_{H_2}$$

Now we can inspect the total energy balance to find the unknown molar flow for hydrogen:

$$E_{H_2,comb} = E_{CaCO_3,reacted} + Q_{preheated\ meal} + Q_{H_2} + Q_{O_2} + Q_{H_2O}$$

To expose the molar flow, we need to split up the hydrogen combustion energy and the energy needed to heat hydrogen, oxygen, and water:

$$\dot{n}_{H_2} * LHV_{H_2} = E_{CaCO_3,reacted} + Q_{preheated\ meal} + (\dot{n}_{H_2} * Cp_{H_2} * \Delta T_{H_2}) + (\dot{n}_{H_2O} * Cp_{H_20} * \Delta T_{H_20}) + (\dot{n}_{O_2} * Cp_{O_2} * \Delta T_{O_2})$$

Then we replace the molar flow of O_2, and H_2O with the molar flow of H_2 to get a shared unknown:

$$\dot{n}_{H_2} * LHV_{H_2} = E_{CaCO_3,reacted} + Q_{preheated\ meal} + (\dot{n}_{H_2} * Cp_{H_2} * \Delta T_{H_2}) + (\dot{n}_{H_2} * Cp_{H_20} * \Delta T_{H_20}) + (\frac{1}{2}\dot{n}_{H_2} * Cp_{O_2} * \Delta T_{O_2})$$

From this we can derive the molar flow of hydrogen:

$$\dot{n}_{H_2} * LHV_{H_2} = E_{CaCO_3,reacted} + Q_{preheated\ meal} + \dot{n}_{H_2}(Cp_{H_2} * \Delta T_{H_2} + Cp_{H_20} * \Delta T_{H_20} + \frac{1}{2} Cp_{O_2} * \Delta T_{O_2})$$

From here, we can isolate the molar flow of hydrogen:

$$\dot{m}_{H_2} * (LHV_{H_2} - \left(Cp_{H_2} * \Delta T_{H_2} + Cp_{H_20} * \Delta T_{H_20} + \frac{1}{2} Cp_{O_2} * \Delta T_{O_2}\right)) = E_{CaCO_3,reacted} + Q_{preheated\ meal}$$

Then:

$$\dot{n}_{H_2} = \frac{(E_{CaCO_3,reacted} + Q_{preheated\ meal})}{LHV_{H_2} - (Cp_{H_2} * \Delta T_{H_2} + Cp_{H_20} * \Delta T_{H_20} + \frac{1}{2} Cp_{O_2} * \Delta T_{O_2})}$$

From here we find the energy needed for heating H_2, O_2 and H_2O:

$$Q_{H_2} = \dot{n}_{H_2} * Cp_{H_2} * \Delta T_{O_2}$$

$$Q_{O_2} = \frac{1}{2}\dot{n}_{H_2} * Cp_{O_2} * \Delta T_{O_2}$$

$$Q_{H_2O} = \dot{n}_{H_2} * Cp_{H_2O} * \Delta T_{H_2O}$$

The rest of the mass balance equations can be obtained by:

$$\dot{m}_{H_2} = \dot{n}_{H_2} * M_{H_2}$$

$$\dot{m}_{O_2} = \frac{1}{2}\,\dot{n}_{H_2} * M_{O_2}$$

$$\dot{m}_{H_2O} = \dot{m}_{H_2} + \dot{m}_{O_2}$$

Now we can calculate the energy from hydrogen combustion:

$$E_{H_2,comb} = E_{CaCO_3,reacted} + Q_{preheated\ meal} + Q_{H_2} + Q_{H_20} + Q_{O_2}$$

4.2.4 Electrolyser

For the hydrogen and oxygen production via electrolysis, the reactant is water. The balanced chemical equation for water electrolysis is:

$$2H_2O \rightarrow 2H_2 + O_2$$

From calciner system we know the mole flow of hydrogen needed to be produced in the electrolyser, then we can obtain the molar flow of oxygen and water:

$$\dot{n}_{O_2} = \frac{1}{2}\dot{n}_{H_2}$$

$$\dot{n}_{H_2O} = \dot{n}_{H_2}$$

The mass balance equations can be obtained by:

$$\dot{m}_{H_2} = \dot{n}_{H_2} * M_{H_2}$$

$$\dot{m}_{O_2} = \dot{n}_{O_2} * M_{O_2}$$

$$\dot{m}_{H_2O} = \dot{n}_{H_2O} + \dot{m}_{O_2}$$

To calculate the energy balance for an electrolyser, we need to consider the energy input from electrical energy and the energy output from chemical energy gained in the hydrogen:

$$E_{in} = E_{out}$$

Where energy in is the electrical energy needed for producing hydrogen and the energy out is the potential combustion energy of hydrogen and the waste heat:

$$E_{el} = E_{H_2,comb} + E_{waste\ heat}$$

Next, when we know that it takes two electrons to produce one molecule hydrogen and the Faradays constant, we can obtain the current:

$$I = e^- * F * \dot{n}_{H_2}$$

Where e^- is number of electrons and F is the Faradays constant.

From this we can obtain the needed energy input from electrical energy:

$$E_{el} = (V_{cell} + V_{tn}) * I$$

4.3 Aspen Plus

Aspen Plus, developed by AspenTech, is a widely used commercial chemical process simulation software that is considered the leading process simulation software in the chemical industry. The software has been developed over 40 years with input from top chemical companies and incorporates an award-winning physical properties database [27]. The steady-state process modelling, and simulation software is utilized by both industrial and academic entities for process engineering purposes.

4.3.1 Overview of Aspen Plus

The Aspen Plus model selection offers a comprehensive selection of blocks for various process equipment, including distillation columns, pumps, reactors, and fans. With its extensive built-in property methods, thermodynamic models, and calculation options, the software can simulate a broad range of processes that involve a range of species and phenomena. These processes includes both batch and continuous operations, as well as solids and biomass processing, carbon capture, hydrogen electrolysis, bioreactors, and polymers.

AspenTech aslo offers Aspen Process Economic Analyzer. This software allows for the estimation of capital and operating expenses, as well as providing in-depth economic analysis over the project's lifetime.

4.3.2 Assumptions

To create a simulation model of the modified concept using Aspen Plus, several assumptions have been made to facilitate system feasibility and reaction processes:

- The calciner combustion only involves hydrogen and oxygen, with no air intrusion. This assumes ideal conditions without the dilution of the nitrogen from air, which can occur due to false air entry in real systems.
- Only the reaction of calcium carbonate ($CaCO_3$) from the meal is considered. The presence of inert solids in the raw meal is simplified to only include silicon dioxide (SiO_2).
- It's assumed that no dust is present in the gas phase exiting the calciner for simplification purposes.
- A compressor is incorporated in the model to counteract an assumed 0.1 Atm pressure drop in the flue gas system.
- The comparative model assumes the use of only coal as fuel, without any alternative fuels.
- It's assumed that 83,400 kg/h of air at 879℃ and hot flue gas from kiln is sufficient to preheat the raw meal to 658℃ in the preheater cyclones, similar to the preheating temperature in the existing system.
- The efficiency of the electrolyser is assumed to be equal to that of NEL Hydrogen's A3880 model.
- The minimum temperature approach in the heat exchangers is assumed to be 20℃.
- The electrolyser cell operates at a temperature of 70℃, with an inlet electrolyte temperature of 20℃.
- The design of the calciner combustion chamber and the cyclone downstream of the calciner is assumed to remain unchanged in the modified system.
- The calcination rate, which depends on CO_2 partial pressure and temperature, is assumed steady at 900℃ and not evaluated in this model.
- For straightforward simulation there is no kinetic and potential energy losses considered, and no heat losses to the atmosphere.
- Freshwater supply is assumed demineralized.

These assumptions provide a framework that allows us to focus on the primary modifications and compare the performance of the modified oxyfuel combustion concept with the existing process.

4.3.3 Coal-fired calciner model approach

A steady-state model was developed in Aspen Plus to replicate the modern coal-fired calciner process system. The model was calibrated against operational data provided by the plant. This simulation model was created to gain an overview of the existing calciner system, the energy dispersion, CO_2 emissions, and the adiabatic flame temperature.

4.3.3.1 Property method

The *PR-BM* (Peng-Robinson with Boston-Mathias modification) method was selected as the property model for simulating the coal-fired system. This choice was made based on Aspen Plus specific software recommendations for coal systems.

The components chosen for the system was:

- CO_2
- H_2O
- SO_2
- NO_2
- N_2
- O_2
- Cl_2
- COAL – Nonconventional
- ASH – Nonconventional
- NO
- S – Solid
- SO_3
- HCl
- C – Solid
- H_2
- $CaCO_3$ – Solid
- SiO_2 – Solid
- CaO – Solid

The thermodynamic properties for the components were using standard values from Aspen Plus, except $CaCO_3$, CaO, C and SiO_2 which were specified as solid, and COAL and ASH, which were specified as Nonconventional. Furthermore, the heat of combustion for COAL was set to 27.7 MJ/kg.

4.3.3.2 Process simulation approach

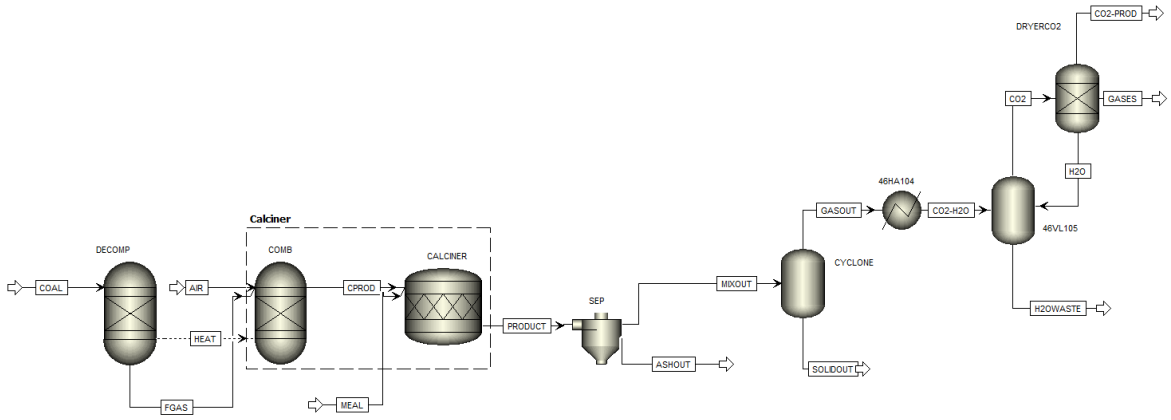

Figure 4.1: Process Flowsheet of Coal Combusted Calciner

The approach for modeling a coal-fired calciner in Aspen Plus is based on the built-in coal combustion example provided within the software. This model serves as a starting point for understanding the system and its parameters specifically the coal handling, which are then customized to fit the specifications of the cement plant in question. The complete model can be seen in figure 4.1.

In this model, the pressure for the entire system is set at atmospheric conditions. This assumption simplifies the modeling process and provides a baseline for understanding the system's behavior.

The model was designed for a preheated meal mass flow rate of 205,000 kg/h at 658ºC. The meal was set to a mass fraction of 0.77 kg/kg $CaCO_3$ and 0.23 kg/kg SiO_2. The calcination reaction, which converts $CaCO_3$ into CaO and CO_2, was modeled in a stoichiometric reactor. As previously mentioned, 94% of the calcination reaction was assumed to occur in the calciner, with the remaining 6% occurring in the kiln (which is not part of this model).

The model was adjusted to achieve a calciner exit temperature of 900ºC, with the flow rate coal being adjusted accordingly. Hence, the flow rates are part of the results of the model.

The coal inlet, characterized by the plant, was set at 20ºC and fed into a decomposition module (*DECOMP*), where it is pyrolyzed into different elements. The energy for pyrolyzing the coal was take out of the combustion block with a heat stream. The coal's ultimate, sulfur, and proximate analysis, as shown in table 4.3, were used for both the coal inlet composition and the decomposition module.

Thermal energy required for calcination is generated combustion in a non-stoichiometric reactor (*COMB*), based on known yield distribution. This reactor combines the carbon, H_2 gas, sulfur, nitrogen (which reacts to form NOx), and ash from the decomposition module with air to generate the necessary heat. The inlet air is set at 190 000 kg/h at 650ºC, the parameter was provided by the plant. This temperature comes from being preheated by the clinker coolers and kiln.

The model also includes a step for the separation of the ash from the coal combustion. The mixture of coal ash is separated in a gas-solid separator using as a cyclone (*SEP*). Following this step, the mixture of combustion gas and CO_2 released from calcination, along with $CaO/SiO_2/CaCO_3$, is fed into another cyclone modelled as a separator (*CYCLONE*) where the solids are separated from the gases.

The flue gas treatment, starting from the heat exchanger *46HA104* and continuing downstream, does not reflect the actual configuration of the cement plant. Instead, this section of the model was designed solely to enable a comparison with the modified concept in terms of CO_2 emissions and cooling requirements. The heat exchanger was set to a temperature of 25°C, and *46VL105* was designed as a flash drum with both liquid and gas outlets. A component separator (*DRYERCO2*) was also incorporated to isolate the CO_2 gas, making it easier to compare with the modified concept model.

This model, while simplified, provides a solid foundation for understanding the energy and mass balances in a coal-fired calciner and serves as a benchmark for evaluating the potential benefits and challenges of the proposed modified oxyfuel combustion concept.

4.3.3.3 Coal characteristics

The combustion fuels at Norcem Brevik include coal, animal meal, and liquid hazardous waste. However, for simplification, this thesis will assume the use of only coal fuel for simulation comparison and simplification. The proximate analyses for coal (moisture, volatiles, fixed carbon and ash) and the ultimate analysis (elemental analysis of C, H, N, O, S and Cl) were provided obtained by the plant, see table 4.3 and 4.4.

Table 4.3: Coal Characteristics Norcem Brevik

Parameter	Value	Unit
Coal heating value	27.7	MJ/kg
Coal ultimate analysis:		
C	71.7	wt%
H	3.9	wt%
O	5.9	wt%
S	1.2	wt%
N	1.7	wt%
Cl	0.1	wt%
Ash	14.3	wt%
Moisture	1.2	wt%
Coal proximate analysis:		
Moisture	1.2	wt%
Volatiles	23.7	wt%
Fixed carbon	60.8	wt%
Ash	14.3	wt%
Coal sulfur:		
Sulfate	0.15	wt%
Pyritic	0.90	wt%
Organic	0.15	wt%

Table 4.4: Coal Ash Composition Norcem Brevik

Component i	Mass content [wt%]
CaO	2.4
Fe2O3	4.1

Al2O3	19.8
SiO2	67.0
Na2O	2.2
K2O	2.9
MgO	1.6

4.3.3.4 Modified coal combustion to match real coal consumption

The coal combustion simulation model was adapted based on experimental results that indicated a higher than expected coal consumption rate. This higher consumption influenced the calculated cost per avoided CO_2 unit (with avoided coal cost), prompting a need to adjust the model to better reflect the actual coal consumption.

The high coal usage in the model can be attributed to several factors that are not accurately modeled in the simulated environment. These include the transfer of heat from kiln flue gas to the calciner, minor exothermic reactions in the meal, and the entrainment of hot particles from the kiln flue gas. The model also utilized heat from combustion to pyrolyze coal into the desired elements, which in real-world conditions might be done by heat from a different system (not evaluated). Moreover, the calculated energy required in the calciner is lower than the software's calculation, which could also contribute to the higher coal consumption from the simulation.

To address these issues, modifications were made to the model to align the coal consumption rate with the actual rate of 12 000 kg/h. The energy required to pyrolyze the coal was simulated to come from another system. Furthermore, the *CALCINER* block was adjusted to include the additional thermal energy necessary to achieve an exit temperature of 900°C with lower coal consumption. These adjustments allow for a more accurate representation of real-world conditions and improve the reliability of the model's results.

4.3.4 Oxy-fuel hydrogen combustion calciner modification with flue gas treatment model approach

The modeling approach for the calciner modification with flue gas treatment in Aspen Plus is designed to maintain consistency with the properties of the existing process plant. The goal is to maintain the same adiabatic flame temperature as coal combustion, the exit temperature of 900ºC, and the production rate, while at the same time enable carbon capture without too much total energy efficiency loss.

The model was developed to investigate multiple aspects, including the adiabatic flame temperature of oxy-fueled hydrogen combustion, recycled flue gas temperature and flow rate needed to match the adiabatic flame temperature for coal, and the optimal relationship between these factors. The model was also designed to evaluate cooling needs, heat exchange optimization, and heat exchange utilization from another system. The model also aimed to investigate if recycling only CO_2, and not CO_2/H_2O, is preferable considering energy efficiency. The model was modified several times to investigate these different possibilities. Including a model for increased allowable adiabatic flame temperature at 3 000ºC. The final model can be observed in figure 4.2.

4.3.4.1 Property method

The *PENG-ROB* (Peng-Robinson) method was selected as the property model for simulating the modified calciner system. This choice was made based on Aspen Plus specific software recommendations for cement systems and complies with Carlson's guidelines [28]. The thermodynamic properties for the components were using standard values from Aspen Plus.

The components chosen for the system was:

- H_2
- CO_2
- H_2O
- O_2
- $CaCO_3$ – Solid
- CaO – Solid
- SiO_2 – Solid
- AIR (for simulation without optimized split heat exchange)

The thermodynamic properties for the components were using standard values from Aspen Plus, except $CaCO_3$, CaO, C and SiO_2 which were specified as solid, and COAL and ASH which were specified as Nonconventional.

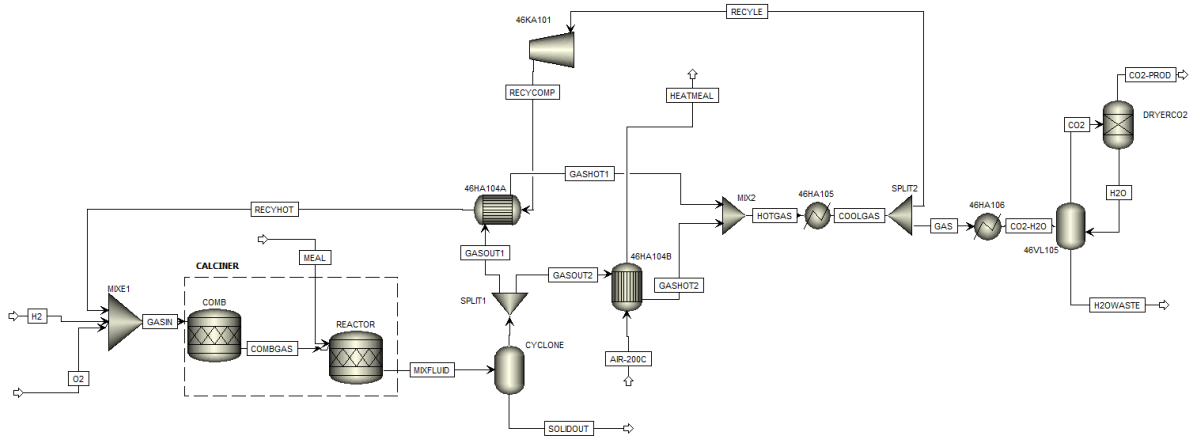

Figure 4.2: Process Flowsheet of Modified Calciner

Hydrogen and oxygen input was defined at 10ºC and 1 atm. The gases were fed into a stoichiometric reactor (*COMB*) for combustion, producing thermal energy for the calcination reaction downstream. The fractional conversion for the hydrogen combustion reaction was set to 100%.

Preheated meal at 658ºC and a rate of 205 000 kg/h, with a composition of 0.77 kg/kg $CaCO_3$ and 0.23 kg/kg SiO_2, was fed into another stoichiometric reactor (*REACTOR*). The fractional conversion for the $CaCO_3$ reaction was also set to 94%. The feed flow rate input of hydrogen and oxygen was adjusted to reach the desired exit temperature out of the calciner at 900 ºC at different recycled rates and temperatures. Therefore, the flow rate of hydrogen and oxygen are part of the results presented in this thesis.

Following this, the mixture of combustion gas (H_2O) and CO_2 released from calcination, along with CaO/SiO2/$CaCO_3$, was fed into a separator block (*CYCLONE*) where the solids are separated from the gases. This block reduces the pressure to 0.9 atm to simulate pressure loss in the system.

Heat exchangers are used to transfer heat with a counter-flow type for the flue gas in *46HA104A/B*, with a minimum approach temperature of 20ºC. The flue gas was split to *46HA104A* and *46HA104B* for heat exchange with the recycled gas and air from the clinker cooler (not modelled) respectively. This was performed with a splitter block where the split flow to 4*6HA104A* were chosen similar to the flow rate of the recycled flue gas flowing counter current. The air from clinker cooler was set to input of 200ºC and 83400 kg/h following provided data from the plant. This heats the air such that it can preheat the raw meal (which is not modelled in this thesis).

Heat exchanger block *46HA105* adjusts the temperature for the recycled gas and determined for different simulation scenarios. The recycled flow rate was determined experimentally to match the same adiabatic flame temperature in the calciner as for coal combustion at different recycled temperatures.

A compressor block (*46KA101*) counters the pressure loss in the system and increases the pressure for the recycled flue gas to 1.0 atm. The compressor is of an isentropic type with 80% efficiency.

The heat exchanger block *46HA106* is set to a temperature of 25°C. *46VL105* is designed as a flash drum with both liquid and gas outlets. A component separator (*DRYERCO2*) is incorporated to dry the CO_2 gas for carbon capture downstream boundary limit.

4.3.5 Alkaline electrolyser model approach

The modeling approach for the alkaline electrolyser in Aspen Plus is designed to assess the feasibility of the oxy-fuel combustion with hydrogen system concept. The model evaluates performance, energy requirements, cooling needs, equipment sizing, and cost evaluation for the proposed system.

The electrolyser process simulation model is based on the NEL A3880 alkaline electrolyser, an industrial-scale system. The model is adjusted to produce the required hydrogen and oxygen gas for the modified calciner. The NEL A3880 electrolyser has a power consumption of 3.8 - 4.4 kWh/Nm3 hydrogen, equal to 42.246 - 48.917 kWh/kg hydrogen [29]. Excess heat generated in the cell is cooled by circulating the electrolyte.

The water electrolysis process model used in this work is simplified, neglecting detailed electrochemistry. The initial plan was to use a more detailed model available within the software. However, due to compatibility issues with the software version used in this thesis, a simplified approach was chosen instead, see the final model in figure 4.3. The electrolyser is designed based on a simulation file provided by KG Engineering Solutions [29]. The property model chosen for the alkaline electrolysis simulation was ELECNRTL, as advised by Aspen Plus software and in compliance with Carlson's guidelines.

4.3.5.1 Property method

The property model chosen for the alkaline electrolysis simulation was *ELECNRTL*. This method was advised by the Aspen Plus software and complies with Carlson's guidelines [28]. The thermodynamic properties for the components were using standard values from Aspen Plus.

The components chosen for the system was:

- H_2O
- H_2
- KOH
- H^+
- K^+
- OH^-

4.3.5.2 Process simulation approach

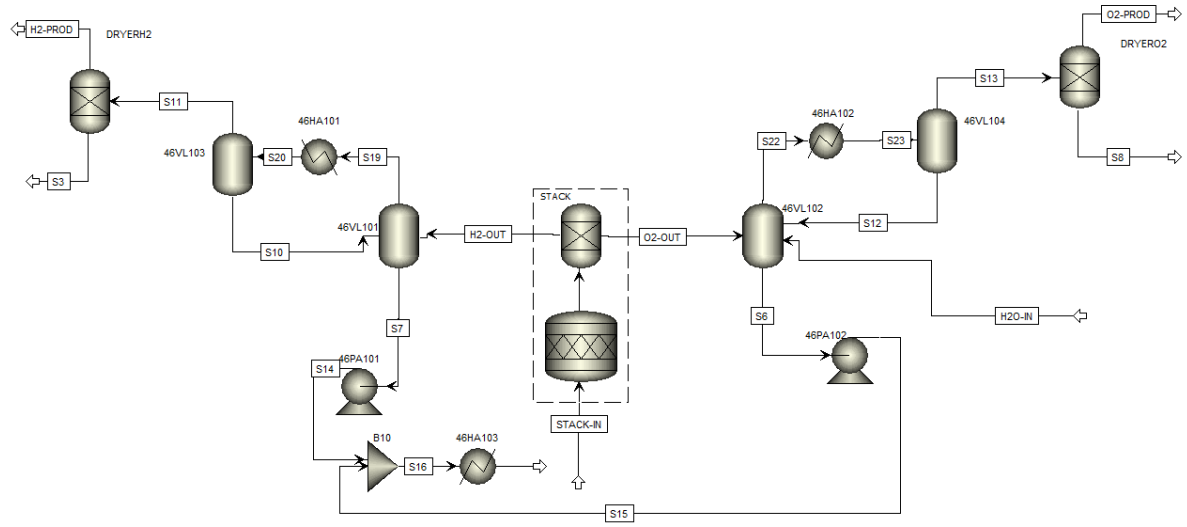

Figure 4.3: Process Flowsheet of Alkaline Electrolyser

The core unit of the model is the alkaline electrolyser (*STACK*), where water is split into hydrogen and oxygen at the cathode and anode, respectively. Water with 25% KOH at 7 bar pressure and 20°C temperature is fed to the *STACK*, which operates at 6.7 bar and 70°C. Water splitting occurs in the reactor, with conversion defined by the cell efficiency, production rate, and resulting cooling need. Produced oxygen and hydrogen gases, and electrolyte are separated with a component separator.

The power consumption input in the cell is calculated for two cases within NEL Hydrogen's provided power consumption and one future case with best theoretical power efficiency:

1. 42.246 kWh/kg hydrogen
2. 48.917 kWh/kg hydrogen
3. Power consumption equal to no heat generation (~39.615 kWh/kg hydrogen)

The following steps have been performed to determine the needed electrolyte flow and the water reaction rate input:

1. Adjust the water reaction rate during simulation based on the energy needed to produce the specified amount of hydrogen and maintain the wanted cell temperature of 70°C.
2. To find the needed electrolyte flow rate, divide the determined mass flow rate of combined hydrogen and oxygen by the mass fraction of water in the electrolyte and the determined water reaction rate.

The gas products from the electrolyser are fed to flash drum separators (*46VL101/102*) to separate hydrogen and oxygen from the electrolyte. The electrolyte is then recycled. The water from both electrodes is recycled with the model pumps *46PA101/102*, cooled in *46HA103* to 20°C, and fed back into the electrolyser along with a freshwater makeup stream *H2O-IN*. The makeup water flow rate is determined by the production rate of hydrogen and oxygen, with temperature and pressure set at 10°C and 9 bar, respectively. The pumps efficiency is set to 70%.

Further condensing occurs by cooling the gases in *46HA101/102* and separation in *46VL103/104*. The distinct gases are then dried by their separate component separator block.

For the simulation with no heat generation in the cell, the *STACK-IN* was set to 70°C and therefore 46HA103 became a heater set to 70°C for the recycled electrolyte. For this simulation case, the water reaction rate in the cell was defined as 30%.

This simplified model allows for the evaluation of the proposed system concept, providing valuable information on energy consumption, cooling need, and mass balance.

4.4 Economic estimation techniques

There are multiple factors affecting the feasibility of expanding a process plant, such as energy design optimalization, maturity of technology, electrical prices, etc.

The primary goal of cost estimating is to determine the entire cost of the project as well as the uncertainties. The dimensions from the designed Aspen Plus models are used in the calculations. The Aspen Process Economic Analyzer was used to calculate prices for all of the elements in the base case process. The primary costs of the project are CAPEX and OPEX. CAPEX is the cost of acquiring and installing equipment, pipes, instruments, electrical equipment, buildings, land, engineering and supervision, construction costs, contingencies, start-up costs, etc. OPEX includes the expenses of operation, utilities, and maintenance, raw material, salary expenditures, etc.

The calculating procedure used for the CAPEX, OPEX, and cost per avoided CO_2 unit will be presented in this subchapter.

4.4.1 Assumptions

The following was assumed for the cost estimation:

- 7200 hour per year operation
- 20 years plant life
- Plant location Amsterdam
- ASME Design code

- Built on clear field
- Additional equipment cost based on US golf location
- Updated cost of equipment to 2023 with Chemical Engineering Plant Cost Index [30]
- Cost of freshwater: 29 NOK/m^3 [31]
- Avoided cost for coal: $178.2/t [32]
- Income from product sale not evaluated
- Assumed stainless steel equipment material is enough up to 450℃
- Assumption of nickel and Inconel material is enough for equipment in the system at higher temperatures

4.4.2 Equipment cost estimation

The main cost estimation method for the modified concept was performed using Aspen Process Economic Analyzer. However, some of the equipment was calculated wrongly by the software. Hence, both cost curves and power law were applied for the calculation of these equipment. The following procedure was used for the manual equipment cost estimation of this project.

1. Finding new dimensions (provided by software), such as heat transfer area or duty.
2. Calculating cost of new equipment with cost curves or power law based on previous common equipment cost from appendix.
3. Finding material factor, based on temperature and corrosion resistance, from appendix.
4. Adjust up to date with ratio of cost indexes with Chemical Engineering Plant Cost Index.
5. For installation cost calculation, insert the calculated equipment cost in Aspen Process Economic Analyzer as quoted cost.

4.4.2.1 Cost curves and power law

The precision of equipment estimates is based on the similarities between the two pieces of equipment or plants. Cost curves and power law method provides a rough estimate and is expressed by the following equations [20]:

$$C_e = a + b * S^n$$

Here, C_e is the purchased equipment cost of new equipment on a U.S. Golf Coast basis in 2010. S is the size parameter, and a and b is costs constants.

$$c_B = c_A * (\frac{S_B}{S_A})^n$$

Where, C_B is the cost of the new equipment, C_A is the cost of the old equipment, and n is an exponent ranging depending on the equipment. S is the wanted new equipment size parameter.

The cost curve equation was used together with cost of equipment at different size in literature [20]. The cost of *46KA101*, *46HA104A* and *46HA104B* was calculated using the following equations:

$$c_{46KA101,CS,2010} = a + b * S^n = 580\,000 + 20\,000 * S^{0,6}$$

$$c_{46HA104A,CS,2010} = a + b * S^n = 28\,000 + 54 * S^{1.2}$$

$$c_{46HA104B,CS,2010} = a + b * S^n = 28\,000 + 54 * S^{1.2}$$

Furthermore, one cost analysis case explored the cost of not utilizing optimized split heat exchange for the flue gas with air from clinker cooler. For this the cost of an electrical heat exchanger was unknow. However, the Aspen software library have cost built in for a 200 kW electrical heater with 304 stainless steel. Hence, the power law equation was used together with the cost of the electrical heat exchanger to calculate the equipment cost of the wanted heat exchanger duty. Normally, equipment cost for heat exchangers are calculated using heat transfer area. However, the heat transfer area for the wanted electrical heater was unknown, so the known duty was utilized.

$$C_{AIR-EX,without\ split\ EX,SS304,17\ 220kW} = C_{AIR-EX,without\ split\ EX,SS304,200kW} * \left(\frac{Q}{Q_B}\right)^e$$

4.4.2.2 Material factor adjustment

Most open literature gives out material costs in carbon steel. Hence, to obtain equipment cost for wanted material, a material factor, f_m, was applied by the following equation:

$$c_{SS} = c_{CS} * f_m$$

When dealing with temperatures as high as 900°C and fluids with CO_2 and H_2O, corrosion resistance and high-temperature strength become even more critical. In such cases for the *46HA104A/B*, stainless steel is not be sufficient. Instead, the use high-temperature nickel-based superalloys was desided.

One of the more suitable materials for this application was nickel and Inconel ($f_m = 1.7$). These alloys are known for their excellent high-temperature strength and resistance to oxidation and corrosion [20]. They maintain their mechanical properties even at elevated temperatures and are widely used in high-temperature applications [20].

$$c_{46HA104A,NI,2010} = c_{46HA104A,CS,2010} * f_{m,NI}$$

$$c_{46HA104B,NI,2010} = c_{46HA104B,CS,2010} * f_{m,NI}$$

For the compressor block 46KA101, the temperature was designed to not be above 450°C. For a high-temperature environment of 400°C with a mixture of CO_2 gas and water content, material selection must prioritize resistance to corrosion and high-temperature strength. In this case, we should consider using 316 stainless steel. 316 offers good corrosion resistance in the presence of water and CO_2 and can withstand high temperatures. Hence, 316 stainless steel ($f_m = 1.3$) was be utilized as material.

$$c_{46KA101,SS,2010} = c_{46KA101,CS,2010} * f_m$$

Note that the exact material choice will depend on the specific operating conditions and other environmental factors. Consulting with a materials engineer or corrosion specialist is highly recommended to determine the most appropriate material for this application.

4.4.2.3 Index adjustment

The cost of process equipment may vary from year to year due to inflation and other variables. To update the base costs published in open literature, cost index from Chemical Engineering Plant Cost Index was used. The following equation shows the cost estimation technique.

$$c_2 = c_1 * \frac{INDEX_2}{INDEX_1}$$

Hence, the equipment can be calculated by:

$$c_{46KA101,SS,2023} = c_{46KA101,SS,2010} * \frac{INDEX_{2023}}{INDEX_{2010}}$$

$$c_{46HA104A,NI,2023} = c_{46HA104A,NI,2010} * \frac{INDEX_{2023}}{INDEX_{2010}}$$

$$c_{46HA104B,NI,2023} = c_{46HA104B,NI,2010} * \frac{INDEX_{2023}}{INDEX_{2010}}$$

4.4.2.4 Electrolyser equipment cost calculation

The CAPEX cost for the electrolyser stack based on energy usage was collected using literature for 2017 cost, updated to 2023, and calculated based on the results for energy usage in the electrolyser from the simulations. Furthermore, an expected 2025 cost was used and calculated to evaluate a future, more mature technology, cost. Using 1 € = 1,1304$, The CAPEX STACK cost is calculated by the following equations:

$$CAPEX_{STACK,2017,123\ 399kW,750\ €/kW} = 92\ 549\ 250\ € = \$104\ 617\ 672$$

$$CAPEX_{STACK,2017,131\ 598\ kW,750\ €/kW} = 98\ 698\ 500\ € = \$111\ 568\ 784$$

$$CAPEX_{STACK,2017,152\ 375kW,750\ €/kW} = 114\ 281\ 250\ € = \$129\ 183\ 525$$

$$CAPEX_{STACK,2023,123\ 399kW,750\ €/kW} = Capex_{STACK,2017,123\ 399kW,750\ €/kW} * \frac{INDEX_{2023}}{INDEX_{2017}}$$

$$= \$104\ 617\ 672 * \frac{567{,}5}{550{,}8} = \$107\ 789\ 631$$

$$CAPEX_{STACK,2023,131\ 598kW,750\ €/kW} = Capex_{STACK,2017,131\ 598\ kW,750\ €/kW} * \frac{INDEX_{2023}}{INDEX_{2017}}$$

$$= \$111\ 568\ 784 * \frac{567{,}5}{550{,}8} = \$114\ 951\ 497$$

$$CAPEX_{STACK,2023,152\ 375kW,750\ €/kW} = Capex_{STACK,2017,152\ 375kW,750\ €/kW} * \frac{INDEX_{2023}}{INDEX_{2017}}$$

$$= \$129\ 183\ 525 * \frac{567{,}5}{550{,}8} = \$133\ 100\ 309$$

$$CAPEX_{STACK,2025,123\ 399kW,480\ €/kW} = 59\ 231\ 520\ € = \$66\ 955\ 310$$

$$CAPEX_{STACK,2025,131\ 598\ kW,480\ €/kW} = 63\ 167\ 040\ € = \$71\ 404\ 022$$

$$CAPEX_{STACK,2025,152\ 375kW,480\ €/kW} = 73\ 140\ 000\ € = \$82\ 677\ 456$$

The cost of the electrolyser was added as input in the Aspen Process Economic Analyser. However, this was done as quoted equipment cost. Hence, the cost was reduced such as the software's calculated added CAPEX is matching the calculated CAPEX of STACK.

The real-life existing equipment in the system model, such as CALCINER, COMB, CYCLONE, REACTOR, and the component splitter for part of the STACK (B2), was added to aspen software as quoted price of 0$.

4.4.3 Aspen Process Economic Analyzer

Aspen Process Economic Analyzer is a tool that provides model-based estimates for capital and operating costs of proposed projects, thus facilitating their comparison and evaluation. In this study, we used this software to evaluate the capital expenditure (CAPEX) and operating expense (OPEX) associated with the process models developed in Aspen Plus.

The Aspen Plus models remained largely unchanged, except for a more detailed representation of heat exchangers to accurately specify their capital costs. Aspen Process Economic Analyzer allows for the combination of multiple Aspen Plus simulation files into a larger system using hierarchy blocks, while still allowing for separate CAPEX and OPEX calculations for each block. This made it easier to debug the system, as individual blocks could be activated or deactivated.

Before importing the models as hierarchy blocks, they were exported as Aspen Plus Backup files (.bkp) for compatibility. Each hierarchy block was assigned property methods and other calculation options according to the respective original simulation files. Figure 4.4 shows how the previously stated system models are brought together using hierarchy blocks.

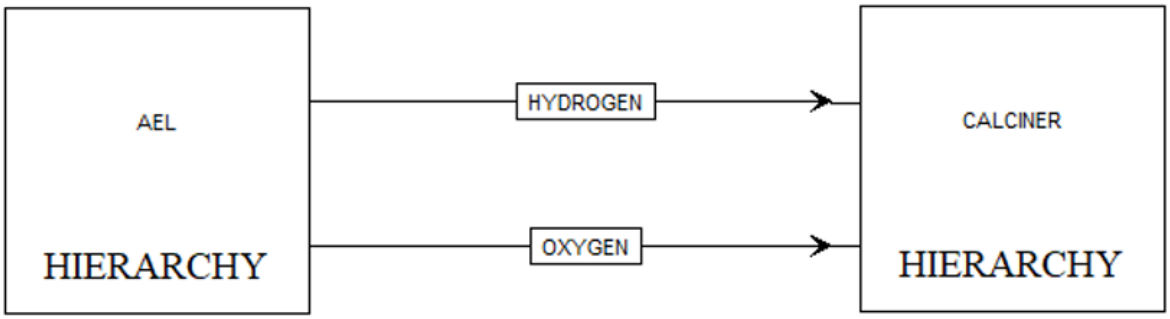

Figure 4.4: Aspen Process Economic Analyzer Hierarchy blocks

4.4.3.1 Raw material stream price

The cost of raw materials, such as freshwater supplied to the electrolyser, was included in the analysis. The avoided cost of coal consumption was not included in the OPEX calculation. However, this cost was manually added to the OPEX after simulation to evaluate the cost per avoided CO2 unit. The cost for other raw materials were not evaluated.

4.4.3.2 Process utilities

Process utilities, primarily water cooling at different temperatures, were also considered in the cost estimation. The costs of these utilities are presented in the appendices of this thesis. The cooling cost consists of standard software used prices.

The electricity price was added manually to the Excel files after simulation due to incompatibility with electricity usage for the manually added quoted electrolyser STACK and the compressor. The electricity price for all centrifugal pumps were also adjusted.

4.4.3.3 Mapping

By activating the economics for the software, the mapping of equipment becomes available. This was performed. The module creates estimates using data from a "standard basis file" that includes geographic cost basis information as well as corporate and project standardization information. The mapping of each simulator model to one or more process equipment is a critical step in the economic evaluation with the integrated evaluation feature Aspen Process Economic Analyzer has.

The Aspen Process Economic Analyzer was a valuable tool for doing pinch analysis on the simulated processes, suggesting configurations for heat exchanger modification.

4.4.3.4 Quoted equipment cost

Equipment costs were further refined by supplying design data to Aspen Process Economic Analyzer. For some equipment, such as heat exchangers and the compressor, the costs were manually calculated and added as quoted equipment. The design data description of heat exchangers *46HA104A/B* (also *AIR-EX*) and the compressor was needed in the cost estimation.

The software has the capacity to override the default mappings and replace them with the user's own mappings. While mapping, the user can modify, remove, and add equipment. The manually calculated equipment cost, including the electrolyser *STACK*, was added as quoted equipment. Real existing equipment was chosen to cost $0.

4.4.3.5 Size

Furthermore, the process equipment was sized using the default sizing technique module and the simulation data. Carbon steel is the standard construction material for all machinery.

4.4.3.6 Material selection

Capital expenses can be sensitive to the materials used in construction. Therefore, material design data was provided to Aspen Process Economic Analyzer to generate more accurate results. All materials calculated by the software were designed with 316 stainless steel due to the corrosive fluid and high temperatures. However, for the heat exchanger operating at higher temperatures (*46HA105*), Nickel and Inconel were used.

4.4.3.7 Simulation

Six scenarios were simulated for the defined most optimal energy utilization case in the calciner, see figure 5.9, each with different electrolysis efficiencies and quoted electrolyser prices. These scenarios were then analyzed with respect to fluctuating electrical prices.

Furthermore, two scenarios; one with less optimized split heat exchange for the flue gas, and one with an allowable 3 000°C adiabatic hydrogen flame temperature were also investigated. For these two scenarios, the electrical price was maintained fixed at $0.3364 per kWh.

Upon completion of the simulations, Excel files containing the results of the economic assessment and a summary of the equipment were produced as a comprehensive project economic report. These files were then slightly adjusted due to minor software errors such as not utilizing provided yearly operational hours.

Overall, the integrated use of Aspen Plus and Aspen Process Economic Analyzer minimized errors caused by manual data transfer between the process design and estimators, thus saving time and reducing potential inaccuracies. This approach facilitated a robust and comprehensive economic evaluation of the designed systems.

4.4.4 Electricity price

The cost evaluation of the simulation cases was conducted under various electricity prices to provide a comprehensive view of the operational cost. Electricity prices have fluctuated over the past few years, with hourly spot prices reaching as high as 8.22 NOK/kWh [33]. However, between 2012 and 2020, prices remained relatively stable for the power intensive industry. The spot price averaged 27.43 øre/kWh from 2012 to 2020 and was as low as 10.40 øre/kWh in 2020. The fixed price for the same period was as low as 29.76 øre/kWh [34].

The increase in spot prices started when Norway commissioned new power cables to Germany and Britain [35], together with the onset of the global energy crisis in late 2021. This event led to a record spot price of 106.2 øre/kWh for 2022. Concurrently, fixed-price contracts for electricity rose to 38.1 øre/kWh in 2021 and 50.2 øre/kWh in 2022. It's important to note that the fixed price averages include many contracts negotiated several years prior.

The electrical price is also dependent on the *energiledd* and the *effektledd* and the reactive effect. The reactive effect price is not evaluated. The total electrical price was calculated by the obtained prices from Porsgrunn's local electricity provider [36] and the following calculation:

$$P_{el,total} = P_{el,contract} + P_{el,energiledd}$$

Where:

$$P_{el,energiledd} = \left(\left(P_{el,energiledd,Nov.-Mar.} * \frac{6}{12}\right) + \left(P_{el,energiledd,Apr.-Oct.} * \frac{6}{12}\right)\right)$$

$$P_{el,energiledd} = \left(\left(0.05\frac{øre}{kWh} * \frac{6}{12}\right) + \left(0.03\frac{øre}{kWh} * \frac{6}{12}\right)\right) = 0.04\frac{øre}{kWh}$$

Furthermore, the *effektledd* was calculated by:

$$C_{el,effektledd} = \left(\left(P_{el,effektledd,Nov.-Mar.} * E_{system,\max month} * \frac{6}{12}\right) + \left(P_{el,effektledd,Apr.-Oct.} * E_{system,\max month} * \frac{6}{12}\right)\right)$$

$$C_{el,effektledd} = \left(\left(P_{el,effektledd,Nov.-Mar.} * E_{system,\max month} * \frac{6}{12}\,\frac{mnd}{year}\right) + \left(P_{el,effektledd,Apr.-Oct.} * E_{system,\max month} * \frac{6}{12}\,\frac{mnd}{year}\right)\right)$$

$$= \left(\left(\frac{\frac{48{,}75NOK}{kW}}{\frac{mnd}{9{,}9506\frac{\$}{NOK}}} * 124\ 175\ kW * \frac{6}{12}\,\frac{mnd}{year}\right) + \left(\frac{\frac{35.74NOK}{kW}}{\frac{mnd}{9{,}9506\ \frac{\$}{NOK}}} * 124\ 175\ kW * \frac{6}{12}\frac{mnd}{year}\right)\right) = \frac{\$527\ K}{year}$$

Then, the total electrical cost was calculated by:

$$C_{el,period} = (P_{el,contract} + P_{el,energiledd}) * E_{system} * t_{op} + C_{el,effektledd}$$

The cost of *effektledd* was added to the cost estimation for the different energy usages and the *energiledd* was used as additional input for the cost simulation. The electricity contract price was, as mentioned, altered with several prices.

4.4.5 Net present value

Net Present Value (NPV) is a method of determining the overall cost of a project by considering capital and operational expenditures over a specific period. For this cost estimation simulation, CAPEX starts at year zero, and OPEX is calculated from year zero onwards. The project's calculation period is 20 years, with an interest rate of 4.5%. The annual OPEX cost is assumed to remain constant throughout the project's calculation period. The following equations were used to calculate the NPV:

$$NPV_{CAPEX} = C_{CAPEX}$$

Here, the NPV_{CAPEX} is equal the total CAPEX cost of the system.

$$NPV_{OPEX} = C_{OPEX} + C_{OPEX} * \frac{1}{(1+i)^1} + C_{OPEX} * \frac{1}{(1+i)^2} + \cdots + C_{OPEX} * \frac{1}{(1+i)^{n-1}}$$

The total NPV was be calculated by adding the NPV_{CAPEX} and NPV_{OPEX}.

4.4.6 Equivalent annual cost

The equivalent annual cost (EAC) accounts for all costs associated with assets throughout their full life cycle. This involves ownership, operation, and maintenance of the asset. An annuity factor must be computed to calculate the EAC. The annuity factor was derived using the following calculation based on the time value of money:

$$a_f = 1 - \frac{\frac{1}{(1+i)^n}}{i} = 1 - \frac{\frac{1}{(1+0.045)^{20}}}{0.045} = 13.008 \frac{1}{year}$$

The interest rate, i, was set to 4.5% and the life cycle of the plant modification, n, was set to 20 years. This calculated value was used for all cost estimation calculation.

Furthermore, the EAC was calculated by dividing the net present value by the annuity factor.

$$EAC = \frac{NPV}{a_f}$$

Considering EAC addresses all costs assessed over the entire plant lifespan, that would be incurred if the expenses were spread evenly over each year, the total capital and operating expenses may be calculated annually using the following equations:

$$EAC_{total} = \frac{NPV_{CAPEX} + NPV_{OPEX}}{a_f}$$

4.4.7 Avoided coal cost

When we assume all CO_2 gas from the flue gas in the existing coal combustion simulation case is avoided, we can calculate the avoided coal cost. As of May 2023, the price of coal is \$178.2/t, though it is important to note that the price of coal has fluctuated significantly due to the global energy crisis [32] . By eliminating coal consumption in the existing coal combustion simulation, we can calculate the avoided coal cost using the following equation:

$$C_{coal\ consumption\ avoided\ cost} = \dot{m}_{coal,period} * C_{coal} = \frac{86\,400\ t}{period} * \frac{\$178{,}2}{t} = \frac{\$15.397\ M}{period}$$

Here, the coal usage was based on the coal input for coal combustion simulation:

$$\dot{m}_{coal,period} = \dot{m}_{coal} * t_{period} = 12.000 \frac{t}{h} * \frac{7200\ h}{year} = \frac{86\,400\ t}{year}$$

The net present value was then updated:

$$NPV_{OPEX,avoided\ coal\ cost} = (C_{OPEX} - C_{coal\ consumption\ cost}) + (C_{OPEX} - C_{coal\ consumption\ cost}) * \frac{1}{(1+i)^1} + \cdots + (C_{OPEX} - C_{coal\ consumption\ cost}) * \frac{1}{(1+i)^{n-1}}$$

4.4.8 Cost per avoided CO_2 unit

When assuming all CO_2 gas from the flue gas, obtained by this thesis's results, in the existing coal combusted simulation case is avoided, we can calculate the cost per avoided CO_2 unit by dividing the EAC total with the annual CO2 emission from coal combustion case:

$$Cost\ per\ tonne\ CO2\ avoided_{total} = \frac{EAC_{total}}{\dot{m}_{CO_2\ emission,coal\ combustion\ case,period}}$$

Where:

$$\dot{m}_{CO_2\ emission,coal\ combustion\ case,period} = \dot{m}_{CO_2\ emission,coal\ combustion\ case} * t_{period}$$

4.4.9 Cost per avoided CO_2 comparison with alternative technology

This thesis cost estimation considered both capital expenditures and operational expenditures per avoided tonne of CO_2, comparing the proposed modification with alternative CO_2 capture technologies. Recent research includes alternative CO_2 capture technologies for the same system at Norcem, such as standard monoethanolamine (MEA) amine, advanced amine with waste heat utilization, and an electrically heated rotary calciner. This thesis compares the technologies with the proposed modification, and this was performed by considering the same avoided coal cost (111 EUR/tonne coal) and the same electrical price (0.033 EUR/kWh) [1]. All six cases were investigated against the alternative technology.

4.4.10 Avoided CO_2 tax

Another crucial aspect in the analysis is the calculation of avoided CO2 tax, which can help ascertain whether the investment in system modification is worthwhile. The same electricity price and avoided coal cost as for the alternative technologies were used for this estimation.

Norway implemented a tax on carbon emissions in 1991, initially set at 260 NOK per tonne of CO2 [37]. This tax has steadily increased over the years, reaching 590 NOK ($59.29) per tonne of CO2 in 2021. According to the climate plan presented to the Norwegian parliament in 2021 by the Norwegian Ministry of Climate and Environment, this tax is planned to rise to 2000 NOK ($200.99) per tonne of CO2 by 2030 [38].

The avoided CO2 emission tax was also considered in the analysis, both for the tax cost in 2021 and the planned tax cost in 2030. In Norway, this tax can be refunded with CO2 capture by submitting an application, making it a significant factor in evaluating the overall cost-efficiency of the project [39].

The cost per avoided tonne of CO2, including the avoided CO2 tax, was calculated for the same avoided coal cost and electricity price as the alternative technology. Additionally, the high electricity price of 2022 (106.2 + 4 øre/kWh) was investigated in calculating the cost per avoided tonne of CO2, including the avoided CO2 tax.

To calculate the avoided 2021 and 2030 CO2 tax cost, the tax was multiplied by the annual avoided CO2 using the following equation:

$$C_{Avoided\ CO2\ tax\ 2021\ price} = Tax_{CO2\ per\ tonne,2021} * \dot{m}_{coal,year} = \frac{\$59.29}{t_{CO_2}} * \frac{696\,744t}{year}$$
$$= \frac{\$41.31M}{year}$$

$$C_{Avoided\ CO2\ tax\ 2030\ price} = Tax_{CO2\ per\ tonne,2030} * \dot{m}_{coal,year} = \frac{\$200.99}{t_{CO_2}} * \frac{696\,744t}{year}$$
$$= \frac{\$140.04\ M}{year}$$

This avoided tax was then subtracted from the OPEX to calculate the updated cost per avoided tonne of CO2. The net present value was adjusted by the following equation:

$$NPV_{OPEX,avoided\ coal\ cost}$$
$$= \left(C_{OPEX} - C_{coal\ consumption\ cost} - C_{Avoided\ CO2\ tax\ price}\right) + (C_{OPEX}$$
$$- C_{coal\ consumption\ cost} - C_{Avoided\ CO2\ tax\ price}) * \frac{1}{(1+i)^1} + \cdots + (C_{OPEX}$$
$$- C_{coal\ consumption\ cost} - C_{Avoided\ CO2\ tax\ price}) * \frac{1}{(1+i)^{n-1}}$$

This approach provides a comprehensive understanding of the total cost of avoided CO2 emissions, including the financial impact of potential tax refunds.

4.5 HAZID

The Hazard Identification (HAZID) study is a fundamental aspect of the risk assessment process, especially when planning the implementation of new systems like the electrolysis hydrogen and oxygen production plant in a cement plant. It is a systematic and proactive approach to identify and understand potential hazards and associated risks that could negatively impact people, the environment, assets, and reputation.

In this thesis, the HAZID study was conducted following a structured methodology. The process began with a comprehensive understanding of the process flow, equipment, and operating procedures related to the electrolysis plant. This initial step ensured that every element of the system was thoroughly considered.

Following this, potential hazards associated with each system element were identified. This identification process considered a wide range of scenarios, including equipment failure, leakage of unignited gas, and leakage of ignited gas. The potential consequences and severity of each hazard were then evaluated to understand the risk level associated with each identified hazard.

Once the hazards were identified and evaluated, risk mitigation measures were proposed. These measures were designed to either eliminate the hazards or reduce the risk associated with them to an acceptable level.

The findings of the HAZID study were documented and are included as an attachment in the appendices.

5 Mass and energy balance calculation results

This chapter will present the results of the mass and energy balance calculations for the calciner system and the electrolyser STACK. These calculations are pivotal in our understanding of the functioning and efficiency of these systems under various operational conditions.

Derived from the methodologies detailed in the preceding chapter, these results offered a quantitative perspective on the operational dynamics of the calciner and the electrolyser STACK. Notably, the balance calculations address the mass flow and energy requirements of these systems, essential parameters that determine the efficiency and feasibility of operations.

By analyzing these calculations, we'll gain insights into the underlying mechanisms of these systems, informing potential strategies for optimization and enhanced performance. The results also serve as a foundation for further simulations and analyses in subsequent chapters.

5.1.1 Calciner

From the mass balance chapter, we can calculate the mass flows in the calciner system:

$$\dot{m}_{CaCO_3} = w_{CaCO_3} * \dot{m}_{preheated\ meal} = 0{,}77 * 205\,000 \frac{kg}{h} = 157\,850\ \frac{kg}{h}$$

$$\dot{m}_{SiO_2} = (1 - w_{CaCO_3}) * \dot{m}_{preheated\ meal} = 0{,}23 * 205\,000 \frac{kg}{h} = 47\,150\ \frac{kg}{h}$$

$$\dot{m}_{CaCO_3,reacted} = \eta_{calc} * \dot{m}_{CaCO_3} = 0{,}94 * 157\,850 \frac{kg}{h} = 148\,379\ \frac{kg}{h}$$

$$\dot{m}_{CaCO_3,non\ reacted} = \left(\dot{m}_{CaCO_3} - \dot{m}_{CaCO_{3\,reacted}}\right) = 9\,471 \frac{kg}{h}$$

$$\dot{n}_{CaCO_3,reacted} = \frac{\dot{m}_{CaCO_3,reacted}}{M_{CaCO_3}} = \frac{148\,379\ \frac{kg}{h}}{\frac{100{,}0869}{1\,000}\ \frac{kg}{mol}} = 1\,482\,460 \frac{mol}{h}$$

$$\dot{m}_{CaO} = \dot{n}_{CaO} * M_{CaO} = 1\,482\,502 \frac{mol}{h} * \frac{56{,}077}{1000}\ \frac{kg}{mol} = 83\,132\ \frac{kg}{h}$$

$$\dot{m}_{CO2} = \dot{n}_{CO_2} * M_{CO_2} = 1\,482\,460 \frac{mol}{h} * \frac{44{,}01}{1000}\ \frac{kg}{mol} = 65\,243\ \frac{kg}{h}$$

The flow of H_2, O_2, and H_2O is dependent upon the energy balance of the system, so we will examine the energy balance before we continue with the mass balance.

From the energy balance, we can calculate the energy into and out of the calciner system:

$$\Delta H^o_{CaCo_3} = \Delta H^o_{f,CaCo_3} - \Delta H^o_{f,CaO} - \Delta H^o_{f,Co_2}$$
$$= \left(-1202{,}06534 - (-640{,}3182495) - (-394{,}9869575)\right)$$
$$= -166{,}760133\ \frac{kJ}{mol}$$

$$E_{CaCO_3,reacted} = \dot{n}_{CaCO_3,reacted} * \Delta H^o_{CaCO_3} = 1\,482\,460 * (-166{,}76) = 247\,215\,226\ \frac{kJ}{h}$$
$$= 68\,670{,}9\ kW = 68{,}671 MW$$

$$\dot{n}_{preheated\ meal}\frac{mol}{h} = \frac{\dot{m}_{CaCO_3}}{M_{CaCO_3}} + \frac{\dot{m}_{SiO_2}}{M_{SiO_2}} = \frac{157\,850\ \frac{kg}{h}}{\frac{100{,}0869}{1000}\ \frac{kg}{mol}} + \frac{47\,150\ \frac{kg}{h}}{\frac{60{,}08}{1000}\ \frac{kg}{mol}} = 2\,361\,916\ \frac{mol}{h}$$

$$Q_{preheated\ meal} = \dot{n}_{preheated\ meal} * Cp_{preheated\ meal} * \Delta T_{prehreated\ meal}$$
$$= 2\,361\,916\ \frac{mol}{h} * \left(\frac{1\,577\,129}{2\,361\,916} * \frac{129{,}7390}{1000} + \frac{784\,786}{2\,361\,916} * \frac{70{,}6915}{1000}\right)$$
$$* (900 - 658))\frac{kJ}{mol} = 62\,942\,400\ \frac{kJ}{h} = 17\,484\ kW = 17{,}484\ MW$$

$$\dot{n}_{H_2} = \frac{(E_{CaCO_3,reacted} + Q_{preheated\ meal})}{LHV_{H_2} - (Cp_{H_2} * \Delta T_{H_2} + Cp_{H_20} * \Delta T_{H_20} + \frac{1}{2} Cp_{O_2} * \Delta T_{O_2})}$$

$$= \frac{(247\,215\,226 + 62\,942\,400)\ \frac{kJ}{h}}{242\frac{kJ}{mol} - \left(\frac{28{,}84}{1000} * (25 - 10) + \frac{45{,}539005}{1000} * (900 - 25) + \frac{1}{2} * \frac{29{,}39}{1000} * (25 - 10)\right)\frac{kJ}{mol}}$$

$$= 1\,539\,241\ \frac{mol}{h}$$

$$\dot{m}_{H_2} = \dot{n}_{H_2} * M_{H_2} = 1\,539\,241\frac{mol}{h} * \left(\frac{2{,}016}{1000}\right)\frac{kg}{mol} = 3\,103{,}11\ \frac{kg}{h}$$

$$\dot{m}_{O_2} = \frac{1}{2}\ \dot{n}_{H_2} * M_{O_2} = \frac{1}{2} * 1\,539\,241\frac{mol}{h} * \left(\frac{32}{1000}\right)\frac{kg}{mol} = 24\,627{,}856\ \frac{kg}{h}$$

$$\dot{m}_{H_2O} = \dot{m}_{H_2} + \dot{m}_{O_2} = 3103{,}11\frac{kg}{h} + 24\,627{,}856\frac{kg}{h} = 27\,731\ \frac{kg}{h}$$

$$Q_{H_2} = \dot{n}_{H_2} * Cp_{H_2} * \Delta T_{O_2} = 1\,539\,241\frac{mol}{h} * \frac{28{,}84}{1000}\frac{kJ}{mol * K} * (25 - 10)K = 665\,875{,}7\frac{kJ}{h}$$
$$= 184{,}97\ kW = 0{,}185\ MW$$

$$Q_{O_2} = \frac{1}{2}\dot{n}_{H_2} * Cp_{O_2} * \Delta T_{O_2} = \frac{1}{2} * 1\,539\,241\frac{mol}{h} * \frac{29{,}39}{1000}\frac{kJ}{mol * K} * (25 - 10)K$$
$$= 339\,287{,}2\frac{kJ}{h} = 94{,}25\ kW = 0{,}094\ MW$$

$$Q_{H_2O} = \dot{n}_{H_2} * Cp_{H_2O} * \Delta T_{H_2O} = 1\,539\,241\frac{mol}{h} * \frac{45{,}539005}{1000}\frac{kJ}{mol * K} * (900 - 25)K$$
$$= 61\,333\,565{,}7\frac{kJ}{h} = 17\,037{,}10\ kW = 17{,}037\ MW$$

$$E_{H_2,comb} = E_{CaCO_3,reacted} + Q_{raw\ meal} + Q_{H_2} + Q_{O_2} + Q_{H_20}$$
$$= (68{,}771 + 17{,}484 + 0{,}185 + 0{,}094 + 17{,}037)MW = 103{,}571\ MW$$

5.1.2 Electrolyser

From calciner system we know the mole flow of hydrogen needed to be produced in the electrolyser:

$$\dot{n}_{H_2} = 1\,539\,241\frac{mol}{h}$$

$$\dot{n}_{O_2} = \frac{1}{2}\dot{n}_{H_2} = \frac{1}{2} * 1\,539\,241\frac{mol}{h} = 769\,620{,}5\frac{mol}{h}$$

$$\dot{n}_{H_2O} = \dot{n}_{H_2} = 1\,539\,241\frac{mol}{h}$$

$$\dot{m}_{H_2} = \dot{n}_{H_2} * M_{H_2} = 1\,539\,241\frac{mol}{h} * \left(\frac{2{,}016}{1000}\right)\frac{kg}{mol} = 3\,103{,}11\frac{kg}{h}$$

$$\dot{m}_{O_2} = \dot{n}_{O_2} * M_{O_2} = 769\,620{,}5\frac{mol}{h} * \left(\frac{32}{1000}\right)\frac{kg}{mol} = 24\,627{,}856\frac{kg}{h}$$

$$\dot{m}_{H_2O} = \dot{m}_{H_2} + \dot{m}_{O_2} = 3103{,}11\frac{kg}{h} + 24\,627{,}856\frac{kg}{h} = 27\,731\frac{kg}{h}$$

The energy balance in the electrolyser STACK is obtained by:

$$I = e^- * F * \dot{n}_{H_2} = 2 * 96{,}485\ \frac{kC}{mol} * 1\,539\,241\frac{mol}{h} = 297\,027\,335{,}8\frac{kC}{h}$$

$$E_{AEL} = (V_{cell} + V_{tn}) * I$$

$$E_{AEL} = (1{,}23 + 0{,}26)\ V * 297\,027\,335{,}8\frac{kC}{h} = 439\,600\,457\frac{kJ}{h} = 122\,936{,}31\ kW$$
$$= 122{,}936\ MW$$

6 Process Simulation

This chapter focuses on the presentation of the results obtained for different cases of the modified calciner system and alkaline electrolyser, providing insight into the proposed system's performance and potential optimization opportunities.

6.1 Process value design parameters

The first step of the simulation process involves verifying and calibrating the model with actual operational data from a cement calciner that uses coal as fuel. Once the model has been calibrated, it is modified to include six different scenarios of gas recycling, with different recycling temperature.

6.2 Aspen Plus model verification

6.2.1 Adiabatic flame temperature and CO_2 emission for coal combustion

In the existing coal combustion process, the results from figure 6.1 showed that a coal usage of 15040 kg/h is necessary for combustion to provide the thermal energy needed in the calciner to reach the exit temperature of 900°C with the provided air usage. The main result shows an adiabatic flame temperature of 2076°C. The energy used to pyrolyze the raw coal amounts to 7.04 MW and is utilized by thermal energy from some of the combusted coal. The total mass flow rate of solids separated from the gas in the cyclone was observed to be 139 756 kg/h, which matches with the manually calculated number. This adiabatic flame temperature will be a parameter for all the following simulations.

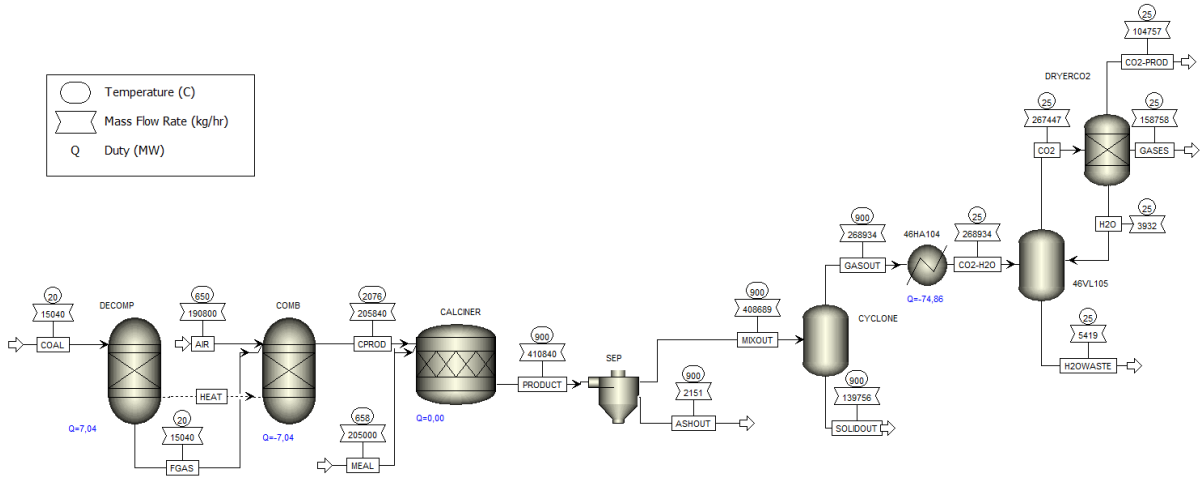

Figure: 6.1: Simulated Coal Combusted Calciner

6.2.2 Modified coal combustion to match real coal consumption

Modifications were made to the original coal combustion model to match the real coal consumption, which was reduced to more realistic 12 000kg/h. The pyrolysis of raw coal was

performed using an external source, and additional thermal energy was supplied to the calciner to maintain the exit temperature of 900℃.

The simulation results in figure 6.2 show that for this coal combustion calciner model, the pyrolysis energy needed from an external source was 5.62 MW. An additional 15.41 MW was needed in the calciner to maintain the desired exit temperature. The CO2 emission was found to be 96 770 kg/h.

The solids out result remained the same at 139 756kg/h with 83 135 kg/h CaO produced, 9 471 kg/h $CaCO_3$ not reacted, and 47 150 kg/h SiO_2 not reacted. The ash out consists of 1 716 kg/h. The energy equivalent in the gas that is needed to be cooled down to 25℃ was 72.93 MW.

The output of H_2O vapor from the calciner was 4 323kg/h. Other gases in the flue gas exiting the calciner included SO_2, N_2, O_2, and others, totaling 165235 kg/h.

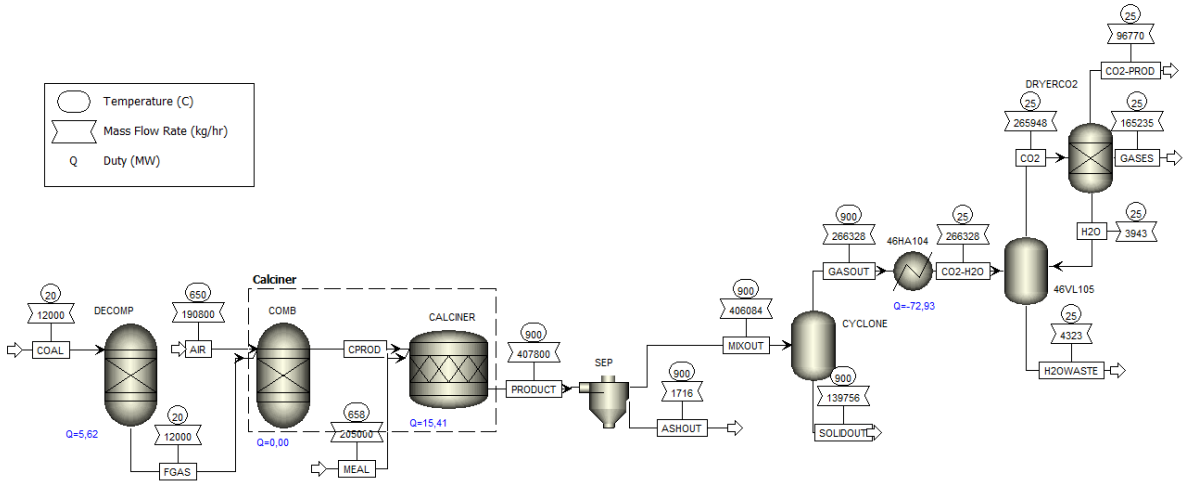

Figure: 5.2: Simulated Modified Coal Combusted Calciner

From this, the coal consumption and the CO_2 emission were used to calculate the cost per avoided tonne CO_2 in this thesis. The annual coal consumption was calculated by the following equation:

$$\dot{m}_{CO_2\ emission,coal\ combustion,year} = \dot{m}_{CO_2\ emission,coal\ combustion} * t_{period}$$
$$= 96.770\frac{t}{h} * 7200\frac{h}{period} = 696\,744\frac{t}{period}$$

6.3 Simulation of calciner modification and flue gas treatment

6.3.1 Adiabatic flame temperature for oxy-fuel hydrogen combustion

In the simulation of oxy-fuel hydrogen combustion, it was found that 3 080 kg/h of H_2 and 24 447 kg/h of O_2 are needed to reach the exit temperature of 900℃ for both the combustion

product (H_2O vapor) and the meal products. This can be observed in figure 6.3. Interestingly, this shows a decrease from the manually calculated need of 3103 kg/h of hydrogen and 24 628 kg/h of oxygen.

The adiabatic flame temperature for hydrogen oxy-fuel combustion was resulted to be 4 734°C. The flow of solids out of the cyclone, downstream of the calciner, remains consistent with previous models and manual calculation results.

To separate the CO_2 from water vapor for carbon capture, the flue gas downstream of the cyclone was cooled to 25°C, requiring an energy input of 50.78 MW. The increased water vapor from hydrogen combustion, separated from CO_2, results in a mass flow rate of 27 530 kg/h. This separation leads to a captured CO_2 mass flow rate of 65 244 kg/h, indicating a reduced CO_2 emission of 31 526 kg/h when compared to coal combustion.

Furthermore, a substantial reduction was observed in the emission of other gases, which was reduced by 165 235 kg/h compared to the coal combustion model. This substantial reduction leads to a cleaner, pure CO_2 outlet stream. This presents a significant advantage as it indicates the potential for effective carbon capture without the need for complex and energy-intensive post-combustion technology.

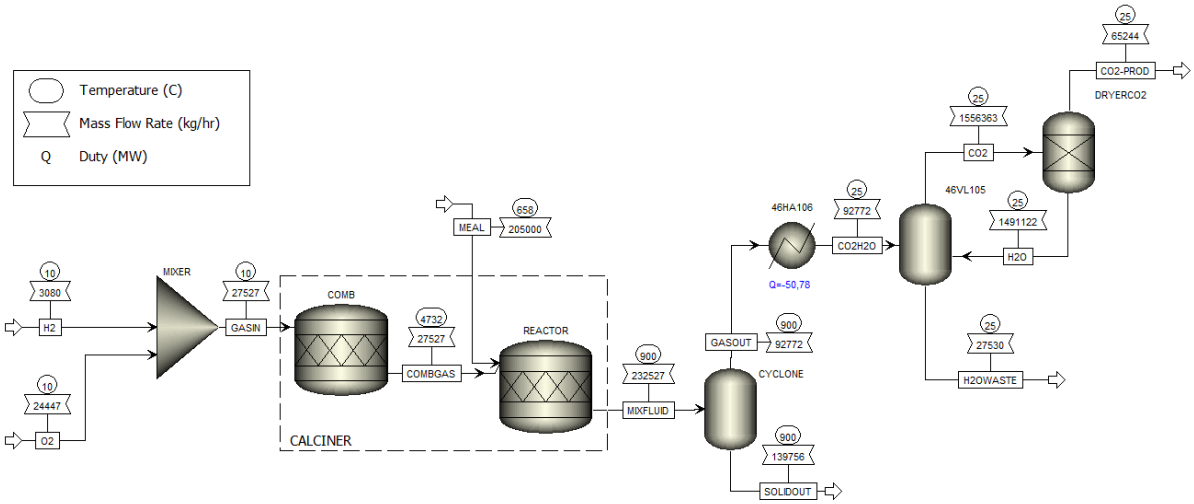

Figure 6.3: Simulated Hydrogen Oxy-Fuel Combusted Calciner

In the same simulation, it was found from figure 6.4 that 71.83 MW is required to react 94% of the $CaCO_3$, and an additional 17.89 MW is needed to heat the meal up to 900°C. This represents an increase of 3.06 MW for the calcination and a minor increase of 0.4 MW for the heating compared to the manually calculated energy results.

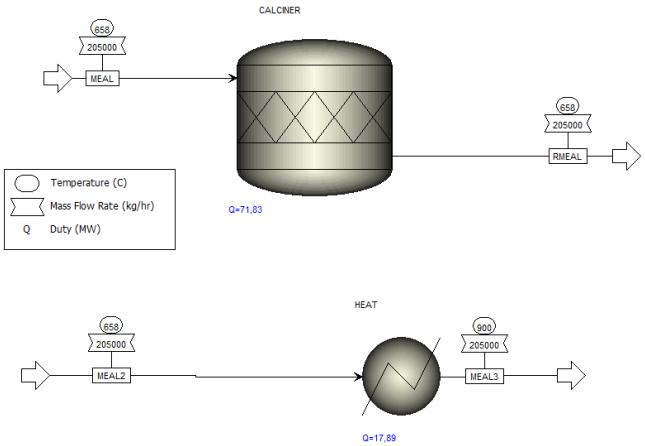

Figure 6.4: Energy Need Calcination Reaction and Heating of Meal

6.3.2 Recycling temperature cases

CO_2 recycling is critical for controlling the high adiabatic flame temperatures associated with H_2/O_2 combustion, resulting in a more regulated and efficient combustion environment.

However, the temperature at which this recycling process is carried out could have significant implications for overall process performance, energy consumption, and emissions. This consideration led to the examination of several different recycling temperature scenarios.

6.3.2.1 H_2/O_2 combustion with 35℃ recycled CO_2

One of the primary objectives of this thesis was to investigate the potential for recycling only CO_2 to moderate the adiabatic flame temperature of the H_2/O_2 combustion, aiming to match the temperature obtained from coal combustion, i.e., 2 076℃. This had to be achieved while still preserving the desired exit temperature of 900℃ in the calciner.

To satisfy these conditions, the flow rates for hydrogen and oxygen input, as well as the recycling rate for CO_2, were adjusted accordingly. The simulation results, in figure 6.5, showed that a hydrogen flow rate of 4 237 kg/h and an oxygen flow rate of 33 631 kg/h were required. Furthermore, the rate of CO_2 recycling needed to be as high as 121 900 kg/h to maintain these parameters. This recycling rate is 54% of the combined total gas flow exiting the calciner.

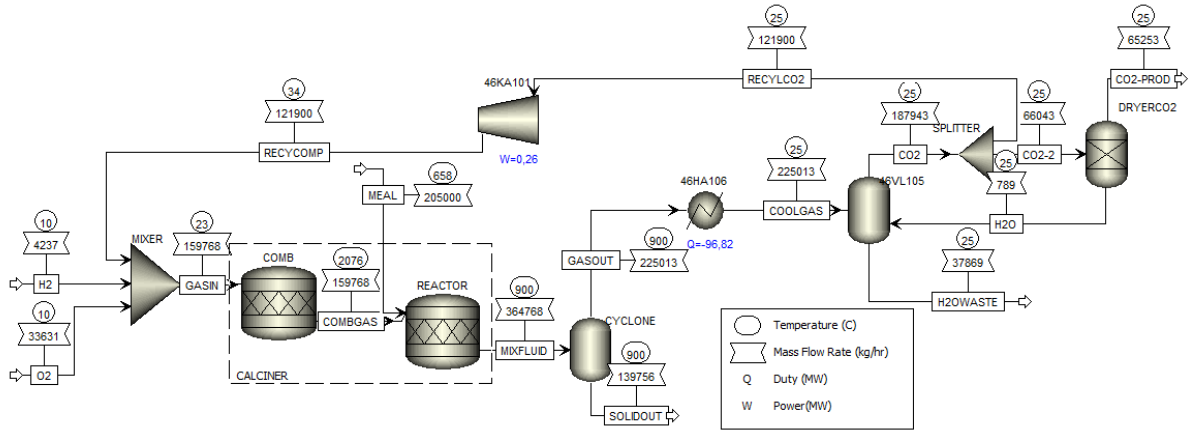

Figure 6.5: H_2/O_2 Combustion with 35℃ Recycled CO_2

The output to the kiln from the cyclone remains unchanged from previous simulation cases. And the energy required for the compressor to recycle the CO_2 resulted in 260 kW.

In terms of the cooling needs for the flue gas, which now includes the recycled CO_2, the required energy increased significantly to 96.82 MW. This is an incredible increase of almost double cooling need, prompting for an energy optimalization need. The amount of CO_2 captured remains consistent with the previous case. Furthermore, the quantity of water vapor condensed from the flue gas increased to 37 869 kg/h. This increase is due to the higher consumption of hydrogen and oxygen in this case. The water separated in *DRYERCO2* block resulted in 789 kg/h.

6.3.2.2 H_2/O_2 combustion with 150℃ recycled CO_2/H_2O

In the simulation showed in figure 6.6, both CO_2 and H_2O vapor are recycled back to the calciner at a temperature of 150℃. The objective was to maintain the adiabatic flame temperature and the desired calciner exit temperature under these new conditions.

To achieve this, the input flow rates for hydrogen and oxygen were adjusted. The results indicate that a decrease in hydrogen flow rate to 4 092 kg/h and an oxygen flow rate of 32 479 kg/h was necessary to maintain the desired parameters. Simultaneously, the recycle rate of CO_2 and H_2O vapor was set to 92 300 kg/h. This recycling rate is 48% of the combined total gas flow exiting the calciner.

This adjusted recycling rate also impacts the energy requirements of the system. Due to the higher recycle temperature, resulting in reduces recycle flow rate and recycled water vapor content, the need for cooling is reduced, with the total cooling capacity required across the now needed two heat exchangers dropping to 91.24 MW.

On the other hand, the energy consumption of the compressor, which is responsible for recycling the CO_2 and H_2O vapor, increases to 400 kW.

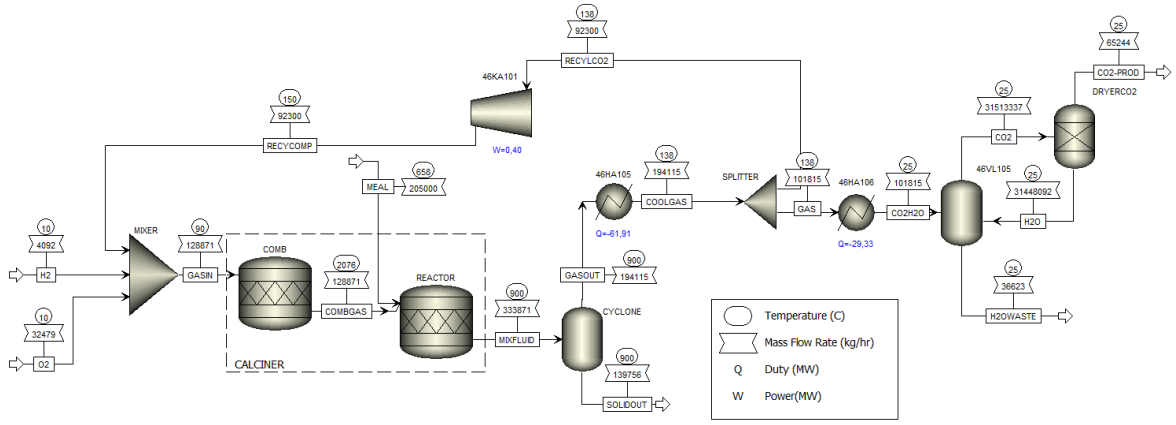

Figure 6.6: H_2/O_2 Combustion with 150℃ Recycled CO_2/H_2O

6.3.2.3 H_2/O_2 combustion with 275℃ recycled CO_2/H_2O

To investigate the effect of further increasing the recycling temperature, simulation in figure 6.7 was run where CO_2 and H_2O vapor were recycled back to the calciner at 275℃. The results showed that a decrease in hydrogen and oxygen flow rates was needed to maintain the adiabatic flame temperature and desired calciner exit temperature. Specifically, the hydrogen flow rate was reduced to 3 959 kg/h and the oxygen flow rate to 31 423 kg/h, while the recycle rate was set at 94 600 kg/h. The recycling rate in this case was 49% of the combined total gas flow exiting the calciner.

Compared to previous simulations, the total cooling needed was further reduced to 86.10 MW. However, the energy consumption of the compressor increased to 530 kW.

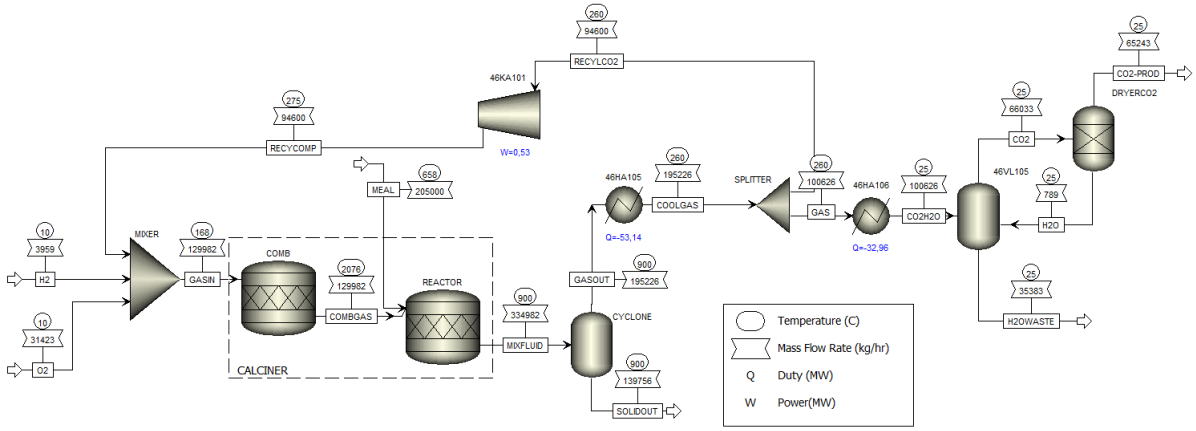

Figure 6.7: H_2/O_2 Combustion with 275℃ Recycled CO_2/H_2O

6.3.2.4 H_2/O_2 combustion with 400℃ recycled CO_2/H_2O

In this simulation, the recycling temperature was further increased to 400°C. This case required a hydrogen flow rate of 3 814 kg/h and an oxygen flow rate of 30 271 kg/h to maintain the adiabatic flame temperature and the desired calciner exit temperature of 900°C. The recycling rate was adjusted to 97 200 kg/h.

The heat exchanger needs have continued to decrease as the recycling temperature increased. In this case, the total cooling energy requirement was reduced to 80.48 MW. The compressor energy consumption, however, increased to 670 kW. The simulation can be observed in figure 6.8.

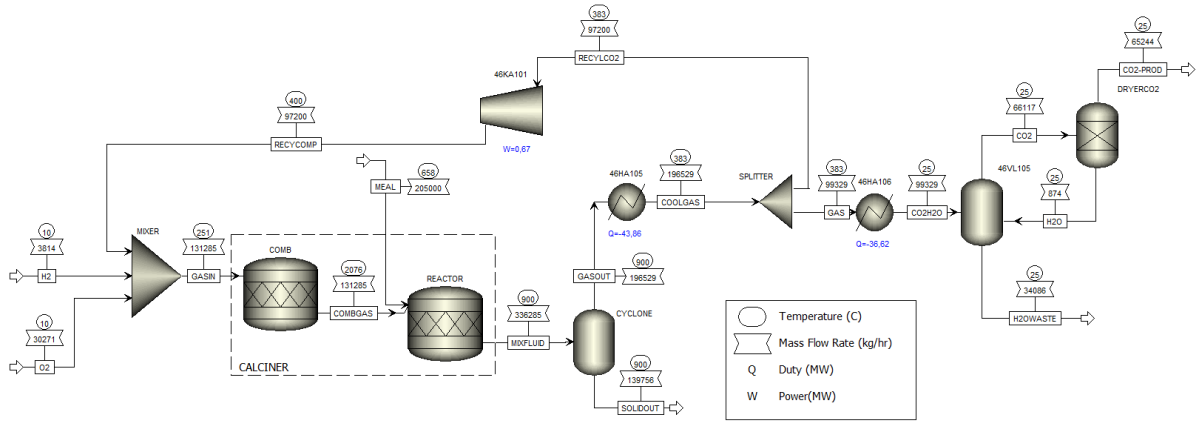

Figure 6.8: H_2/O_2 Combustion with 400℃ Recycled CO_2/H_2O

6.3.2.5 H_2/O_2 combustion with optimized heat exchange at 878℃ recycled CO_2/H_2O

Intrigued by the observations from the previous simulations, we proceeded to create a model with an even higher recycling temperature, see figure 6.9. For this purpose, a 2-stream counter current heat exchanger block (*46HA104*) was utilized to heat exchange the flue gas at 900℃ with the recycled CO_2/H_2O gas at 417℃ downstream the compressor. This resulted in a recycled gas temperature of 878℃ (without exceeding the set minimum pinch temperature of 20℃).

The flue gas temperature was lowered to 659℃ through *46HA104*, which was further cooled to 400℃ by *46HA105* for the split recycling flow rate entering the compressor. To maintain the adiabatic flame temperature and the desired calciner exit temperature, the hydrogen flow rate was reduced to low 3 115 kg/h and the oxygen flow rate to 24 719 kg/h. This is almost as low as the calciner modification without recycling use. The recycle rate was increased to 110 050 kg/h.

Notably, the total energy required for cooling continued to decrease, dropping to 52.79 MW in this case. As the recycling temperature increased and flowrate, the compressor energy consumption rose to 740 kW.

The recycling rate for this case rose to 54% of the combined total gas flow exiting the calciner, a further increase from the previous cases. This indicates that higher recycling temperatures could potentially lead to higher recycling rates and lower H_2/O_2 consumption. However, these benefits must be balanced against the increased energy consumption for compression.

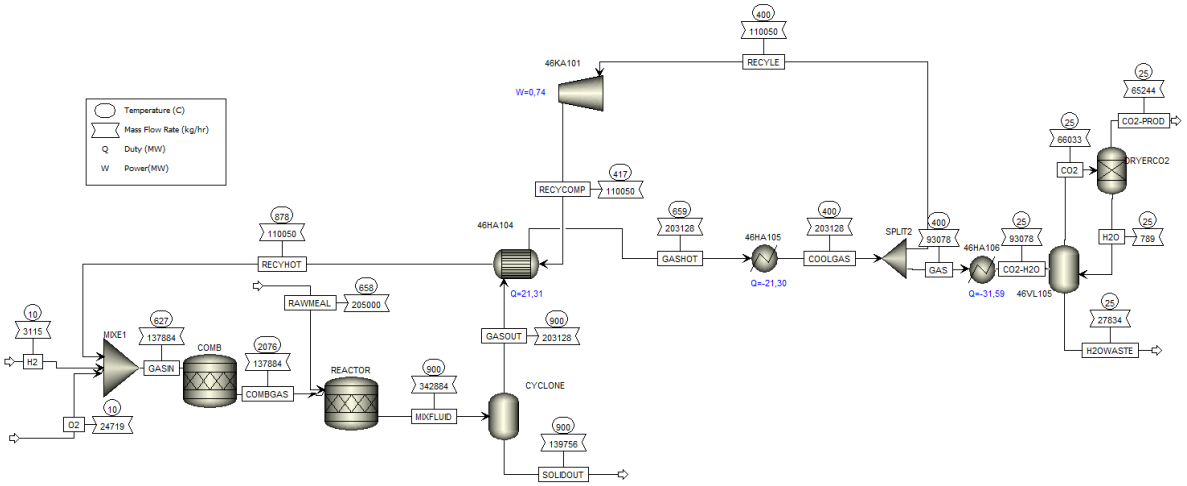

Figure 6.9: H_2/O_2 Combustion with Optimized Heat Exchange at 878℃ Recycled CO_2/H_2O

6.3.3 H_2/O_2 combustion with optimized split heat exchange with Clinker Cooler air

An intriguing opportunity surfaced from the plant's ability to utilize 83 400 kg/h of air at 200℃, sourced from the Clinker Cooler. This air could serve the dual purpose of cooling down the flue gas while simultaneously preheating the meal in the cyclone preheaters within this modified process.

To implement this, a split in the flue gas downstream of the *Cyclone* was introduced. One stream continues to heat the recycled flue gas in heat exchanger block *46HA104A*, while the other stream is cooled by the air from the *Clinker Cooler* (not modelled), necessitating an additional 2-stream counter current heat exchanger block (*46HA104B*). see figure 6.10.

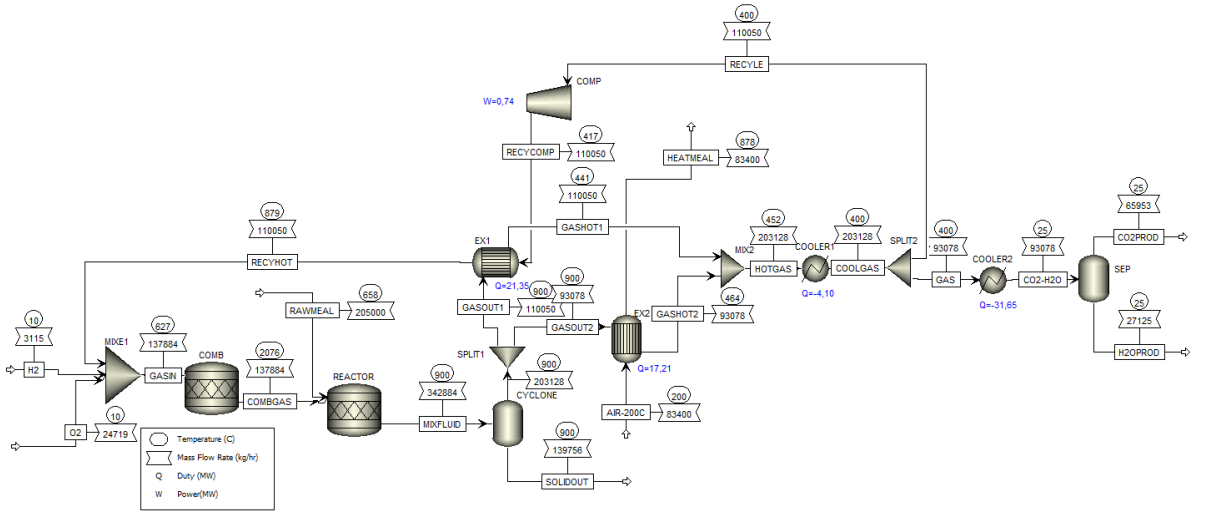

Figure 6.10: H_2/O_2 Combustion with Optimized Split Heat Exchange with Clinker Cooler Air at 879℃ Recycled CO_2/H_2O

The heat exchange between the split flue gas at 900°C and the recycled CO_2/H_2O gas at 417°C results in the flue gas being cooled to 441°C, thereby maintaining the recycled gas temperature at 879°C, without exceeding the set minimum pinch temperature of 20°C.

The other split flue gas stream, now at 464°C, is further cooled to 400°C before it joins the split recycling flow rate entering the compressor. This adjustment lowers the cooling requirement to only 35.75 MW, which is less than that of the original H_2/O_2 combustion modification without recycling. The rest of the system remains unaffected by this change.

Moreover, the energy exchanged in heat exchanger block *46HA104B* to increase the air temperature to 878°C was noted to be 17.21 MW, showcasing an efficient utilization of heat energy.

6.3.4 H_2/O_2 combustion at 3000°C adiabatic flame temperature

Exploring the potential for higher operating temperatures in the calciner, up to an adiabatic flame temperature of 3 000°C, could bring intriguing shifts in both CAPEX and OPEX. This increase in temperature could be possible with advancements in calciner material, strategies to protect the calciner wall such as swirling the meal around the burner, having a shorter hydrogen jet flame compared to coal, or through other innovative methods.

The system model for this case is the same as the previous case, with the significant alteration being the acceptance of a higher adiabatic flame temperature. As a result, the simulation shows intriguing shifts in the process parameters and resultant efficiencies. See figure 6.11.

The hydrogen usage is reduced to 3 092 kg/h, and oxygen usage is decreased to 24 543 kg/h. The recycling rate drops considerably to 39 550 kg/h, leading to a lower power requirement for the compressor, now only consuming 266 kW. The energy transferred in heat exchanger block 46HA104A also decreases significantly. This enables lower CAPEX cost for *46HA104A*, *46KA101*, and *46HA105*. For manual equipment cost calculation, the software provided the lower required heat transfer area for *46HA104A* (190 m^2) and the lower power used by *46KA101* (266 kW).

The requirement for cooling falls to as low as 34.30 MW.

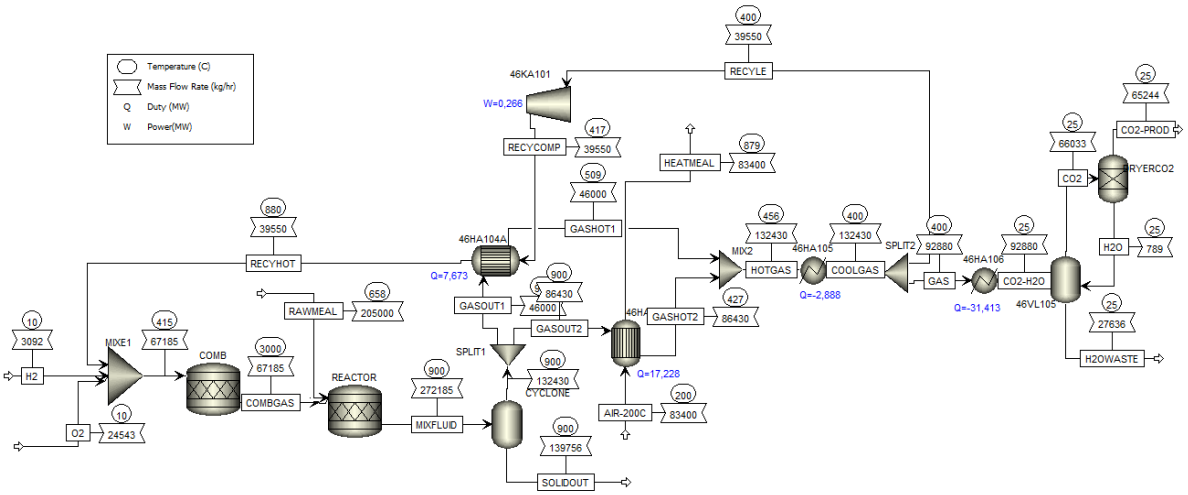

Figure 6.11: H_2/O_2 Combustion at 3000°C adiabatic flame temperature

6.4 Simulation of alkaline electrolyser

The simulation of the alkaline electrolyser system was carried out using four models, with one model specifically set to match the hydrogen production requirement determined from the mass and energy balance calculations equal to 3 103 kg/h. The goal of that model was to validate the calculated energy requirements using an Aspen Plus model to ensure consistency and accuracy in the process design. The rest of the models are investigating the energy usage at different energy efficiencies in current existing technology and one possible future efficiency, for the hydrogen production requirement determined from the calciner simulation result for combustion with optimized heat exchange at 878℃ recycled CO_2/H_2O equal to 3 103 kg/h hydrogen.

6.4.1 Alkaline electrolyser model validation

The electrolyser model was established with a water reaction rate of 30%, with the remaining electrolyte circulating through the system. This rate was chosen to represent the circulation need for optimized cell response for an industrial-scale alkaline electrolyser.

The simulation, seen in figure 6.12, resulted in the production of the required hydrogen amount of 3 103 kg/h and a corresponding energy requirement in the *STACK* was shown to be 122.936 MW. This result is perfectly consistent with the calculated energy requirement from the mass and energy balance calculations, which provides confidence in the accuracy of the model and the assumptions made.

Notably, there was no heat generation within the *STACK*, which indicates that all the input energy was utilized in the electrolysis process. However, there was a minor heating requirement of 1.24 MW to raise the electrolyte temperature to the desired inlet temperature of 70℃. This heating demand arises due to the cooling effect of the fresh make-up water on the circulating electrolyte, which lowered the electrolyte temperature to 59℃ before it was subsequently heated.

In addition, the energy required to condense the water vapor from the hydrogen and oxygen gas streams was resulting to be 1.08 MW and 0.32 MW, respectively. These results underline the cooling requirements associated with the gas product streams in the electrolysis process.

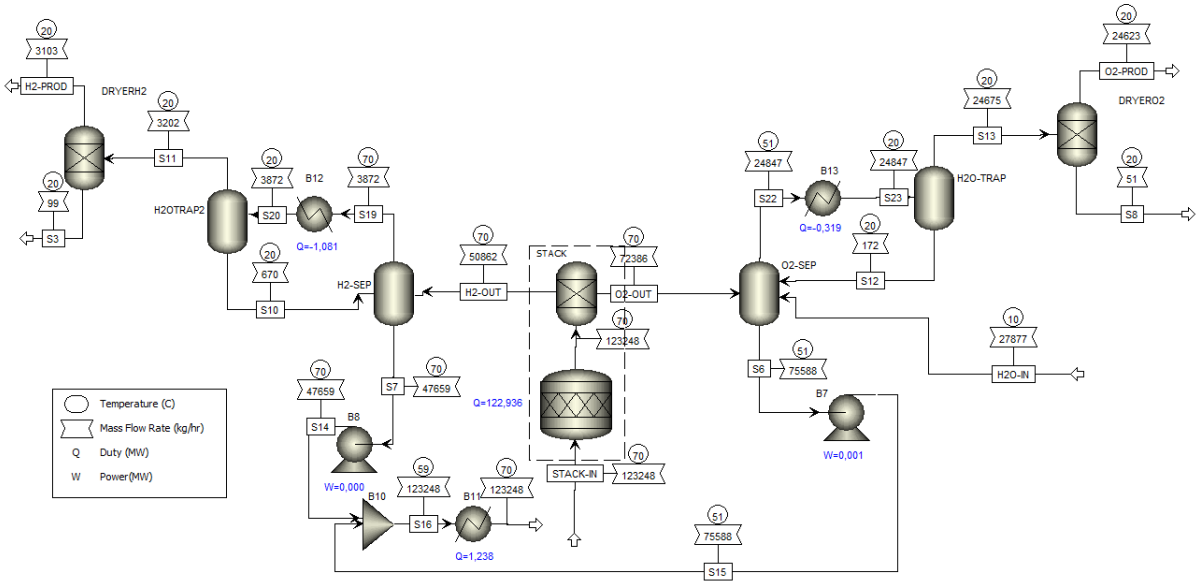

Figure 6.12: Alkaline Electrolyser Model Validation

6.4.2 Possible future efficiency

With the validation of the electrolyser model established, the next step in the analysis was to simulate an increased hydrogen production scenario. This increase in hydrogen production mirrors the requirements set by the increased hydrogen consumption in the calciner, as discussed in the previous sections.

In this scenario, the hydrogen production was increased to 3 115 kg/h. The purpose of this simulation was to observe the effect of increased hydrogen production on the energy usage and cooling requirements of the system, providing a more complete picture of the potential operational changes required in response to the increased hydrogen demand.

Following the simulation in figure 6.13, it was observed that the cooling requirement for the electrolyte in the heat exchanger *46HA103* increased to 1.20 MW. This increase is a direct consequence of the higher hydrogen production rate, which raises the thermal load on the system.

Similarly, the cooling requirements for the hydrogen and oxygen gas streams also increased. The cooling need for the hydrogen side (*46HA101*) increased to 1.11 MW, and for the oxygen side (*46HA102*), it increased to 0.33 MW. This represents an increase in the thermal duty of these cooling operations, reflecting the increased thermal load associated with the increased hydrogen and oxygen production.

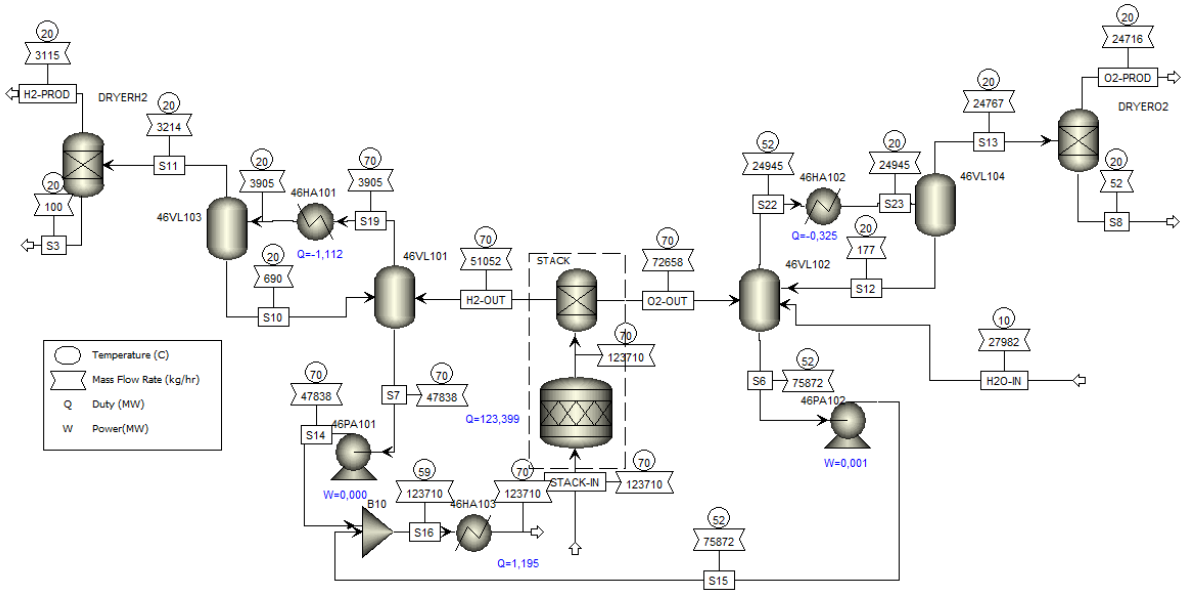

Figure 6.13: Alkaline Electrolyser 123MW

6.4.3 Peak electrolyser efficiency

Another important consideration in the analysis of the electrolyser system was to simulate its operation at peak efficiency. This simulation was based on NEL Hydrogen's highest real-world efficiency value within their efficiency range. The aim was to determine the energy usage in the *STACK* required to produce the desired hydrogen output of 3 115 kg/h, a figure that corresponds to the simulation results for the optimized heat exchange in the calciner.

Through calculation, the energy required in the *STACK* was determined to be 131.598 MW. As this efficiency is no longer theoretical, but instead based on real-world performance data, this results in an increase in excess heat in the *STACK*. Consequently, an increase in electrolyte flow circulation was required to maintain the desired *STACK* temperature of 70°C.

To achieve this, the inlet temperature was adjusted down to 20°C, and the H_2O reaction rate was experimentally adjusted to maintain the *STACK* temperature. It's important to note that the circulation rate is directly affected by the reaction rate. The unreacted H_2O will continue to circulate in the system, and the production rate of hydrogen is also affected by this reaction rate. This necessitates adjusting the circulation rate and water make-up filling accordingly to manage the system effectively.

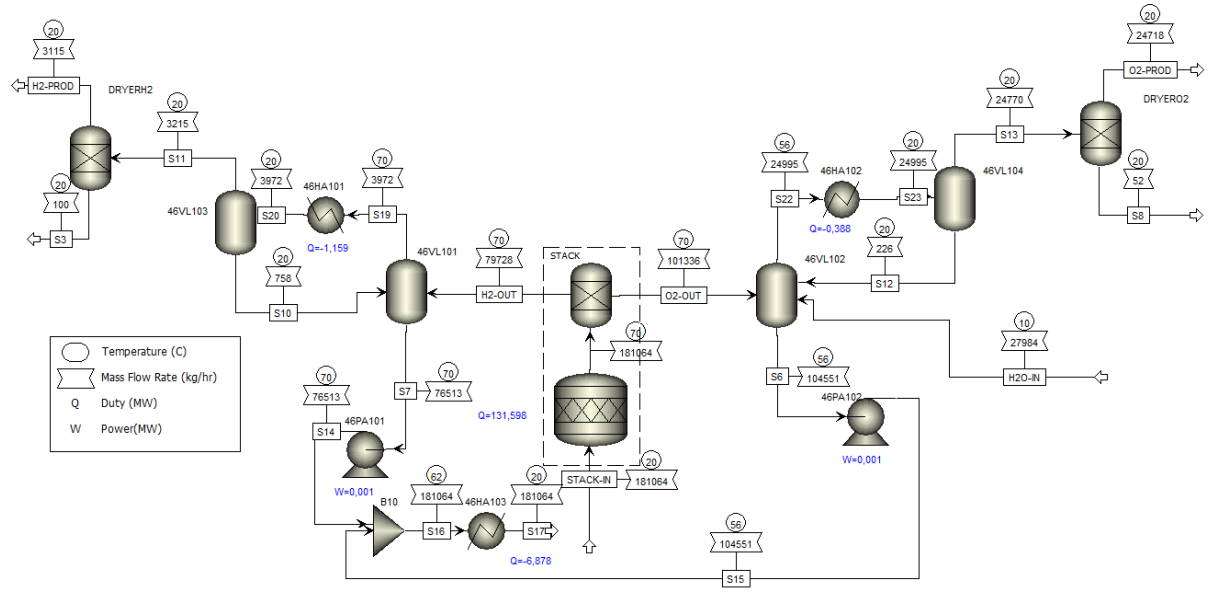

Figure 6.14: Alkaline Electrolyser 131MW

In the simulation in figure 6.14, the reaction rate of H_2O was adjusted to 20.5% to maintain the desired temperature within the *STACK*. As a result, the cooling needs of the system changed notably. The cooling requirement for the circulating electrolyte in the *46HA103* heat exchanger increased to 6.88 MW, necessary to reduce the electrolyte temperature from 62°C down to the lower inlet temperature of 20°C.

Meanwhile, the cooling needs for the *46HA101* and *46HA102* exchangers showed a slight increase to 1.16 MW and 0.39 MW, respectively. These values are quite like those from the previous simulation, which produced the same quantity of hydrogen (3115 kg/h). This similarity indicates that the cooling needs for condensation are primarily dependent on the gas production rate, rather than the overall system efficiency.

However, the cooling requirements for the electrolyte saw a significant increase. This is largely due to the higher circulation rate required to manage the excess heat from the *STACK*, along with the need to cool the electrolyte to a lower inlet temperature of 20°C (as opposed to heating it to 70°C in the previous simulation). This result highlights the increased thermal management demands when operating the electrolyser at less optimized efficiency.

6.4.4 Minimum electrolyser efficiency

In the scenario shown in figure 6.15, it was simulated the operation of the electrolyser using NEL Hydrogen's lowest real efficiency in their range. This was done to determine the energy usage in the *STACK* needed to produce the desired amount of 3 115 kg/h of hydrogen. Based on calculations, the energy requirement was determined to be 152.373 MW. This level of energy use in the *STACK* results in more excess heat, necessitating a greater electrolyte flow circulation to maintain the temperature within the *STACK*.

The reaction rate of H_2O was adjusted downward experimentally, resulting in a rate of 5.8% to maintain the desired *STACK* temperature.

Consequently, the cooling requirement for the circulating electrolyte in the *46HA103* heat exchanger significantly increased to 27.42 MW. This cooling effort is required to bring down the electrolyte temperature from 68℃ to the lower inlet temperature of 20℃.

Meanwhile, the cooling needs for the *46HA101* and *46HA102* exchangers showed changes as well. The cooling requirement for *46HA101* remained quite like the previous simulations at 1.12 MW. However, *46HA102* had a higher cooling need of 0.539 MW. The latter increase is mainly due to the decreased cooling effect from the water make-up in the knockout drum *46VL102*. This is a result of the higher electrolyte circulation.

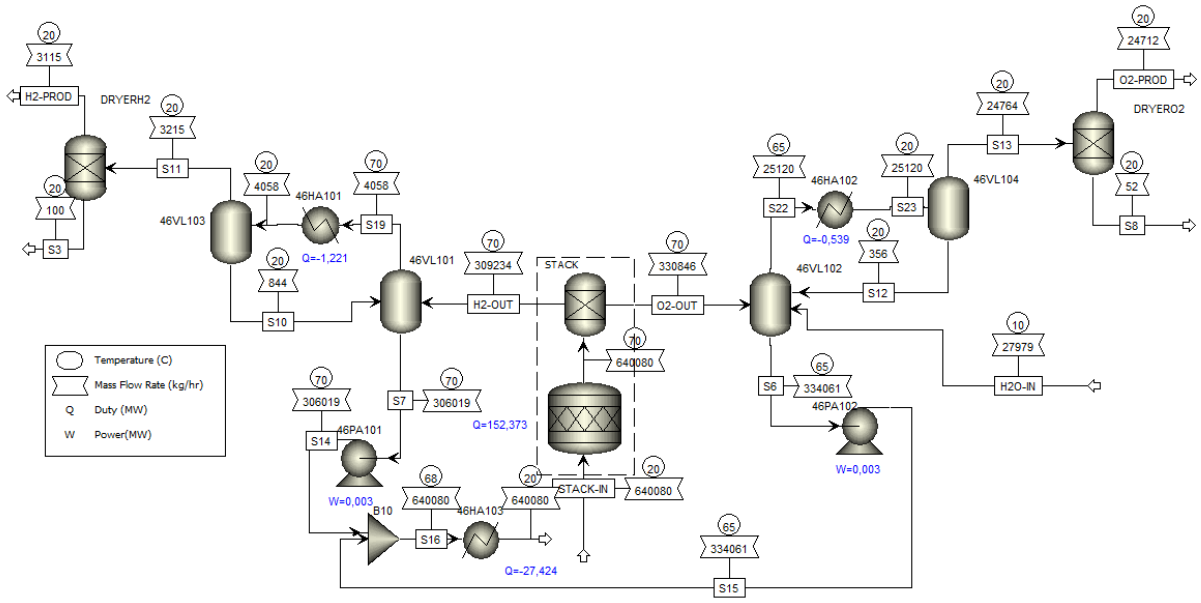

Figure 6.15: Alkaline Electrolyser 152MW

6.4.5 Electrolysis for H_2/O_2 combustion at 3000℃ adiabatic flame temperature

The simulation case for the calciner with H_2/O_2 combustion at an adiabatic flame temperature of 3 000℃ necessitated a hydrogen production rate of 3 090 kg/h. This electrolyser scenario was modeled for the minimum efficiency scenario.

Minimum Efficiency Scenario: Operating at its minimum efficiency, the electrolyser requires a slightly lower energy input of 151.25 MW and a water reaction rate of the same 5.8%. The electrolyte heating demand was similar at 27.12 MW. Cooling requirements for the hydrogen and oxygen gas sides are 1.20 MW and 0.53 MW, respectively. This can be observed in figure 6.16.

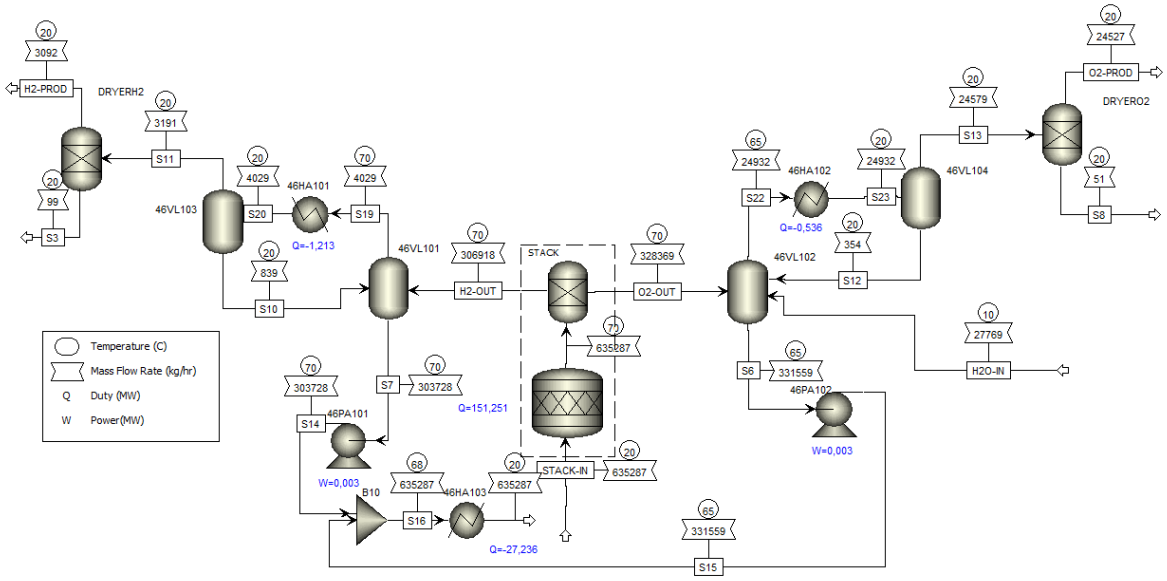

Figure 6.16: 3000°C H_2 prodution Alkaline Electrolyser 151MW

7 Cost Estimation of Modified System

This chapter delves into the detailed cost estimation of the proposed system modification, including the estimation of capital investment costs, operational expenses, and cost per avoided tonne of CO_2 emissions utilizing Aspen Process Economic Analyzer.

7.1 Equipment cost estimation

To provide supplementary cost information on some heat exchangers and a compressor that encounter errors in the cost calculation within the Aspen software, we will calculate the equipment cost using known cost estimation techniques.

The compressor equipment cost was calculated by:

$$c_{COMP,CS,2010} = a + b * S^n = 580\,000 + 20\,000 * 740^{0,6} = \$1\,633\,341$$

$$c_{COMP,SS,2010} = c_{COMP,CS,2010} * f_m = \$1\,633\,341 * 1.3 = \$2\,123\,343$$

$$c_{COMP,SS,2023} = c_{2010} * \frac{INDEX_{2023}}{INDEX_{2010}} = \$2\,123\,343 * \frac{801,4}{550,8} = \$3\,089\,410$$

Some of the heat exchanger equipment costs was calculated according to:

$$c_{46HA104A,CS,2010} = a + b * S^n = 28\,000 + 54 * 1126^{1,2} = \$275\,879$$

$$c_{46HA104A,NI,2010} = c_{46HA104A,CS,2010} * f_m = \$275\,879 * 1,7 = \$468\,994$$

$$c_{46HA104A,NI,2023} = c_{46HA104A,NI,2010} * \frac{INDEX_{2023}}{INDEX_{2010}} = \$468\,994 * \frac{801,4}{550,8} = \$682\,375$$

$$c_{46HA104B,CS,2010} = a + b * S^n = 28\,000 + 54 * 210^{1,2} = \$61\,041$$

$$c_{46HA104B,NI,2010} = c_{46HA104B,CS,2010} * f_m = \$61\,041 * 1,7 = \$103\,770$$

$$c_{46HA104B,NI,2023} = c_{46HA104B,NI,2010} * \frac{INDEX_{2023}}{INDEX_{2010}} = \$103\,770 * \frac{801,4}{550,8} = \$150\,983$$

For the case without split exchange, it was calculated manually the equipment cost of *46HA104* and an electrical heater, *AIR-EX*, for the air from Clinker Cooler:

$$c_{46HA104,CS,2010,274m2} = a + b * S^n = 28\,000 + 54 * 274^{1,2} = \$73\,467$$

$$c_{46HA104,NI,2010,274m2} = c_{46HA104,CS,2010,274m2} * f_m = \$73\,467 * 1,7 = \$124\,894$$

$$c_{46HA104,NI,2023,274m2} = c_{46HA104,NI,2010,274m2} * \frac{INDEX_{2023}}{INDEX_{2010}} = \$124\,894 * \frac{801,4}{550,8} = \$181\,716$$

Heat exchangers of different size is normally compared by their area, however we do not know the size of the needed electrical heat exchanger, as there is modest literature on the size and cost of electrical heat exchangers, we can therefore compare the known needed energy

usage to the energy usage for the cost of a 200 kW stainless steel electric heater in Aspen Plus's library:

$$C_{AIR-EX,without\ split\ EX,SS304,200kW} = \$13\ 600$$

$$C_{AIR-EX,without\ split\ EX,SS304,17\ 220kW} = C_{AIR-EX,without\ split\ EX,SS304,200kW} * \left(\frac{Q}{Q_B}\right)^e$$

$$= \$13\ 600 * \left(\frac{17\ 220\ kW}{200\ kW}\right)^{0.68} = \$281\ 410$$

7.2 Aspen Process Economic Analyzer cases

In this section, we conduct cost estimation simulations for the modified calciner and electrolyser systems under varying conditions. The analysis considers three different electrolysis efficiencies, two quoted electrolyser prices, and fluctuating electricity prices for energy intensive industry. These diverse scenarios provide a robust understanding of the systems' economic viability under a range of potential real-world conditions.

Furthermore, one simulation is modified to be directly cost comparable with recent alternative technologies research for the same system. In addition, a scenario with less optimized heat exchange for the flue gas was explored. Lastly, a cost estimation scenario with an allowable higher adiabatic hydrogen flame temperature of 3000℃ was investigated.

The simulations are performed using the Aspen Process Economic Analyzer, a powerful tool that allows us to comprehensively evaluate the costs associated with each scenario. Through these simulations, we gain insights into the economic implications of specific operational decisions, providing a foundation for informed strategic planning.

7.2.1 Base parameters

The base parameters for the cost simulation are the production need of 3115 kg/h from the electrolyser with the optimized split exchange scenario in the calciner model. All three electrolysers will be investigated.

7.2.2 Cost estimation calculation example

The Aspen Plus simulation results, with electricity price of $0.0336412 per kWh, showed the following result seen in Table 7.1.

Table 7.1: Electricity price 33.475 øre/kWh + 4 øre/kWh (*energiledd*)

Energy usage electrolyser	CAPEX		OPEX	
	2023	2025	2023	2025
123MW	$125.479 M	$84.656 M	$\frac{\$36.220\ M}{year}$	

131MW	\$133.098 M	\$89.563 M	$\frac{\$38.466\ M}{year}$
152MW	\$152.655 M	\$102.247 M	$\frac{\$44.345\ M}{year}$

This table shows the CAPEX is 33% higher for the 2023 compared to the estimated cost in 2025. The results indicate a significant difference in CAPEX between the 2023 and 2025 scenarios. Specifically, the CAPEX for a 152 MW electrolyser is \$152.655 M for 2023 and \$102.247 M for 2025—a decrease of \$50.408 M.

For the 123 MW electrolyser, the CAPEX was \$125.479 M for 2023 and \$84.656 M for 2025, with an OPEX of \$36.220 M/year. For the 131 MW electrolyser, the corresponding figures were \$133.098 M (2023), \$89.563 M (2025), and an OPEX of \$38.466 M/year. For the 152 MW electrolyser, the OPEX was \$44.345 M/year.

The OPEX, however, shows a consistent increase from the 123 MW to the 131 MW to the 152 MW electrolyser energy usage. This increase is primarily due to the higher electricity consumption in the electrolyser and a minor increase in utility usage for cooling the recirculating electrolyte.

To calculate the cost per avoided tonne CO2 for the 123 MW electrolyser case with 2023 STACK CAPEX, we consider an electricity price of \$0.0336412 per kWh. Detailed calculations for this scenario are provided as follows:

$$NPV_{CAPEX,123MW,2023} = \$125.479\ M$$

$$NPV_{OPEX,123MW,2023} = 36.22 + 36.22 * \frac{1}{(1+0.045)^1} + 36.22 * \frac{1}{(1+0.045)^2} + \cdots + 36.22 * \frac{1}{(1+0.045)^{19}} = \$492.343\ M$$

$$NPV_{total,123MW,2023} = NPV_{CAPEX,123MW,2023} + NPV_{OPEX,123MW,2023} = \$125.479\ M + \$492.343\ M = \$617.822\ M$$

$$EAC_{CAPEX,123MW,2023} = \frac{NPV_{CAPEX,123MW,2023}}{a_f} = \frac{125\ 479\ 000}{13.008} = \frac{\$9.646\ M}{year}$$

$$EAC_{OPEX,123MW,2023} = \frac{NPV_{OPEX,123MW,2023}}{a_f} = \frac{\$492.343\ M}{13.008\ \frac{1}{year}} = \frac{\$37.849\ M}{year}$$

$$EAC_{total,123MW,2023} = \frac{NPV_{total,123MW,2023}}{a_f} = \frac{\$617.822\ M}{13.008 \frac{1}{year}} = \frac{\$47.496\ M}{year}$$

$$Cost\ per\ tonne\ CO2\ avoided_{CAPEX,123MW,2023} = \frac{EAC_{CAPEX,123MW,2023}}{\dot{m}_{CO_2,coal\ combustion,year}} = \frac{\frac{\$9.646\ M}{year}}{696\ 744\frac{t}{year}} = \frac{\$13.844}{t_{CO_2\ avoided}}$$

$$Cost\ per\ tonne\ CO2\ avoided_{OPEX,123MW,2023} = \frac{EAC_{OPEX,123MW,2023}}{\dot{m}_{CO_2,coal\ combustion,year}} = \frac{\frac{\$37.849\ M}{year}}{696\ 744\frac{t}{year}} = \frac{\$54.323}{t_{CO_2\ avoided}}$$

$$Cost\ per\ tonne\ CO2\ avoided_{total,123MW,2023} = \frac{EAC_{total,123MW,2023}}{\dot{m}_{CO_2,coal\ combustion,year}} = \frac{\frac{\$47.496\ M}{year}}{696\ 744\frac{t}{year}} = \frac{\$68.168}{t_{CO_2\ avoided}}$$

By eliminating the coal consumption in the existing coal combustion simulation, we can remove the coal cost seen below.

$$C_{coal\ consumption\ avoided\ cost} = \frac{\$15.397\ M}{year}$$

Then:

$$NPV_{OPEX,123MW,2023,avoided\ coal\ cost} = (37.86 - 15.40) + (37.86 - 15.40) * \frac{1}{(1+0.045)^1} + (37.86 - 15.40) * \frac{1}{(1+0.045)^2} + \cdots + (37.86 - 15.40) * \frac{1}{(1+0.045)^{19}} = \$283.055\ M$$

$$NPV_{total,123MW,2023,avoided\ coal\ cost} = NPV_{CAPEX,123MW,2023} + NPV_{OPEX,123MW,2023,avoided\ coal\ cost} = 125.479\ M\$ + \$283.055\ M = \$408.534\ M$$

$$EAC_{OPEX,123MW,2023,avoided\ coal\ cost} = \frac{NPV_{OPEX,123MW,2023,avoided\ coal\ cost}}{a_f} = \frac{\$283.055\ M}{13.008\ \frac{1}{year}} = \frac{\$21.760M}{year}$$

$$EAC_{total,123MW,2023,avoided\ coal\ cost} = \frac{NPV_{total,123MW,2023,avoided\ coal\ cost}}{a_f} = \frac{\$408.534\ \ M}{13.008\frac{1}{year}} = \frac{\$31.406\ M}{year}$$

When assuming all CO_2 gas from the flue gas in the existing coal combusted simulation case is avoided, we can calculate the cost per avoided CO_2 unit by the following equation:

$$\dot{m}_{CO_2\ emission,coal\ combustion,year} = \dot{m}_{CO_2\ emission,coal\ combustion} * t_{period}$$
$$= 96.770\frac{t}{h} * 7200\frac{h}{year} = 696\,744\frac{t}{year}$$

$$Cost\ per\ tonne\ CO2\ avoided_{OPEX,123MW,2023,avoided\ coal\ cost}$$
$$= \frac{EAC_{OPEX,123MW,2023,avoided\ coal\ cost}}{\dot{m}_{CO_2,coal\ combustion,year}} = \frac{\frac{\$21.760\ M}{year}}{696\,744\frac{t}{year}} = \frac{\$31.231}{t_{CO_2\ avoided}}$$

$$Cost\ per\ tonne\ CO2\ avoided_{total,123MW,2023,avoided\ coal\ cost}$$
$$= \frac{EAC_{total,123MW,2023,avoided\ coal\ cost}}{\dot{m}_{CO_2,coal\ combustion,year}} = \frac{\frac{\$31.406\ M}{year}}{696\,744\frac{t}{year}} = \frac{\$45.076}{t_{CO_2\ avoided}}$$

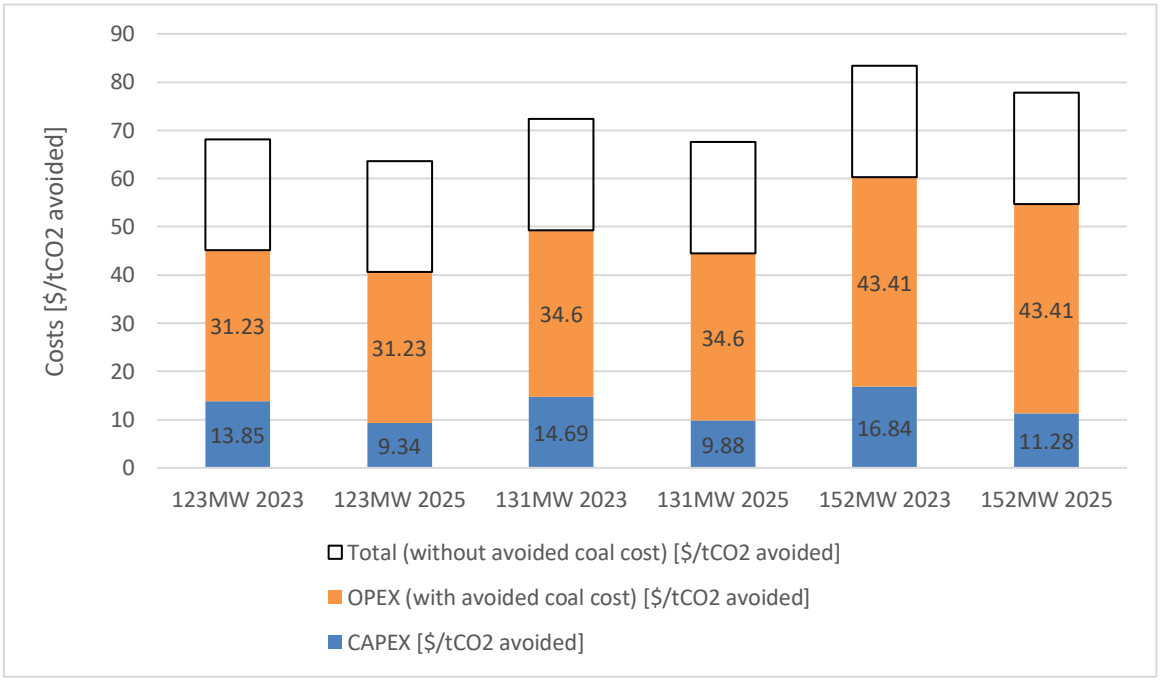

Figure 7.1: Cost per avoided tonne CO_2 – Electricity price 33.475 øre/kWh = $0.03364/kWh

Figure 7.1 in this section depicts the calculated cost per avoided tonne CO2 considering CAPEX, OPEX (with and without the avoided coal cost), for all simulated scenarios. The graph illustrates how the CAPEX cost is influenced by the energy consumption in the STACK and the technology maturity, evidenced by the significantly lower installation cost for future STACK CAPEX estimated in 2025 compared to 2023.

7.2.3 Average electricity spot price 2012-2020

In this section, we explore the impact of average electricity spot prices from 2012 to 2020 on the operational costs of the system. These historic figures provide a realistic context for assessing the potential cost implications of the modified system.

When considering the average electricity spot price from 2012 to 2020, the CAPEX remains unchanged, but the OPEX decreases due to the lower electricity costs for operating the electrolyser STACK and other equipment. The resulting OPEX for the 123 MW, 131 MW, and 152 MW electrolysers were $30.786 M/year, $32.673 M/year, and $37.643 M/year, respectively, see table 7.2.

Table 7.2: Average electrical spot price 2012-2020 (27,43 øre/kWh + 4 øre/kWh)

Energy usage electrolyser	OPEX	
	2023	2025
123MW	$\frac{\$30.786\ M}{year}$	
131MW	$\frac{\$32.673\ M}{year}$	
152MW	$\frac{\$37.643\ M}{year}$	

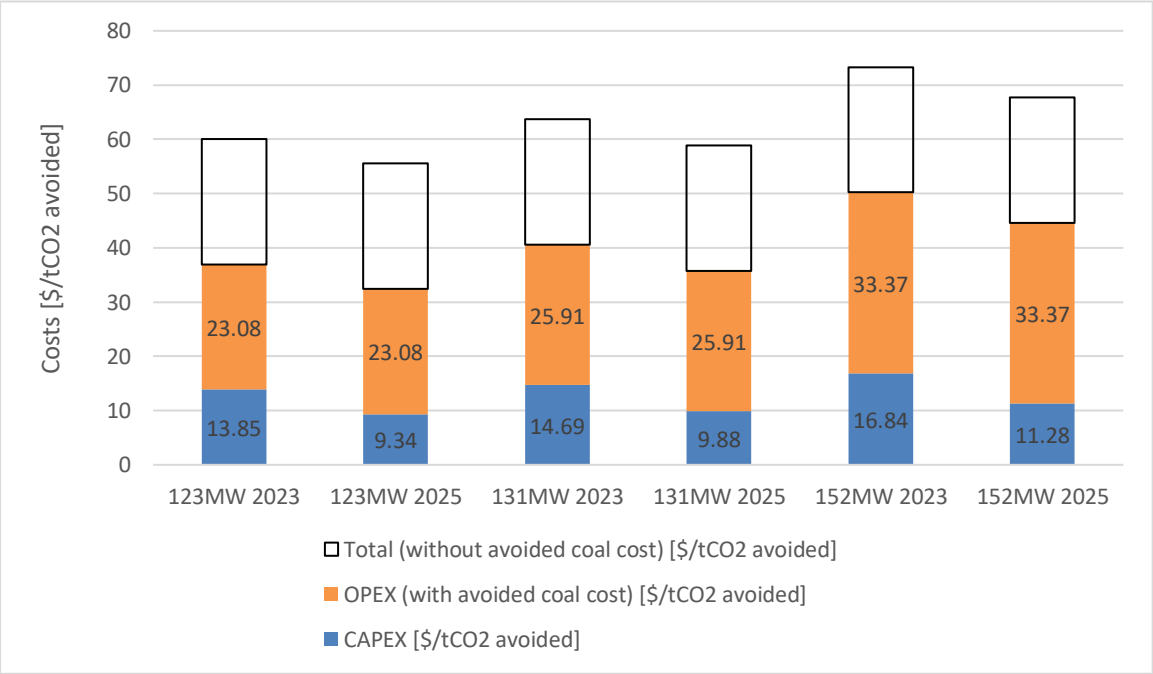

Figure 7.2: Cost per avoided tonne CO_2 – Electricity price 27,43 øre/kWh + 4 øre/kWh

The cost per avoided tonne CO2 is also examined within this context. The figure 7.2 shows the results. The costs concerning the avoided coal consumption and CAPEX remain the same; however, the cost per avoided tonne CO2 concerning OPEX decreases. The OPEX cost per avoided tonne CO2 (including avoided coal consumption in the calciner) is lower, as follows: $\$23.08 t_{CO2\ avoided}$ (123 MW), $\$25.91 t_{CO2\ avoided}$ (131 MW), $\$33.37 t_{CO2\ avoided}$ (152 MW).

This decrease in cost per avoided tonne CO2 concerning OPEX is attributable to the lower average electricity costs between 2012 and 2020. These results underscore the importance of electricity prices in the overall operational costs of the system, highlighting the need for strategic energy procurement and management in this context.

7.2.4 Fixed electricity price 2020

In this section, we explore the impact of a fixed electricity price, specifically the price from 2020, on the operational costs of the system. This analysis provides valuable insight into how fluctuations in electricity prices can significantly affect the economic feasibility of the system.

For the 123 MW electrolyser, the OPEX increases to $40.377 M/year due to the higher electricity costs for the electrolyser STACK and other minor equipment. Similarly, the OPEX for the 131 MW electrolyser rises to $42.898 M/year, and for the 152 MW electrolyser, it reaches $49.472 M/year. This is shown in table below, see table 7.3.

Table 7.3: Electrical fixed price 2020 38,1 øre/kWh +4 øre/kWh

Energy usage electrolyser	OPEX	
	2023	2025
123MW	$\frac{\$40.377\ M}{year}$	
131MW	$\frac{\$42.898\ M}{year}$	
152MW	$\frac{\$49.472\ M}{year}$	

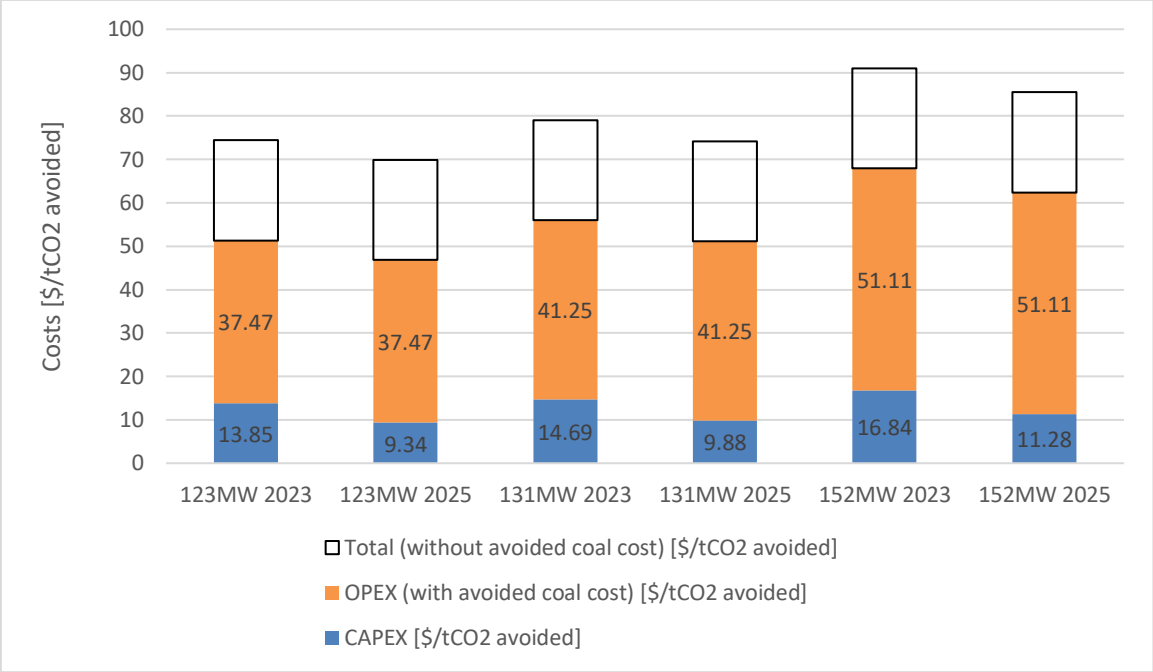

Figure 7.3: Cost per avoided tonne CO_2 – Electrical fixed price 2020 38,1 øre/kWh +4 øre/kWh

Given the fixed electricity price from 2020, the cost per avoided tonne CO2 in relation to the OPEX increases, see figure 7.3. Specifically, the OPEX cost per avoided tonne CO_2 (including avoided coal consumption in the calciner) is higher, as follows: $\$37.47 t_{CO2\ avoided}$ (123 MW), $\$41.25 t_{CO2\ avoided}$ (131 MW), and $\$51.11 t_{CO2\ avoided}$ (152 MW).

7.2.5 Fixed electricity price 2021

This subchapter investigates the implications of a fixed electricity price based on the cost from 2021 on the operation costs of the electrolysis system.

With the 2021 electricity price, the operational expenditures of the system increase due to the higher electricity costs for the electrolyser STACK and other minor equipment. For the 123 MW electrolyser, the OPEX rises to $51.254 M/year. The OPEX for the 131 MW electrolyser increases to $54.493 M/year, and for the 152 MW electrolyser, it ascends to $62.866 M/year, table 7.4.

Table 7.4: Electrical fixed price 2021 50,2 øre/kWh + 4øre/kWh

Energy usage electrolyser	OPEX	
	2023	2025
123MW	$\frac{\$51.254\ M}{year}$	

131MW	$\frac{\$54.493\ M}{year}$
152MW	$\frac{\$62.866\ M}{year}$

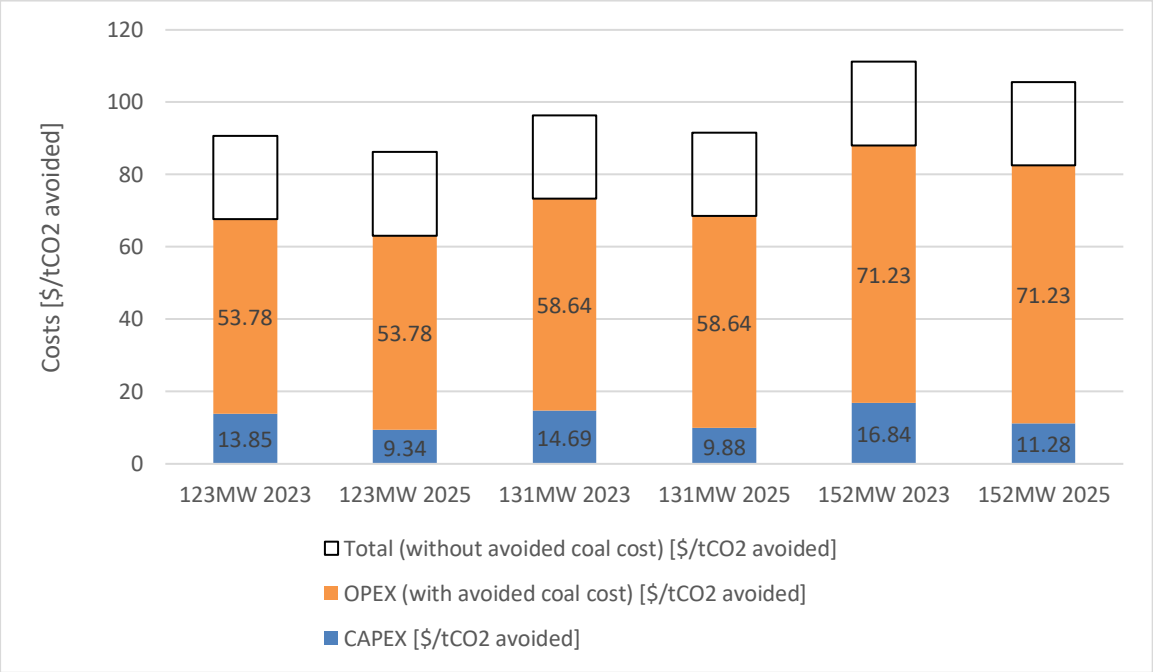

Figure 7.4: Cost per avoided tonne CO_2 – Electrical fixed price 2020 38,1 øre/kWh +4 øre/kWh

The OPEX cost per avoided tonne CO2 (including avoided coal consumption in the calciner) is as follows, see figure 7.4:

- For the 123 MW electrolyser, it is $53.78/tonne CO2 avoided.
- For the 131 MW electrolyser, it is $58.64/tonne CO2 avoided.
- For the 152 MW electrolyser, it is $71.23/tonne CO2 avoided.

7.2.6 Average electricity spot price 2022

This section analyzes the impact of the average electricity spot price for the year 2022 on the operating costs of the electrolysis system. The variability of electricity costs is a significant factor in the economic assessment of such systems, and the 2022 prices offer a recent and relevant benchmark for analysis.

The OPEX for the 123 MW electrolyser rises to $101.594 M/year, while it reaches $108.115 M/year for the 131 MW electrolyser, and soars to $124.969 M/year for the 152 MW electrolyser, see table 7.5.

Table 7.5: Electrical spot price 2022 106,2 øre/kWh + 4 øre/kWh

Energy usage electrolyser	OPEX	
	2023	2025
123MW	$\frac{\$101.594\ M}{year}$	
131MW	$\frac{\$108.155\ M}{year}$	
152MW	$\frac{\$124.969\ M}{year}$	

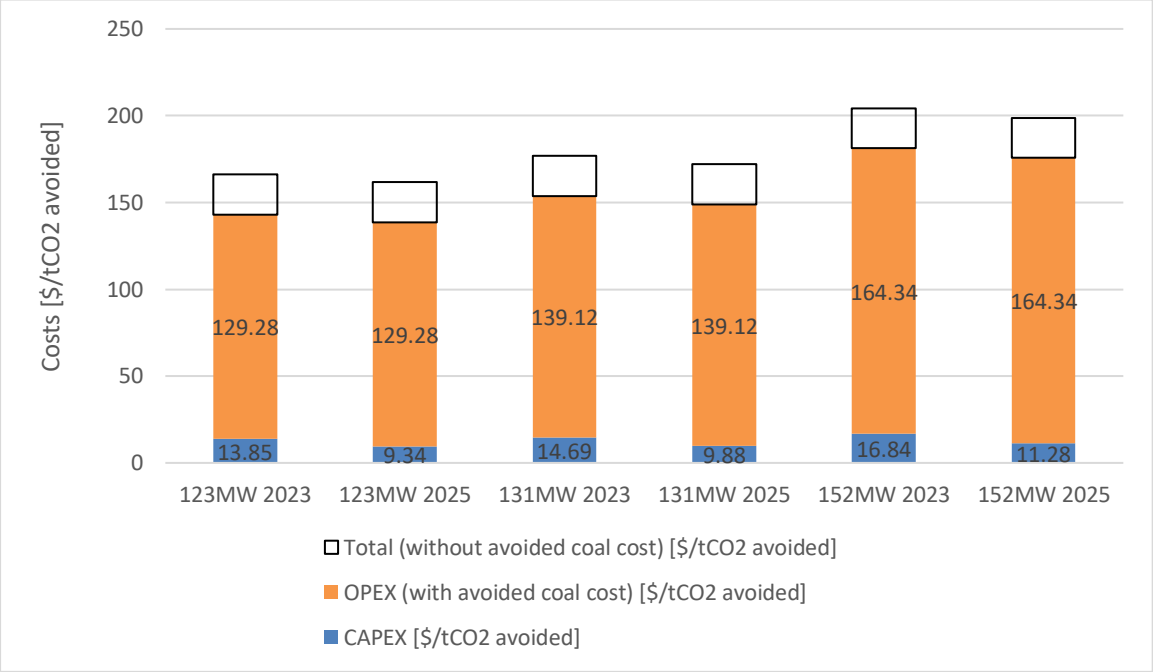

Figure 7.5: Cost per avoided tonne CO_2 – Electrical spot price 2022 106,2 øre/kWh + 4 øre/kWh

Similarly, the cost per avoided tonne CO2, especially with regard to the OPEX, also increases notably. The OPEX cost per avoided tonne CO2 (factoring in avoided coal consumption in the calciner) are as follows, see table 7.5:

- For the 123 MW electrolyser, it is $129.28/tonne CO2 avoided.
- For the 131 MW electrolyser, it is $139.12/tonne CO2 avoided.
- For the 152 MW electrolyser, it is $164.34/tonne CO2 avoided.

In this scenario, both the OPEX and the OPEX cost per avoided tonne CO2 significantly overshadow the impact of the capital expenditure (CAPEX), highlighting the critical role that electricity prices play in the economic viability of modified system.

7.2.7 Comparison with recent research alternative technologies

This section compares the economic efficiency and CO2 avoidance rate of the proposed hydrogen oxy-fuel combustion modification with several alternative technologies as reported in recent research. The comparison considers the standard MEA, advanced amine with waste heat utilization, and the electrically heated rotary calciner. The same electricity cost of 0.033 EUR/kWh and the same avoided coal cost of 111 EUR/tonne as alternative technologies were used for equal comparison.

Table 7.6: Electrical price (0.033EUR/kWh) and avoided coal consumption cost equal alternative technology.

Energy usage electrolyser	CAPEX		OPEX	
	2023	2025	2023	2025
123MW	$125.479 M	$84.656 M	$\frac{\$34.212\ M}{year}$	
131MW	$133.098 M	$89.563 M	$\frac{\$36.326\ M}{year}$	
152MW	$152.655 M	$102.247 M	$\frac{\$41.869\ M}{year}$	

The resulting OPEX for our model was: $34.212 M/year for the 123 MW electrolyser, $36.326 M/year for the 131 MW electrolyser, and $41.869 M/year for the 152 MW electrolyser, as seen in table 7.6.

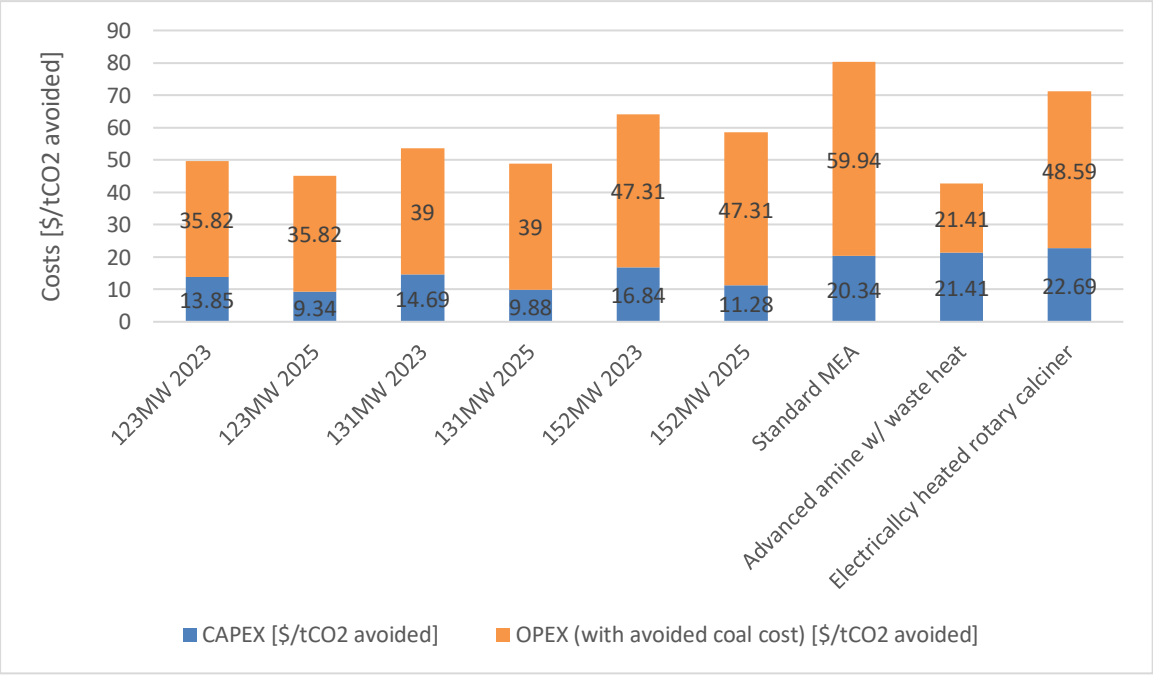

Figure 7.6: Comparison with alternative technologies

Figure 7.6 shows the alternative technologies have demonstrated the following costs:

1. Standard MEA: CAPEX - $20.34/ton of CO2 avoided; OPEX - $59.94/ton of CO2 avoided; CO2 avoidance rate - 85%
2. Advanced amine with waste heat utilization: CAPEX - $21.41/ton of CO2 avoided; OPEX - $21.41/ton of CO2 avoided; CO2 avoidance rate - 48%
3. Electrically heated rotary calciner: CAPEX - $22.69/ton of CO2 avoided; OPEX - $48.59/ton of CO2 avoided; CO2 avoidance rate - 72%

The proposed hydrogen oxyfuel combustion modification, in comparison, presents a lower CAPEX cost per ton of CO2 avoided than all alternative technologies. In terms of OPEX costs, the proposed system presents higher costs than the advanced amine with waste heat utilization but lower costs than the standard MEA and electrically heated rotary calciner. Moreover, the oxyfuel combustion modification achieves a similar CO2 avoidance rate as the electrically heated rotary calciner, outperforming the other technologies in terms of overall CO2 capture efficiency.

The OPEX cost per avoided tonne CO2 (including avoided coal consumption in the calciner) was $35.82/tonne CO2 avoided for the 123 MW system, $39.00/tonne CO2 avoided for the 131 MW system, and $47.31/tonne CO2 avoided for the 152 MW system. The CAPEX cost per avoided tonne CO2 remained the same as previously calculated.

This analysis underscores the competitiveness of the oxyfuel combustion modification in terms of both economic efficiency and CO2 avoidance rate when compared to other recent alternative technologies.

7.2.8 Avoided CO_2 tax

An important component of our economic assessment is the calculation of the avoided CO2 tax. This measure not only indicates the system's environmental effectiveness but also provides a financial advantage that can make the investment in system modification more economically viable.

In this study, we calculated the avoided CO2 tax based on two different tax rates: the tax rate in 2021 and the planned tax rate in 2030. We also considered the high electricity price of 2022 (106.2 + 4 øre/kWh) alongside the projected 2030 tax rate to estimate the cost per avoided tonne of CO2, including the avoided CO2 tax.

7.2.8.1 $59.29 per saving CO2 avoided

The figure below results showed significant savings in CO2 tax across all scenarios when using the 2021 tax rates. However, for the 152MW system, the results showed a slightly positive figure of +$2.19/tonne CO2 avoided in 2023, turning to a saving of -$3.37/tonne CO2 avoided in 2025.

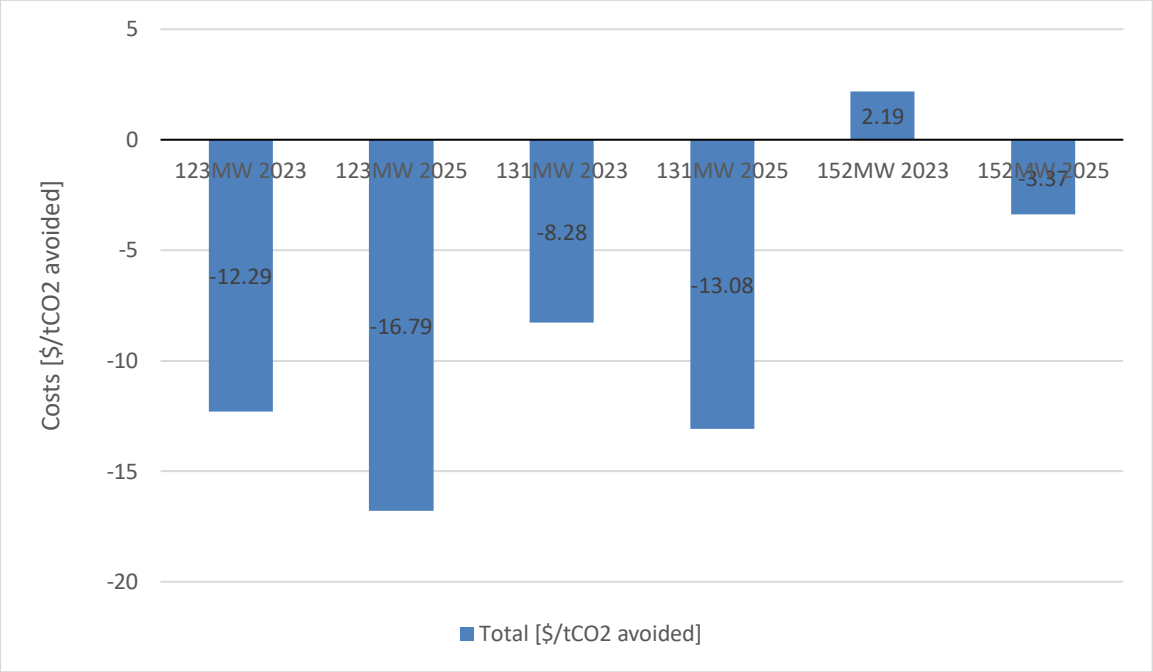

Figure 7.7: Cost per avoided tonne CO_2 with $59.29 per saving CO2 avoided

The negative cost values indicate the cost savings achieved through the avoided CO2 tax for the proposed modified calciner system at the given electricity price. The only scenario that did not yield savings was the one involving the 152MW electrolyser with the 2023 price. See results in figure 7.7.

These findings underscore the potential of the proposed system to mitigate CO2 emissions cost-effectively. As the CO2 tax increases over time, the savings achieved through CO2 capture and avoidance could offset the initial investment in system modification, thereby improving the overall economic feasibility of the project.

7.2.8.2 $200.99 saving per tonne CO2 avoided

Looking towards the future, it was also assessed the avoided CO2 tax using the planned 2030 tax rates. The results from figure were striking, with the cost per avoided tonne CO2 significantly in the negative for all cases. The average was a substantial saving of $156.68/tonne CO2 avoided.

These findings highlight the considerable financial benefits of investing in CO2 capture and avoidance technologies now, in anticipation of future tax increases. By implementing such systems today, companies can offset the higher CO2 taxes that will be imposed in the coming years, thereby improving their long-term economic sustainability.

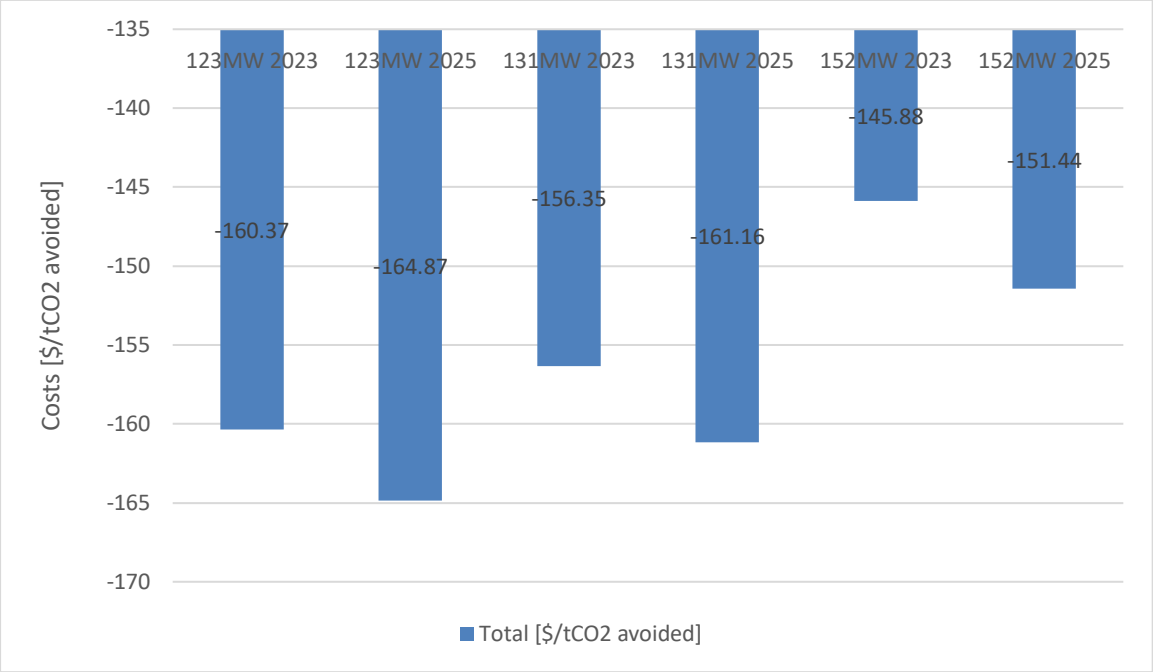

Figure 7.8: Cost per avoided tonne CO_2 – with \$200.99 per saving CO_2 avoided

\$200.99 saving per tonne CO2 avoided at high electricity price (106,2 øre/kWh + 4 øre/kWh)

Next, we considered the impact of a high electricity price (106.2 øre/kWh + 4 øre/kWh) on the avoided CO2 tax using the projected 2030 tax rates. Here, the results were still notably in the negative, but to a lesser degree, with an average saving of \$45.54/tonne CO2 avoided. The 152MW (2023) scenario had the lowest saving, but this still represented a saving of \$21.25/tonne CO2 avoided.

Even under conditions of high electricity prices, our proposed system still delivers significant savings in avoided CO2 tax. These savings are slightly lower than those achieved under normal electricity prices, but they still represent a considerable financial advantage. As such, these results further reinforce the economic viability of investing in CO2 capture and avoidance technologies.

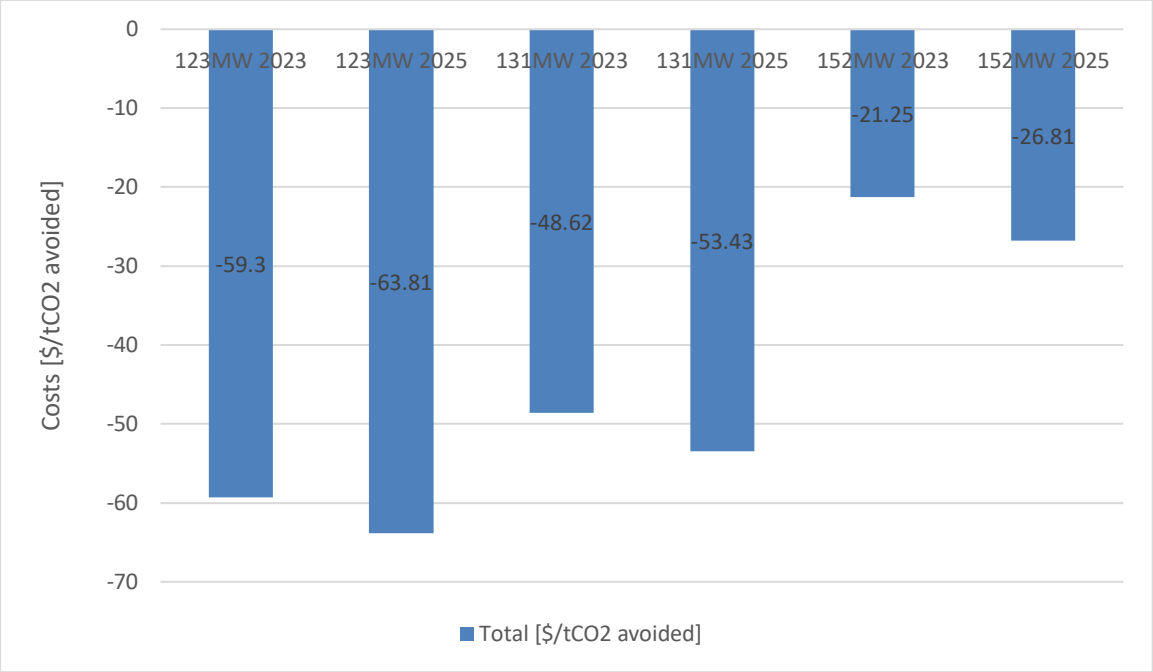

Figure 7.9: Cost per avoided tonne CO_2 – with $200.99 per saving CO_2 avoided and high electricity price

7.2.9 Cost estimation of non-optimized split exchanger in calciner

The economic evaluation of a non-optimized split exchanger in the calciner revealed certain considerations. The simulation results indicated the necessity of an additional heat exchanger, AIR-EX, to heat the air from the Clinker Cooler. As per the project's commitment to renewable energy, the design of this heat exchanger relies on electricity to generate thermal energy for the air. The cost estimation was performed considering an electricity price of $0.0336412 per kWh. This estimation encompassed the entire system, including the electrolyser with an energy usage of 152 MW.

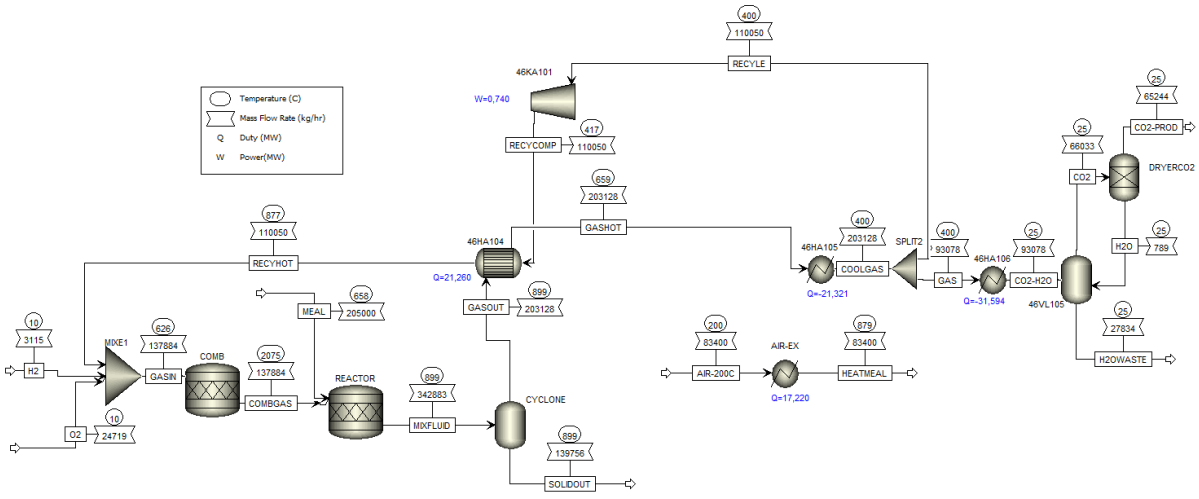

Figure 7.8: Not optimized split exchange with heater for air from Clinker Cooler.

Table 7.8: CAPEX and OPEX comparison without split exchange

	With split exchange	Without split exchange
Total CAPEX	$\$152{,}396\ M$	$\$152{,}655\ M$
Total OPEX	$\frac{\$49{,}213\ M}{\text{year}}$	$\frac{\$44{,}345\ M}{\text{year}}$
Utility increase	-	$\frac{\$4.852\ \text{M}}{\text{year}}$
Maintenance increase	-	$\frac{\$1\ 753}{\text{year}}$
CAPEX Cost per avoided tonne CO_2	$\frac{\$16.843}{t_{CO_2\ avoided}}$	$\frac{\$16.815}{t_{CO_2\ avoided}}$
OPEX Cost avoided per tonne CO_2	$\frac{\$43.417}{t_{CO_2\ avoided}}$	$\frac{\$50.718}{t_{CO_2\ avoided}}$
Total Cost per avoided tonne CO_2	$\frac{\$60.261}{t_{CO_2\ avoided}}$	$\frac{\$67.533}{t_{CO_2\ avoided}}$

The findings showed an increase in the utility needed to heat AIR-EX by 17.22 MW, and a corresponding need to cool the flue gas with an additional 17.22 MW in 46HA105. Table 7.1 displays a slight decrease in CAPEX cost. However, the OPEX cost rises significantly, almost by $7 million per year, resulting in a substantial increase in the total cost per avoided tonne of CO2.

The cost increase in utility for the AIR-EX was $4.684 M per year, and only $94,733 per year for the increased cooling of 46HA105. This indicates that the cost for the system without a split exchanger is highly dependent on the electricity price.

Table 7.9: Equipment cost comparison without split exchange.

	With split exchange	Without split exchange
Cost *46HA104*	-	181 700 $
Cost *46HA104A*	$682 375	-
Cost *46HA104B*	$150 983	-

Cost *AIR-EX*	-	$281 410
Cost *46HA105*	$28 000	$359 900

Table 7.2 illustrates the capital equipment cost for the heat exchangers in the two scenarios, which differ due to their heating needs. However, as seen in Table 7.1, the capital cost is similar for both cases. Therefore, although there are big differences in the cost of equipment, the OPEX is the main difference between the two scenarios, making it the decisive factor in choosing between the two configurations.

7.2.10 Cost estimation of modified system with 3000℃ adiabatic flame temperature

For the cost estimation of the modified system that allows for a 3000℃ adiabatic flame temperature, a few equipments required recalculation prior to cost simulation due to changes in their size and energy. These components include the heat exchanger 46HA104A, the Compressor 46KA101, and the STACK.

The modified compressor equipment cost was calculated by:

$$c_{46KA101,CS,2010} = a + b * S^n = 580\,000 + 20\,000 * 266^{0,6} = \$570\,690$$

$$c_{46KA101,SS,2010} = c_{46KA101,CS,2010} * f_m = \$570\,690 * 1.3 = \$741\,724$$

$$c_{46KA101,SS,2023} = c_{46KA101,SS,2010} * \frac{INDEX_{2023}}{INDEX_{2010}} = \$741\,724 * \frac{801,4}{550,8} = \$1\,078\,925$$

Some of the heat exchanger equipment costs was calculated according to:

$$c_{46HA104A,CS,2010} = a + b * S^n = 28\,000 + 54 * 190^{1,2} = \$57\,302$$

$$c_{46HA104A,NI,2010} = c_{46HA104A,CS,2010} * f_m = \$57\,302 * 1,7 = \$77\,814$$

$$c_{46HA104A,NI,2023} = c_{46HA104A,NI,2010} * \frac{INDEX_{2023}}{INDEX_{2010}} = \$77\,814 * \frac{801,4}{550,8} = \$100\,477$$

The CAPEX STACK cost of the modified system with lower hydrogen production was obtained by:

$$CAPEX_{STACK,2017,151\,251kW,750\,€/kW} = 113\,438\,250\,€ = \$128\,230\,598$$

$$CAPEX_{STACK,2023,151\,251kW,750\,€/kW} = Capex_{STACK,2017,151\,251kW,750\,€/kW} * \frac{INDEX_{2023}}{INDEX_{2017}}$$

$$= \$128\,230\,598 * \frac{567,5}{550,8} = \$132\,118\,490$$

The updated cost of the compressor significantly decreased, alongside the heat exchanger *46HA104A*. There was also a slight decrease in the cost of the *46HA105*. In line with the reduced energy requirements for the reaction due to a slightly lower hydrogen production of 3 092kg/h, the *STACK* also saw a reduction in its cost.

The resulting changes had some impact on the overall cost profile of the system, seen in table 7.10. The CAPEX witnessed a reduction of $5 million, while the OPEX saw a smaller decrease,

dropping by less than half a million per year. As a result, the total cost per avoided tonne of CO_2 was also reduced, achieving a lower cost of \$1.3 per tonne CO_2 avoided.

Overall, these results suggest that adjusting the system to allow for a 3000℃ adiabatic flame temperature can lead to some savings, both in terms of capital expenditure and operational costs.

Table 7.10: Comparison with 3000℃ Adiabatic flame temp.

	2076℃ Adiabatic flame temp.	3000℃ Adiabatic flame temp.
Total CAPEX	$\$152.655\ M$	$\$147.126\ M$
Total OPEX	$\frac{\$44.345\ M}{\text{year}}$	$\frac{\$43{,}889\ M}{\text{year}}$
Utility cost	$\frac{\$42.682\ \text{M}}{\text{year}}$	$\frac{\$42.233\ \text{M}}{\text{year}}$
Raw material cost	$\frac{\$607\ 071}{\text{year}}$	$\frac{\$602\ 515}{\text{year}}$
CAPEX Cost per avoided tonne CO_2	$\frac{\$16.843}{t_{CO_2\ avoided}}$	$\frac{\$16.233}{t_{CO_2\ avoided}}$
OPEX Cost avoided per tonne CO_2	$\frac{\$43.417}{t_{CO_2\ avoided}}$	$\frac{\$42.734}{t_{CO_2\ avoided}}$
Total Cost per avoided tonne CO_2	$\frac{\$60.261}{t_{CO_2\ avoided}}$	$\frac{\$58.967}{t_{CO_2\ avoided}}$

8 Discussion

In this chapter, the simulation results and cost estimations are analyzed and interpreted, comparing the proposed system to alternative CO_2 capture technologies, and evaluating its energy efficiency and environmental impact. The chapter also suggests avenues for future research and potential improvements to the proposed process concept.

8.1 Calciner simulations

The Aspen Plus simulations carried out for the calciner offered insightful results concerning the implementation of oxy-fuel hydrogen combustion, the adiabatic flame temperature, and the effects of different recycling temperature scenarios.

8.1.1 Modified Coal Combustion to Match Real Coal Consumption

The first adjustment made to the model was the modification of coal combustion to match real coal consumption. This step was crucial in ensuring that the simulation results were representative of the actual process, providing a solid foundation for the subsequent simulations. The accuracy of this model's input parameters significantly enhanced the reliability of the study and provided a more realistic assessment of the impact of the proposed modifications. The importance of the obtained 96 700kg/h CO_2 emission and 2076°C adiabatic flame temperature was significant for the rest of this thesis. The CO_2 emission also showed the huge emission making the plant Norway's third largest CO_2 emission source.

8.1.2 Adiabatic Flame Temperature for Oxy-Fuel Hydrogen Combustion

The investigation of the adiabatic flame temperature for oxy-fuel hydrogen combustion revealed a significant influence on the system's energy dynamics. Higher adiabatic flame temperatures were associated with increased thermal efficiency, but also raised concerns about material limitations. This observation highlighted the need for a balance between achieving optimal combustion conditions and ensuring flue gas recirculation for longevity of the equipment. This simulation provided somewhat good correlation to the manual calculated mass and energy balance of the calciner system, except for the slightly higher calcination energy used by the software. The model successfully managed to capture the total CO_2 flow rate of 65 244 kg/h, with an reduced CO_2 production of 31 456kg/h.

8.1.3 Different Recycling Temperature Cases

The simulations exploring different recycling temperature cases were crucial in understanding the impact on the energy balance within the calciner, particularly regarding cooling needs for the flue gas. The recycling of CO2/H2O at varying temperatures influenced the required compressor work and the cooling needs of the system, and the hydrogen consumption. By varying the temperature of the recycled CO_2/H_2O, it was possible to assess the impact on energy efficiency and hydrogen consumption.

The introduction of recycled flue gas at 35°C marked the start of an increased total flue gas flow, leading to an initial increase in the cooling demand. This was expected, as the recycling

process introduced additional volume of gas into the system, thereby raising the total amount of flue gas requiring cooling. The recycled flue gas also introduced a large increase in hydrogen consumption need. This recycled flue gas was performed by a compressor and A temperature of 35℃ for recycled CO_2 displayed the lowest energy consumption of the compressor due to the low recycling temperature and lacking water vapor. The simulation managed to maintain the desired production parameters with carbon capture. However, this case showed the highest cooling need at almost double the cooling need as without recycled flue gas. Furthermore, the recycled flue gas flow rate was the highest due to the lack of water vapor present in the flue gas. Implying that the temperature and the water vapor has significant impact on the reduced flame temperature.

The scenario with 150℃ recycled CO_2/H_2O indicated that increasing the recycle temperature could lead to a lower cooling need of the flue gas. However, energy consumption of the compressor was slightly higher compared to the 35℃ scenario. The recycled rate was much lower. Furthermore, the hydrogen consumption was reduced.

Continuing, as the recycling temperature increased, the cooling demand for the flue gas began to decrease. This counterintuitive result can be explained by the fact that the recycled flue gas temperature was increased, reducing the amount of cooling required to reach the temperature need for the splitted flue gas for recycling. This was valid although the recycled flow was increasing. The cooling needed for the captured carbon and condensed water at lower temperature of 25℃ was still the same. The cooling demand was therefore inversely proportional to the recycling temperature, with higher recycling temperatures requiring less cooling.

The compressor power, on the other hand, demonstrated a direct relationship with the recycling temperature. As the temperature and flowrate of the recycled flue gas increased, so did the power required to drive the compressor. This was due to the increased work needed to handle the larger volume of gas at a higher temperature.

Perhaps the most intriguing finding was the decrease in hydrogen consumption with increased recycling temperature. Initially, the increased volume of gases in the system necessitated a higher rate of hydrogen combustion to maintain the required calciner temperature. However, as the recycled gas temperature rose, less hydrogen was required for combustion to achieve the desired temperature. This was because the incoming recycled gas was already at a higher temperature, reducing the energy needed from hydrogen combustion.

8.1.4 Optimized Heat Exchange at 878℃ Recycled CO_2/H_2O

The optimization of heat exchange at 878℃ recycled CO_2/H_2O represented a significant improvement in the system's thermal efficiency. It demonstrated that strategic heat recovery with exit and inlet flue gas, could offset the increased compressor power demand associated with higher recycling temperatures. Thus, the design and operation of heat exchangers play a crucial role in the process's overall energy efficiency. By optimizing the heat exchanger, it was possible to recover a significant amount of heat from the flue gas, reducing the cooling requirement and improving the system's overall energy efficiency. The reduced hydrogen consumption need is also significant.

8.1.5 Optimized Split Heat Exchange with Clinker Cooler Air

The integration of the split heat exchanger with the Clinker Cooler air presented a unique opportunity to further enhance the system's energy efficiency. By utilizing waste heat to preheat the air, the overall energy demand of the calciner could be significantly reduced. This air is sent to the preheater cyclones to preheat the meal. This energy would be needed to come from somewhere else if not integrated into this model.

In conclusion, the Aspen Plus simulations provided valuable insights into the potential for oxy-fuel hydrogen combustion in a calciner. The results suggested that careful temperature management, coupled with strategic heat recovery and recycling strategies, could enhance energy efficiency, reduce hydrogen consumption, meanwhile maintaining production and introducing carbon capture. Nevertheless, further research and optimization are needed to fully realize the potential of this technology.

Across all recycling scenarios, the simulations successfully achieved the desired process parameters and included carbon capture. This demonstrated the feasibility of oxy-fuel hydrogen combustion in a calciner, provided that careful attention is paid to managing the temperature and cooling needs of the system.

8.1.6 Non-optimized split exchanger

The simulation results for the non-optimized split exchanger system revealed important insights into the system's practical implementation and potential challenges. A critical finding from the simulation was the necessity of an additional heat exchanger, AIR-EX, to heat up the air from the Clinker Cooler. This requirement presented a significant increase in the operational expenditure (OPEX) due to the extra electrical energy demand.

The cost estimation showed that using renewable electricity to generate thermal energy for the AIR-EX led to a substantial increase in the OPEX, by almost $7 million per year. This escalation significantly impacted the total cost per avoided tonne of CO2, making the system less economically viable compared to the optimized split exchange system.

The increase in utility cost for the AIR-EX was quite substantial, around $4.684 million per year, indicating the system's high dependency on electricity prices. As such, the non-optimized split exchanger system could be significantly affected by fluctuations in energy prices, further challenging its economic feasibility.

Interestingly, the capital equipment cost for the heat exchangers in the two scenarios was quite different due to different heating needs. However, the overall capital expenditure was similar for both cases, indicating that the main difference between the two scenarios lies in the OPEX.

Hence, while the non-optimized split exchanger system is technically feasible, its economic viability may be compromised due to high operational costs, primarily due to additional energy requirements. Future research could focus on optimizing this system to reduce its energy demand and, consequently, its operational costs.

8.1.7 H_2/O_2 combustion at 3000℃ adiabatic flame temperature

The investigation into H2/O2 combustion at an elevated adiabatic flame temperature of 3000℃ revealed several significant findings. Firstly, it is crucial to note that this temperature elevation had a profound impact on the system's cost dynamics. In particular, the costs associated with the compressor and certain heat exchangers, like 46HA104A, were considerably reduced. The STACK also observed a decrease in cost due to the slightly lower energy needed for the reaction, stemming from the reduced hydrogen production rate of 3092 kg/h.

The result was a substantial decrease in capital expenditure (CAPEX) by $5 million. While the operational expenditure (OPEX) did not observe a significant decrease (less than half a million per year), the overall cost impact was beneficial. The total cost per avoided tonne of CO2 was lower by $1.3 per tonne, indicating increased economic efficiency of the system under these conditions.

The observed reduction in costs underlines the importance of optimizing combustion conditions. Higher flame temperatures seem to increase the overall efficiency of the combustion process, thereby reducing the energy requirements of various system components. However, it's essential to note that elevated flame temperatures could also potentially lead to increased equipment wear and maintenance needs, which would have to be factored into the long-term operational costs.

Overall, the results suggest that combustion at 3000℃ adiabatic flame temperature could present a viable strategy for cost reduction in hydrogen combusted oxyfuel systems. However, a careful balance must be struck to ensure that the benefits of higher combustion temperatures are not offset by increased maintenance and replacement costs. Future research should focus on this aspect to provide a more comprehensive understanding of the cost dynamics under elevated combustion temperatures.

8.2 Electrolyser simulations

The electrolyser simulation played a pivotal role in understanding the hydrogen production system's operational dynamics and economic implications. The electrolyser simulations successfully achieved the target hydrogen and oxygen production rates of 3115kg/h, demonstrating the system's capability to meet the intended operational parameters. The model was also validated for the calculated mass and energy results, that indicated perfect correspondence when when the efficiency was optimal. The electrolyser, which was designed to operate at different power levels (123MW, 131MW, and 152MW), exhibited distinct performance characteristics that offered valuable insights into the system's behavior under varying operational conditions.

One of the key findings from the simulations was the direct relationship between the electrolyte circulation rate and the energy usage of the electrolyser. As the energy usage increased, so did the thermal heat generated within the system, necessitating a higher circulation rate to distribute the heat effectively and maintain optimal system operation. This relationship underscores the critical role of effective heat management in ensuring the system's efficiency, particularly at higher power levels.

Moreover, the simulations revealed a direct correlation between the electrolyser's energy usage and the cooling demand. The higher the energy usage, the greater was the cooling demand, due to the increased thermal heat generated. This result emphasizes the importance of efficient cooling systems in managing the thermal load, particularly in scenarios involving higher energy usage.

The electrolyser simulation results, therefore, offer significant practical insights for designing and operating electrolyser systems in real-world conditions. They underline the importance of careful management of energy usage and heat loads, and highlight the role of effective thermal management in optimizing system performance and cost-effectiveness. Future work may focus on refining these thermal management strategies to further enhance the system's operational efficiency and economic viability.

8.3 Capital investment costs (CAPEX)

CAPEX plays a crucial role in the financial analysis of any industrial project. It represents the initial cost required to build the infrastructure, purchase the equipment, and establish the project. It is a critical factor that significantly influences the economic feasibility and the decision-making process for implementing new technologies or systems.

In the context of this study, the CAPEX analysis provided important insights into the financial implications of implementing our proposed system, encompassing the electrolyser unit and the modifications to the calciner. The capital costs were largely driven by the size and complexity of the equipment, with the electrolyser representing a significant proportion of the total CAPEX due to its high energy consumption and the need for advanced materials and complex design to ensure efficient operation. The cost of heat exchangers, compressors, and other auxiliary equipment also contributed to the overall capital expenditure. The CAPEX showed significant decrease of the installation cost due to the anticipated future maturity of electrolyser technology.

However, it's important to note that while a lower CAPEX is beneficial, it is not certain, and it is important to look at the cost as an estimation. However, it is not the sole determining factor for the financial viability of a project. Operational expenditure also plays a significant role and must be considered alongside CAPEX for a comprehensive understanding of the total cost of ownership. In some scenarios, a system with higher CAPEX but lower OPEX might prove more economically viable over its lifetime compared to a system with lower CAPEX but higher OPEX.

Moving forward, it would be beneficial to explore strategies to further reduce the capital costs, such as optimizing the design and operation of the electrolyser and other major equipment. It will also be important to keep up to date of developments in relevant technologies, as advancements could lead to reductions in equipment costs, further enhancing the economic feasibility of the proposed system.

8.4 Operational expenses (OPEX)

Operational expenditure is as important as the initial capital investment when it comes to assessing the overall financial feasibility of a project. In this study, OPEX was primarily influenced by the cost of electricity and the maintenance costs associated with the

electrolyser and other key equipment in the system. The cost of electricity emerged as a critical factor in determining OPEX. As the electrolyser is an energy-intensive process, variations in the electricity price significantly impacted the overall operating costs. This was clearly demonstrated in the scenarios where different electricity prices were considered. The higher the electricity price, the greater the OPEX. It's important to note that electricity prices can be volatile and are subject to fluctuations based on market conditions and policy changes, which adds an element of uncertainty to the OPEX estimates.

In scenarios with higher electricity prices, the OPEX costs greatly overshadowed the CAPEX costs, underscoring the profound impact of electricity price on the overall cost-effectiveness of the system.

These results highlight the importance of achieving a balance between CAPEX and OPEX. A system with a low initial investment but high operational costs might not necessarily be more economical over its lifetime compared to a system with a higher initial investment but lower operational costs.

In conclusion, managing OPEX is critical for the economic success of the proposed system. Future work should focus on strategies to reduce operational costs, such as improving energy efficiency, optimizing maintenance practices, and exploring opportunities for lower-cost fixed electricity contracts. Additionally, ongoing monitoring and management of OPEX will be important to ensure the long-term financial sustainability of the project.

8.5 Cost per avoided tonne CO_2

The cost per avoided tonne CO2 is a key indicator of the economic feasibility and environmental effectiveness of any carbon capture and storage (CCS) project. It essentially quantifies the cost-effectiveness of a system in reducing CO2 emissions.

In this study, the cost per avoided tonne CO2 was determined for various scenarios and system configurations. The results indicated that this cost was sensitive to changes in both the capital investment and operational expenditure.

The CAPEX contributed significantly to the cost per avoided tonne CO2. However, the analysis showed that the OPEX, particularly the cost of electricity, had a more substantial impact. As the electrolyser operation is energy-intensive, any increase in electricity prices led to a notable increase in the cost per avoided tonne CO2.

Interestingly, the simulations indicated that despite variations in system configuration and design, the CAPEX remained relatively constant. Therefore, it was the variability in OPEX, especially the cost of electricity, that primarily drove changes in the cost per avoided tonne CO2. This highlights the importance of energy efficiency and the use of low-cost renewable electricity in reducing the cost per avoided tonne CO2.

The simulations also revealed that increasing the recycling temperature in the calciner system led to a reduction in the cost per avoided tonne CO2. This was due to a decrease in hydrogen production need. It was also due to the decreased cooling demand for the flue gas, which in turn reduced the energy consumption and hence the OPEX.

Overall, the results underscore the importance of a balanced approach in designing and operating CCS systems. While system modifications and operational improvements can help

reduce costs, it is also essential to consider the impact of external factors such as energy prices. Future research should continue to explore strategies to minimize both CAPEX and OPEX, thus lowering the cost per avoided tonne CO2 and making CCS a more economically viable solution for carbon emission reduction.

8.5.1 Comparison with alternative CO_2 capture technologies

Comparing the CAPEX of the proposed system with other alternative technologies revealed some interesting findings. The proposed hydrogen oxyfuel combustion modification demonstrated a lower CAPEX cost per ton of CO2 avoided compared to all alternative technologies, which suggests a competitive edge in terms of initial investment requirements.

The comparison of the proposed system with alternative technologies showed mixed results. While the proposed system had a lower OPEX than some alternatives, it was higher than post-combustion with advanced amine with waste heat utilization.

8.6 Avoided CO2 tax

The estimation of avoided CO2 tax is a crucial component of the financial analysis of any system aimed at reducing carbon emissions. In this study, we found that even under a conservative electricity price scenario, the avoided CO2 tax could result in significant savings, thereby providing a strong financial incentive for the adoption of our proposed CO2 capture system.

This finding becomes even more compelling when considering the future trajectory of CO2 tax rates. Governments worldwide are expected to increase these rates to motivate industries to reduce their carbon footprints. The analysis of the planned 2030 CO2 tax rates shows that investing in CO2 capture and avoidance technologies now could result in considerable savings in the long run.

Interestingly, our model showed that the benefits of CO2 tax avoidance remained significant even under high electricity price conditions. This scenario is particularly relevant given the volatility of electricity prices and the potential for future increases. Despite higher operational costs under this scenario, the savings from CO2 tax avoidance still outweigh these costs, indicating the system's resilience under different economic conditions.

However, it's essential to consider that these findings are based on current and planned tax rates, which could change. Future legislation could lead to even higher CO2 taxes or introduce new taxes or incentives that might affect the economic feasibility of CO2 capture and avoidance systems. Therefore, continuous monitoring of the policy landscape is crucial.

In conclusion, the potential for significant savings from avoided CO2 tax reinforces the economic viability of investing in CO2 capture and avoidance technologies. As such, these technologies could play a key role in helping industries transition towards a low-carbon future, in line with the goals of the Paris Agreement and other climate commitments.

8.7 HAZID

The HAZID methodology applied in this thesis has been instrumental in the early identification of potential hazards. It allowed for a comprehensive understanding of how the electrolysis system could impact the current operation of the cement plant, and what measures would be necessary to ensure a safe integration. The HAZID can be viewed in the attached appendix.

The analysis identified several potential hazards, including the risk of hydrogen leakage and accumulation, oxygen enrichment, the dangers associated with high-pressure equipment, potential electrolyte leakage, and electrical hazards. For each identified risk, it was proposed mitigation measures to effectively manage these hazards.

The HAZID study demonstrated the importance of regular inspection and maintenance of the electrolysis equipment, the need for adequate training for staff, and the implementation of safety measures such as leak detection sensors, proper ventilation, and pressure relief devices.

The results also emphasized the importance of proper grounding of electrical equipment and the importance of containment measures for potential electrolyte leaks.

Through the HAZID study, it has been shown that while the introduction of an electrolysis system in a cement plant comes with its set of challenges, these challenges can be effectively managed with the right safety measures and operational procedures in place. This ensures the safety of the plant, its employees, and the surrounding environment.

8.8 Primary energy losses, energy efficiency and environmental impact

Primary energy losses represent the energy dissipated in the system that is not utilized effectively in the desired process. In this case, the electrolyser and the heat exchanger operations were the primary energy-intensive components. It was observed that higher recycling temperatures led to reduced primary energy losses, primarily due to decreased cooling demands for the flue gas. This underlines the importance of optimizing the recycling temperature for improved energy efficiency and minimized energy losses.

Energy efficiency is a crucial factor in any carbon capture system as it directly affects the operational costs and carbon footprint of the process. In the present system, energy efficiency was primarily influenced by theoretically changing the electrolyser operation efficiency, which is inherently energy intensive. However, improvements in energy efficiency were observed with increased recycling temperatures in the calciner. This can be attributed to the reduction in cooling demands and hydrogen consumption with higher recycling temperatures. Therefore, optimizing the recycling temperature appears to be an effective strategy for enhancing the system's energy efficiency.

The environmental impact was assessed based on the amount of CO2 avoided per unit cost. Despite the energy-intensive operations, the system demonstrated a promising potential for CO2 capture. The system's environmental performance was seen to be strongly dependent on the operational expenditure (OPEX), particularly the electricity cost. As such, the use of renewable low-cost energy sources could significantly enhance the environmental sustainability of the process. Moreover, the system achieved a similar or better CO2

avoidance rate to more traditional technologies, indicating its potential as an effective carbon capture solution.

8.9 CO_2 emission reduction and capture

The proposed system's potential for CO2 emission reduction and capture is an essential aspect of its viability, especially in the context of the prevailing environmental targets and commitments at the company, national, and international levels.

8.9.1 Alignment with emission goals for Norway and the Paris agreement

The carbon capture rate achieved by the system in this study aligns well with Norway's ambitious climate goals. Norway has committed to significantly reduce its greenhouse gas emissions by 2030 and even further by 2050. This commitment is in line with the Paris Agreement, which aims to limit global warming to below 2 degrees Celsius above pre-industrial levels. With its considerable CO2 capture potential, the proposed system can make a significant contribution to achieving these targets.

8.9.2 Carbon capture

For Norcem the results are also promising. Cement production is a significant source of CO2 emissions worldwide, and Norcem has been proactively working on reducing its carbon footprint. The system’s potential to capture CO2 effectively can help Norcem further its environmental objectives and reduce CO2 emission tax. With the right implementation and collaboration with projects like Longship, this system could play a significant role in the global fight against climate change.

8.10 Future research

The results from this study provide a strong foundation for further research. While the proposed system demonstrates potential for carbon capture and cost efficiency, there are several areas where further investigation could provide a more comprehensive view of the system and uncover opportunities for optimization.

8.10.1 Kiln Inclusion

Including the kiln in future simulation models could provide a more accurate picture of the system's overall CO2 emissions and energy usage and provide the option to capture/avoid more carbon. It could also help understand the complex interactions between the kiln and calciner operations, potentially revealing ways to improve system efficiency.

8.10.2 Alternative Combustion Processes

Further exploration of combustion processes could also be fruitful. For instance, studying the combustion of coal with oxy-fuel without hydrogen, or the conversion of methane to hydrogen with carbon capture and oxy-fuel from air separation unit, could potentially provide insights into more efficient or cost-effective ways to reduce CO2 emissions.

8.10.3 Use of Alternative Fuels

The actual cement plant uses a mix of coal, animal meal, and liquid hazardous waste as fuel. A comparison between the results obtained in this thesis, which uses coal exclusively, and a scenario that includes the combustion of animal meal and liquid hazardous waste, could be informative. This could also lead to a better understanding of how different fuels impact CO2 emissions and system efficiency.

8.10.4 Detailed Analysis of Cooling Equipment

A more detailed investigation of energy usage and costs associated with cooling equipment could also be beneficial. Cooling is an essential part of the process, and any improvement in this area could have a significant impact on the system’s overall energy efficiency and operational costs.

8.10.5 Comprehensive Cost Analysis

A more comprehensive analysis of operational costs could consider raw material costs, cement sales, and potentially the cost of transporting CO2 to storage facilities in the North Sea. This would provide a more complete picture of the system's economic feasibility.

8.10.6 Calcination Rate Exploration

Finally, further research could explore how the calcination rate is dependent on the CO2 partial pressure and temperature in the calciner. This could potentially reveal more about how these variables affect the energy required in the calciner and provide insights into how to optimize this process.

9 Conclusion

This chapter summarizes the key findings and conclusions drawn from the simulation and the economic exploration, highlighting the potential of electrolysis-generated hydrogen and oxygen for decarbonizing cement production.

This thesis embarked on a comprehensive exploration of the implementation of an oxyfuel combustion modification in a cement plant calciner, with a focus on the Norcem Brevik cement plant. The overarching goal was to assess the feasibility of this modification as a strategy to reduce carbon emissions in line with the goals set out in the Paris Agreement and the specific objectives of Norway and Norcem.

The investigation covered a broad range of aspects, including a detailed analysis of calciner simulations with hydrogen oxy-fuel combustion, an examination of alkaline electrolyser cases, an evaluation of capital and operational expenditure, and a consideration of CO2 emissions reduction and capture. The simulation results provided valuable insights into the potential benefits and challenges associated with the proposed modification.

The calciner simulations indicated that the introduction of recycled flue gas significantly increased the hydrogen consumption rate, although this consumption rate decreased proportionally with increased recycled temperature. The electrolyser simulations highlighted that the circulation rate of the electrolyte and the cooling need were directly affected by the energy usage.

From a cost perspective, the results showed that the proposed hydrogen oxy-fuel combustion modification could demonstrate a lower CAPEX cost per tonne of CO2 avoided compared to alternative technologies. Although the operational expenditure was higher than one alternative technology, the overall cost per avoided tonne CO2 was competitive, especially when considering the avoided CO2 tax, which could result in considerable cost savings.

The results also pointed towards the considerable environmental benefits. The proposed system achieved a similar CO2 avoidance rate as the electrically heated rotary calciner, outperforming some technologies in terms of overall CO2 capture efficiency. The proposed system also aligns well with the Longship project, with the ease of captured CO2 being potentially transported and permanently stored in the North Sea.

Additionally, the investigation of the non-optimized split exchanger highlighted that the system's cost without a split exchanger is highly dependent on the electricity price. However, the simulation of H2/O2 combustion at an elevated adiabatic flame temperature of 3000°C showed the potential for cost savings due to increased combustion efficiency.

Future research directions should include exploring the inclusion of the kiln in the model to avoid more CO2 emission, investigating the combustion of the alternative fuels used today, a detailed exploration of cooling equipment energy usage and costs, and a deeper dive into the interplay between CO2 partial pressure, temperature, and calcination rate in the calciner.

In conclusion, this thesis has provided a comprehensive analysis of the potential for the implementation of calcination driven by oxy-fuel combustion of green hydrogen in a cement plant, presenting a promising pathway towards achieving substantial CO2 emission reductions in the cement industry. The insights generated contribute valuable knowledge to the ongoing global effort to mitigate the impacts of climate change.

References

[1] L. A. Tokheim, “COMBINED CALCINATION AND CO2 CAPTURE IN CEMENT CLINKER PRODUCTION BY USE OF ELECTRICAL ENERGY,” presented at the The 10th Trondheim Conference on CO2 Capture, Transport and Storage, 2019.

[2] F. W. Locher, *Cement principles of production and use*. Düsseldorf: Verl. Bau und Technik, 2006.

[3] L.-A. Tokheim, “The impact of staged combustion on the operation of a precalciner cement kiln,” 1999.

[4] A. Hasanbeigi, L. Price, and E. Lin, “Emerging energy-efficiency and CO2 emission-reduction technologies for cement and concrete production: A technical review,” *Renewable and Sustainable Energy Reviews*, vol. 16, no. 8, pp. 6220–6238, Oct. 2012, doi: 10.1016/j.rser.2012.07.019.

[5] M. J. Mølnvik and E. F. Silva, “Carbon Capture & Storage - CCS research from SINTEF,” *SINTEF*, May 02, 2023. https://www.sintef.no/en/sintef-research-areas/ccs/ (accessed May 10, 2023).

[6] K. L. Scrivener, V. M. John, and E. M. Gartner, “Eco-efficient cements: Potential economically viable solutions for a low-CO2 cement-based materials industry,” *Cement and Concrete Research*, vol. 114, pp. 2–26, Dec. 2018, doi: 10.1016/j.cemconres.2018.03.015.

[7] F. Dr Birol, Ed., “Net Zero by 2050 - A Roadmap for the Global Energy Sector,” *International Energy Agency*, Oct. 2021.

[8] M. Ditaranto and J. Bakken, “Study of a full scale oxy-fuel cement rotary kiln,” *International Journal of Greenhouse Gas Control*, vol. 83, pp. 166–175, Apr. 2019, doi: 10.1016/j.ijggc.2019.02.008.

[9] Ø. Kirsten Å., “Her skal utslippene kuttes med 4,3 millioner tonn,” Apr. 07, 2022. https://energiogklima.no/nyhet/her-skal-utslippene-kuttes-med-43-millioner-tonn/ (accessed May 10, 2023).

[10] C. Chen and S. Yang, “The energy demand and environmental impacts of oxy-fuel combustion vs. post-combustion capture in China,” *Energy Strategy Reviews*, vol. 38, p. 100701, Nov. 2021, doi: 10.1016/j.esr.2021.100701.

[11] European Cement Research Academy, “Cement industry launches an industrial-scale carbon capture project,” Jan. 29, 2018.

[12] D. J. Barker, S. A. Turner, P. A. Napier-Moore, M. Clark, and J. E. Davison, “CO2 Capture in the Cement Industry,” *Energy Procedia*, vol. 1, no. 1, pp. 87–94, Feb. 2009, doi: 10.1016/j.egypro.2009.01.014.

[13] C. B. Gemini.no, “Dette må du vite om fangst og lagring av CO2,” *SINTEF*, Oct. 10, 2019. https://www.sintef.no/siste-nytt/2019/dette-ma-du-vite-om-ccs-karbonfangst-og-lagring/ (accessed May 10, 2023).

[14] A. G. Olabi *et al.*, “Assessment of the pre-combustion carbon capture contribution into sustainable development goals SDGs using novel indicators,” *Renewable and*

Sustainable Energy Reviews, vol. 153, p. 111710, Jan. 2022, doi: 10.1016/j.rser.2021.111710.

[15] NHO, "CO2-fangst og lagring (CCS)," 2023. https://www.nho.no/tema/energi-miljo-og-klima/artikler/co2-fangst-og-lagring-ccs/ (accessed May 10, 2023).

[16] Heidelberg Materials, "Heidelberg Materials og karbonfangst," *Heidelberg Materials Sement Norge*, 2023. https://www.sement.heidelbergmaterials.no/no/CCS (accessed May 13, 2023).

[17] O. energidepartementet, "Spørsmål og svar om Langskip-prosjektet," *Regjeringen.no*, Oct. 13, 2021. https://www.regjeringen.no/no/tema/energi/landingssider/ny-side/ccs/id2863902/ (accessed May 10, 2023).

[18] J. Piispa, "Techno-economic analysis and Aspen Plus process simulation of a Power-to-Gas system integrated to waste incinerator," Dec. 2021.

[19] E. Eikeng and O. Rogneby, "A Feasibility Study of Large Scale Wind Powered Hydrogen Production," Bachelor thesis, NTNU, 2021. Accessed: May 1, 2023. [Online]. Available: https://ntnuopen.ntnu.no/ntnu-xmlui/handle/11250/2779955

[20] G. Towler and R. Sinnott, "Chemical Engineering Design - Principles, Practice and Economics of Plant Process Design," in *Chemical Engineering Design*, in Second Edition. Elsevier, 2013, p. i. doi: 10.1016/B978-0-08-096659-5.00022-5.

[21] L. A. Tokheim, "Task background - CO2 capture combined with calcination driven by oxyfuel combustion of green hydrogen." University of South-Eastern Norway, 2022.

[22] R. M. Jacob and L.-A. Tokheim, "Electrified calciner concept for CO2 capture in pyro-processing of a dry process cement plant," *Energy*, vol. 268, p. 126673, Apr. 2023, doi: 10.1016/j.energy.2023.126673.

[23] *Useful Conversions and Thermodynamic Properties lower heating value*. Washington, DC: National Academies, 2023. doi: 10.17226/10922.

[24] NIST, "The NIST reference on constants: Faraday constant," 2023. https://physics.nist.gov/cgi-bin/cuu/Value?f (accessed May 10, 2023).

[25] "Hydrogen ion," *Wikipedia*. Feb. 14, 2023. Accessed: May 11, 2023. [Online]. Available: https://en.wikipedia.org/w/index.php?title=Hydrogen_ion&oldid=1139221420

[26] M. W. Chase, "NIST-JANAF Themochemical Tables, Fourth Edition," *J. Phys. Chem. Ref. Data, Monograph 9*, pp. 1–1951, 1998.

[27] Aspen Tech, "Aspen Plus | Leading Process Simulation Software | AspenTech," 2023. https://www.aspentech.com/en/products/engineering/aspen-plus (accessed May 5, 2023).

[28] E. C. Carlson, "Don't Gamble With Physical Properties For Simulations," *CHEMICAL ENGINEERING PROGRESS*, 1996.

[29] KG Engineering Solutions, "Alkaline simulation file Aspen Plus," Mar. 31, 2023.

[30] C. Maxwell, "Cost Indices," May 28, 2020. https://toweringskills.com/financial-analysis/cost-indices/ (accessed May 11, 2023).

[31] Porsgrunn kommune, “Gebyrliste,” 2023. https://pub.framsikt.net/2023/porsgrunn/bm-2023-hp23-26_bs-vedtak (accessed May 12, 2023).

[32] Trading Economics, “Coal - 2008-2022 Historical data,” 2023. https://tradingeconomics.com/commodity/coal (accessed May 10, 2023).

[33] Dagsavisen, “Strømprisen når nye rekorder – over 10 kroner på det meste,” *Dagsavisen*, Aug. 28, 2022. https://www.dagsavisen.no/nyheter/innenriks/2022/08/28/stromprisen-nar-nye-rekorder-over-10-kroner-pa-det-meste/ (accessed May 5, 2023).

[34] “09366: Kraftpriser i sluttbrukermarkedet, etter kontraktstype (øre/kWh) 2012 - 2022. Statistikkbanken,” *SSB*, 2023. https://www.ssb.no/system/ (accessed May 01, 2023).

[35] N. Frøystad Delebekk, “Slik endte vi med 17 strømlinjer til utlandet,” *faktisk.no*, Jan. 13, 2022. https://www.faktisk.no/artikler/jn2m2/slik-endte-vi-med-17-stromlinjer-til-utlandet (accessed May 12, 2023).

[36] Lede, “Nettleie priser 2023,” May 20, 2022. https://lede.no/priser/ (accessed May 9, 2023).

[37] K. D. Haug, L. Reiakvam, and H. Solheim, “Avgifter på utslipp er fortsatt lave som andel av produksjonsverdi,” Feb. 22, 2022. https://www.norges-bank.no/bankplassen/arkiv/2022/avgifter-pa-utslipp-er-fortsatt-lave-som-andel-av-produksjonsverdi/ (accessed May 10, 2023).

[38] K. miljødepartementet, “Meld. St. 13 (2020–2021) Klimaplan for 2021-2030,” *Regjeringa.no*, Jan. 08, 2021. https://www.regjeringen.no/nn/dokumenter/meld.-st.-13-20202021/id2827405/ (accessed May 10, 2023).

[39] Skatteetaten, “Refusjon av særavgifter for næringsdrivende,” *Skatteetaten*, 2023. https://www.skatteetaten.no/bedrift-og-organisasjon/avgifter/saravgifter/rapportere/soke-refusjon-av-saravgifter/ (accessed May 10, 2023).

Appendices

Appendix A Master’s thesis signed task description

Appendix B Prosjektplan

Appendix C Work breakdown structure

Appendix D HAZID

Appendix F Aspen Plus Simulation files

Appendix G Cost simulation files